BIOTECH STUDIES

TAGEM JOURNALS

Aims and Scope

"Biotech Studies" is the successor to the "Journal of Field Crops Central Research Institute" which has been published since 1992. The journal publishes articles on agro-biotechnology, plant biotechnology, biotechnology for biodiversity, food biotechnology, animal biotechnology, microbial biotechnology, environmental biotechnology, industrial biotechnology and bioprocess engineering, applied biotechnology, omics technologies, system biology, synthetic biology, nanobiotechnology, and bioinformatics.

The journal of Biotech Studies has been published twice a year (June & December). Original research papers, critical review articles, short communications, and scientific research of the journal are published in English. It is an international refereed journal.

The journal is aimed for researchers and academicians who work in or are interested in the topics of research in biotechnology.

Biotech Studies is indexed in Scopus, ULAKBIM TR Index, Scientific Indexing Services, and CrossRef.

Further information for "*Biotech Studies*" is accessible on the address below indicated:

http://www.biotechstudies.org/

You can reach table of contents, abstracts, full text and instructions for authors from this home page.

Corresponding Address

As a Publisher, Biotech Studies is pleased to declare its commitment to the United Nations Sustainable Development Goals (UN SDGs) Publishers Compact. The purpose of this Compact is to accelerate progress to achieve SDGs by 2030. Signatories aspire to develop sustainable practices and act as champions of the SDGs during the Decade of Action (2020-2030), publishing books and journals that will help inform, develop, and inspire action in that direction. Furthermore, as a signatory of SDG Publishers Compact, Biotech Studies commit to:

1. **Committing to the SDGs**: Stating sustainability policies and targets on our website, including adherence to this Compact; incorporating SDGs and their targets as appropriate.

2. **Actively promoting and acquiring content** that advocates for themes represented by the SDGs, such as equality, sustainability, justice and safeguarding and strengthening the environment.

3. **Annually reporting on progress towards achieving SDGs**, sharing data and contribute to benchmarking activities, helping to share best practices and identify gaps that still need to be addressed.

4. **Nominating a person who will promote SDG progress,** acting as a point of contact and coordinating the SDG themes throughout the organization.

5. **Raising awareness and promoting the SDGs among staff** to increase awareness of SDG-related policies and goals and encouraging projects that will help achieve the SDGs by 2030.

6. **Raising awareness and promoting the SDGs among suppliers,** to advocate for SDGs and to collaborate on areas that need innovative actions and solutions.

7. **Becoming an advocate to customers and stakeholders** by promoting and actively communicating about the SDG agenda through marketing, websites, promotions, and projects.

8. **Collaborating across cities, countries, and continents** with other signatories and organizations to develop, localize and scale projects that will advance progress on the SDGs individually or through their Publishing Association.

9. **Dedicating budget and other resources towards accelerating progress** for SDG-dedicated projects and promoting SDG principles.

10. **Taking action on at least one SDG goal**, either as an individual publisher or through your national publishing association and sharing progress annually.

Besides these 10 action points, Biotech Studies endorses the SDGs, and explicitly concentrate on eight of 17 goals:

BIOTECH STUDIES

BIOTECH STUDIES

CONTENTS

BIOTECH STUDIES

RESEARCH PAPER

Assessment of the usability of four molecular markers to identify potato genotypes suitable for processing

Caner Yavuz[1]* ⓘ, Ufuk Demirel[1] ⓘ, Mehmet Emin Caliskan[1] ⓘ

[1]Agricultural Genetic Engineering Department, Faculty of Agricultural Sciences and Technology, Nigde Omer Halisdemir University, 51240, Niğde, Türkiye

Abstract

The development of processing potato cultivars through a conventional breeding program requires a detailed analysis of post-harvest traits, which is a process that demands high labor and is often time-consuming. Visual selection by breeders is biased and difficult in the field, particularly for quality traits, which shows the importance of marker-assisted selection over conventional techniques. In this study, four allele-specific markers, *AGPsS-9a, Stp23-8b, StpL-3e*, and *Pain1-8c*, developed from tuber quality-related genes, were used to screen a breeding population of the NOHU for processing traits to check the efficiency of these markers in processing trait selection. Marker association with tuber quality trait results showed that *AGPsS-9a* (0, absent) and *StpL-3e* (0) individually were associated with increased chips quality, yet their individual presence improved the reducing sugar content. Further, *Pain1-8c* presence was associated with high levels of reducing sugar accumulation and lower dry matter content, specific gravity, and starch content. The marker combination *Stp23-8b* (0) and *StpL-3e* (0) reached statistical significance (P≤0.05) for better chips quality in the NOHU population. However, the markers (individual and combination) showed poor selection efficiency as a diagnostic marker, possibly reasoning from the multigenic inheritance of tuber quality traits, population structure, and environment.

Introduction

Potato breeding using conventional approaches is a laborious and time-consuming process because of its dependence on many years of selection, along with a means of measuring desired traits such as tuber yield, processing quality, disease resistance, and abiotic stress tolerance in the laboratory and field (Milczarek et al., 2014). Molecular marker studies evaluating the quality properties of potato tubers after harvest are very limited compared to other marker studies in potato because of their multigenic inheritance. However, the development and validation of markers related to processing quality in potato will largely decrease labor

and provide a reliable selection approach for breeding programs (Li et al., 2013).

Labor-intensive quality traits, such as dry matter, starch, reducing sugar content, and French fry/crisp quality, are screened in routine potato breeding programs, and scientists argue the applicability of molecular markers for selection in breeding programs. The selection process during a potato breeding program requires visual evaluation in order to keep the promising breeding line for the next year; however, the measurement of tuber quality traits is possible only at the post-harvest stage. Unfortunately, this latter

circumstance results in the loss of several promising processing breeding lines that are selected based on appearance. In addition, many of the methods currently used to measure tuber quality traits rely on destructive screening. It is, therefore, very critical, especially regarding breeding efforts, to develop a non-destructive mechanism that allows selection of breeding lines for processing purposes during the vegetation period (before the harvest). Therefore, implementing marker assisted selection for tuber quality traits in potato is one of the main concerns of a few scientists today.

There are a limited number of molecular mapping studies regarding dry matter content, and they have reported that the relevant loci are located on chromosomes 2, 5, 8, 9, and 11 (Manrique-Carpintero et al., 2015). In particular, an earlier study observed that a QTL region on chromosome 5 had a minor effect on increasing dry matter content; interestingly, the same QTL region was also associated with maturity and tuber shape (Bradshaw et al., 2008). Unfortunately, the application of the genomic selection model in another study did not produce a reliable and predictable selection approach for dry matter content across different breeding MASPOT populations in potato (Sverrisdottir et al., 2017). Another work screening specific gravity using marker assisted selection (isozymes, RFLP, and RAPD) in a diploid population had an achievement in different trial locations, and several QTLs were mapped on different chromosomes (1, 2, 3, 5, 7, 11). However, this study had restriction on application in tetraploid level (Freyre and Douches, 1994). The use of novel systems, such as the SolCAP SNP array in breeding programs, has exploited the association of several genomic regions with several tuber quality traits, starch content (Schönhals et al., 2017), and browning after fry (D'hoop et al., 2014). Although there are more studies on these particular tuber quality traits, they were not found to be statistically significant (Sharma et al., 2018). However, several novel QTLs, such as *cPHO1B-1b, PHO1B-1a, Stl024-e, PHO1A-b, Stl013-a*, and *SSR327-a*, have been identified for starch content and specific gravity (Urbany et al., 2011). Several SNPs, later related to starch content, have been known to have loci primarily on chromosome 10, revealed using genotyping by sequencing strategy in potato (Sverrisdóttir et al., 2017). These regions are related to a role in carbohydrate metabolism and making the main task of major studies for processing traits in marker development studies (Li et al., 2008, 2013; Schreiber et al., 2014). Novel QTL regions have been investigated for several other processing traits, such as cold-induced sweetening during storage and fry color (Sołtys-Kalina et al., 2020).

Four SSCP markers, *Pain1-8c, AGPsS-9a, StpL-3e*, and *Stp23-8b*, have been associated with tuber yield, starch content, starch yield, crisp color, and French fry color stored at 4°C for three-four months and verified as diagnostic markers for these traits (Li et al., 2013; Schreiber et al., 2014; Schönhals et al., 2016). The effect of *PHO1* alleles, *Stp23-8b (PHO1a-Ha),* and *StpL (PHO1b)-3b*, on starch content was observed independently in two different German populations, CHIPS-ALL with 243 potato cultivars and breeding populations (BNC and SKC clones). Furthermore, the aforementioned molecular markers have been found to be related to decreased sugar content (glucose and fructose) as well (Schreiber et al., 2014). The presence of *Stp23-8b* was associated with increased starch content and positively related to starch yield and chip quality (Li et al., 2013).

In this study, the NOHU population developed in the breeding program of Nigde Omer Halisdemir University was screened with molecular markers developed by Li et al. (2013) to test the reproducibility of these markers for the selection of promising processing breeding lines.

Materials and Methods

Plant material

This study was conducted at Nigde Omer Halisdemir University, Nigde, Turkiye. A breeding population named "NOHU" combining breeding lines from the crosses between four different parental combinations, *04.123 x Hermes, 06.62 x Hermes, 01.536 x Hermes,* and *Pomqueen x CIP 397039.51*, was used for screening. The parental potato genotypes *Hermes* (Austria), *01.536* (Hungary), and *CIP 397039.51* (Peru) were chosen for chips purposes, while *Pomqueen*, 06.62 (Hungary), and *04.123* (Hungary) were chosen for French fry purposes (ECPD, 2017). In total, 182 individuals were included in the study. Three seed tubers at the third year of the potato breeding scheme stage for each crossing combination were planted in the field by hand on May 6, 2015, with a 33 cm in-row distance and 70 cm inter-row spacing. The plants were irrigated regularly using a sprinkler irrigation system. Standard agricultural practices for potato were applied during the growth period. Tubers were harvested by hand 175 days after planting, and all genotypes were kept at 8°C and 90% humidity for post-harvest analysis (Cottrell et al., 1993).

Specific gravity, dry matter, and starch content

Specific gravity (SG) was determined by analyzing potatoes (approximately 1500 g) with a PW2050 Digital Potato Hydrometer. Breeding lines with an SG greater than 1.080 were considered suitable for processing. The dry matter content (DMC) was calculated based on specific gravity. Breeding lines with DMC greater than 20% are considered suitable for processing (Lisinska et al., 2009). Starch content (SC) was calculated according to the following formula (Haase, 2003);

SC = (183 x Specific gravity) - 183

Reducing sugar (glucose and fructose) content

The tuber samples were placed in refrigerator bags without peeling and kept at −20°C for at least 24 h. The

samples were then freeze-dried in a lyophilizer (Labconco) at −80°C and 0.5 mBar conditions for five days. The freeze-dried samples were homogenized using a blender to obtain powder. The tuber skin, which was difficult to break, was crushed using a mortar. The powder was filtered through a sieve (Friedman et al., 2009). Potato powder (200 mg) was weighed and placed in a 15 mL centrifuge tube. Ultrapure water (three mL) was added to the centrifuge tube. The mixture was vortexed for three min then seven mL of pure ethanol (≥ 99.9) was added to the mix, and the mixture was gently shaken. The mixture was then centrifuged for 10 min at 1600 x g. The supernatant was collected using a syringe and passed through 0.45 μm filters. An Inertsil NH$_2$ (GL Science) column was used for the HPLC (Shimadzu Prominence Series) analysis. The pure glucose and fructose (HPLC grade-Merck) were used as the standards for HPLC analysis of reducing sugar content (RSC). A mixture of acetonitrile and water (80:20, V/V) was used as the mobile phase. The column conditions were determined to be one mL flow rate per minute at 40°C. Solid-phase extraction is not required (Yavuz, 2016).

Crisp and french fry color

Tubers meeting the criteria of tuber shape and size for processing purposes were selected for crisp and French fried potato color analysis and quantified using colorimetric measurements. The peeled tuber samples were sliced to a thickness of two mm for crisp processing. These slices were fried in sunflower oil at 180°C for three min (REMTA). The L, a, and b values were measured using a colorimeter (Konica Minolta- CR700) to analyze French fry L value (FLV) and crisp L value (CLV). The tuber samples were cut into strips of 10x10 mm for French fry analysis. The same procedures were followed for the color measurement of French fried potato samples.

DNA extraction

Young leaf samples were ground using TissueLyser II for three min. DNA was extracted from powdered tissue samples using the GeneJET Plant Genomic DNA Purification Mini Kit (Thermo Scientific) according to the manufacturer's protocol. DNA quantity was measured using spectrophotometer (BioSpec-SHIMADZU).

Molecular screening

Four of the most promising candidate molecular markers, *StpL-3e, Stp23-8b, AGPsS-9a*, and *Pain1-8c*, associated with tuber quality traits (Li et al., 2013), were tested on 182 potato breeding lines and parents, *04123, 0662,* and *Pomqueen*, to determine their diagnostic precision. In addition, *Agria*, a non-parental processing variety, was also included in the study as an external control, but we lacked tubers for *01536, Hermes*, and *CIP 397039.51*, so we could not screen these genotypes. For PCR optimization, the DNA samples of the potato cultivars *Diana, Satina, Theresa, Solana*, and *Leyla*

provided by Dr. Christiane Gebhardt were used as positive or negative control based on the marker in the molecular screening studies (*Satina* for *Pain1-8c* and *Solana* for three other markers as positive control and *Leyla* as negative control for all four markers). Primers were constructed as described by Li et al., 2013.

The PCR was performed in 25 μl volume solution containing 10x DreamTaq buffer (Thermo), 0.2 mM dNTP, 1 μM primer (for each forward and reverse primer), 1 unit Taq DNA polymerase, and 50 ng genomic DNA. While a touchdown PCR method was used to screen the NOHU population to increase the specificity of the *StpL-3e, Stp23-8b*, and *Pain1-8c* primers and avoid non-specific amplification, a standard PCR method was used for *AGPsS-9a* because the reaction was already very specific for the target. The thermal cycling conditions of the PCR consisted of an initial incubation at 95°C for three min, followed by 35 cycles of denaturation at 95°C for 15 s, annealing, and elongation at 72°C for 30 s. For the touchdown PCR, the first annealing temperature was set to 5°C above the optimal annealing temperature. The annealing temperature was decreased by 1°C during each subsequent cycle during the five cycles. The reaction was continued for 30 more cycles at the final annealing temperature. The annealing temperatures were set as 63°C-58°C for *Pain1-8c* and *Stp23-8b*, 65°C-60°C for *StpL-3e*. A constant annealing temperature of 63°C was used for *AGPsS-9a*. Depending on the size of the PCR product, the elongation time was set to 30 s for those smaller than 500 bp, and 45 s for the range of 500-750 bp at 72°C. The PCR products were run on a 2% agarose gel at 7 V/cm and produced scorable band sizes of 703 bp for *Pain1-8c*, 348 bp for *Stp23-8b*, 360 bp for *StpL-3e* and 210 bp for *AGPsS-9a*. After ethidium bromide staining of the gels, images were captured using the Bio-Rad UV Transilluminator machine. Single bands were scored based on their absence (0) or presence (1).

Statistical analysis

A total of 186 individuals (182+three parents+one non-parental external control) in the NOHU population were analyzed using the SAS Software. Single marker-trait associations were tested using t-test, and multiple marker combination (based on presence or absence in two-, three-, and four-marker relations) associations with phenotypic traits were statistically analyzed by ANOVA. Statistical significance was set at P≤0.05.

Results and Discussion

Assessment of processing traits of potato tuber in breeding population

A total of 186 individuals along with parents and non-parental external controls in the NOHU were investigated for processing traits such as SG, SC, DMC, FLV, CLV, and RSC. The L-score values determining the brightness of the fried samples were measured using a colorimeter. A brighter chip/French fry color was
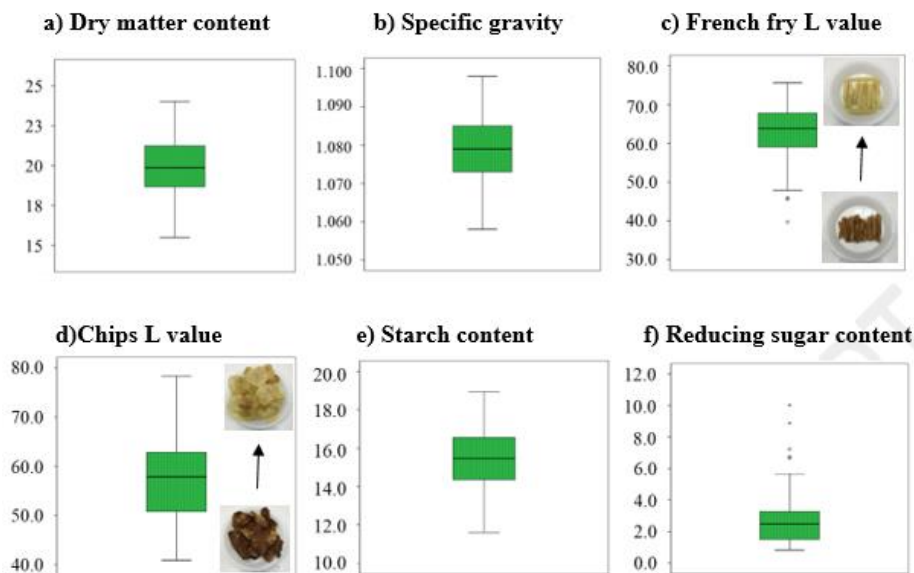
Figure 1. Whisker-box plots of a) dry matter content (%), b) specific gravity, c) French fry L value, d) chips L value, e) starch content (%), f) reducing sugar content (g/100 g DW) (circle and asterisk are indication of outlier values).

previously shown to be closely associated with better processing quality (Sobol et al., 2020). The whisker box plots for processing traits are shown in Figure 1. The phenotypic data showed that the mean values were uniformly distributed for all traits, and the lowest/highest values for each trait are depicted in plots. Browning in French fry was less common in comparison to chips, which was associated with better processing quality in French fry. The accumulation of this brown pigmentation in processed potatoes is not desirable, as it causes a bitter taste, as reported earlier by Roe et al. (1990). Therefore, the processing quality is inversely proportional to browning (Rodriguez-Saona and Wrolstad, 1997). In addition to its taste, color is also an important parameter that determines the final consumer preference for consumption, and a dark brown color is undesirable for consumers (Mestdagh et al., 2008). Overall, the population in this study provided a reliable and suitable system/structure in order to validate the selected molecular markers for processing traits.

Pearson correlation analysis showed that RSC was negatively correlated with all tuber quality traits in our population; however, there was a positive correlation for the rest (P≤0.05) (Table 1). As the FLV and CLV levels increased, the processing quality improved. However, an increase in RSC had the opposite effect, as it reduced the accumulation of sugars following the breakdown of

starch, thereby negatively affecting tuber quality traits. The findings of our study regarding tuber quality traits were consistent for the processing population.

Reducing sugars (glucose and fructose) and several amino acids (asparagine and glutamine) form a carcinogenic compound, acrylamide, which causes browning/darkening via a reaction called Maillard in potatoes and other processed foods (Mestdagh et al., 2008). It is important to ensure that the reducing sugar level in potatoes is below 1 g/kg of average fresh weight, as higher levels of reducing sugar can negatively impact the quality characteristics of potatoes (Rodriguez-Saona and Wrolstad, 1997; Mestdagh et al., 2008).

Genotyping the NOHU population for processing traits

We screened the NOHU population with four diagnostic markers, *Stp23-8b, StpL-3e, AGPsS-9a*, and *Pain1-8c*, for French fry/chip quality traits, dry matter content, specific gravity, starch, and reducing sugar content. *Stp23-8b* was developed from one of the *PHO1* alleles, *PHO1$_a$-H$_a$* and *StpL-3e* was derived from the *plastidic starch phosphorylase* gene (Li et al., 2008). Both *Stp23-8b* and *StpL-3e* were strongly correlated with tuber quality traits. The *AGPsS-9a* marker was developed using the *ADP-glucose pyrophosphorylase* (or *glucose-1-phosphate adenyltransferase*) enzyme (Ballicora et al., 2004; Li et al., 2013). The *Pain1-8c* marker was developed using the *vacuolar acid invertase*

Table 1. Pearson correlation analysis of the NOHU population

Correlation	DMC	SG	FLV	CLV	SC	RSC
DMC	1	0.993*	0.376*	0.206*	0.993*	-0.485*
SG	0.993*	1	0.367*	0.201*	1.000*	-0.468*
FLV	0.376*	0.367*	1	0.433*	0.367*	-0.564*
CLV	0.206*	0.201*	0.433*	1	0.201*	-0.415*
SC	0.993*	1.000*	0.367*	0.201*	1	-0.468*
RSC	-0.485*	-0.468*	-0.564*	-0.415*	-0.468*	1

gene (Li et al., 2013). These molecular markers produced a single scorable marker size of 348 bp for *Stp23-8b*, 360 bp for *StpL-3e*, 210 bp for *AGPsS-9a*, and 703 bp for *Pain1-8c*, as suggested (Li et al., 2013); the same pattern was also observed in our study, as the gel results are shown in Figure 2. A score table for the NOHU population is provided in Supplementary Table 1.
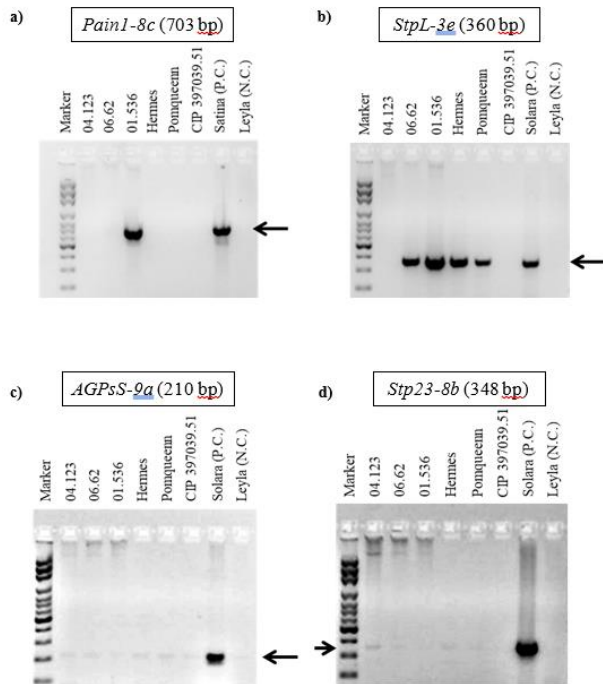
Figure 2. Screening of parental genotypes and positive/negative controls with a) *Pain1-8c*, b) *StpL-3e*, c) *AGPsS-9a* and d) *Stp23-8b*. P.C. : Positive control, N.C.: Negative control.

The study conducted by Li et al. (2013) found that the frequency of positive markers in the BNC population (including 76 genotypes) was 46.0% for *Stp23-8b*, 61.8% for *StpL-3e*, and 36.8% for *Pain1-8c*. The frequency rates in our study were 68.8, 88.2, and 5.9% for the three molecular markers, respectively. Despite consistent positive marker frequency in the SKC population, as

observed in a previous study by Li et al. (2013), the positive band rate was found to be higher for *StpL-3e* and lower for *Pain1-8c* in our study. The "1" frequency of *AGPsS-9a* in Li and colleagues study were 23.6 - 34.9% (BNC and SKC populations) (Li et al., 2013) as the frequency of 1 (present) was almost three times more in our study. The frequency rate is not a definite and constant parameter, which we can infer in a population, as it may be greatly affected by population size and structure; however, it provides a general banding pattern for each molecular marker, that is, *Pain1-8c* had 5.9% in the present study, unlike in previous reports. The BNC population contained individuals from different parental lines, whereas SKC was generated from the progeny of a single parental line, Diana x Candella. The frequency of *Pain1-8c* (1) changed in these two populations as well as in different years (42% in 2009 and 62% in 2010) in the SKC (Li et al., 2013). It is obvious that the marker frequency, especially *Pain1-8c*, can vary in populations with different genetic backgrounds, which might explain the reason to have low frequency of *Pain1-8c* (1) in our study. As these markers are allele specific, they are valuable for providing information about the frequency of alleles in a population. Given that our study population is a segregating population, this information will be useful for other researchers who may wish to employ these markers in future.

Marker associations with tuber quality traits

In the current study, it was observed that the presence (1) of *AGPsS-9a* and *StpL-3e*, unlike to *Pain1-8c* (0), was closely correlated with increased RSC (Table 2). RSC mean value was ranged between 2.76 - 2.82 in the presence of these single markers. The association of RSC with *AGPsS-9a*, *StpL-3e*, and two other allele-specific markers has not been tested by Li et al. (2013). However, a subsequent study by Schreiber et al. (2014) found that 12 different alleles were associated with RSC (reasoning from cold-induced sweetening). They generated a new population named SUGAR40, indicating that the absence of all four validation markers in the SUGAR40 population was significantly associated

Table 2. Correlation of single markers with several tuber quality traits

Marker	Trait	0/1	Number of Genotype[a]	Mean[b]
AGPsS-9a	French fry L value	0	19	*67.36↓
	Chips L value	0	19	*63.89↑
	Reducing sugar content	1	163	*2.76↑
Stp23-8b	Chips L value	0	54	*59.66↑
StpL-3e	Reducing sugar content	1	134	*2.82↑
Pain1-8c	Dry matter content	0	171	*19.84↓
	Specific gravity	0	171	*1.078↓
	Starch content	0	171	*15.31↓
	Reducing sugar content	0	171	*2.74↑
	French fry L value	1	11	*67.80↑
	Chips L value	1	11	*66.37↑

[a]Number of genotypes showing either 0/1 banding pattern

[b] Statistical significance by t-test, *$P \leq 0.05$

with higher RSC. The finding of our work, as it mainly showed an increase in RSC in the presence of *AGPsS-9a* and *StpL-3e* contradicted previous reports, while the absence of *Pain1-8c* reinforced the earlier findings (Table 2).

Negative (0) banding patterns in *AGPsS-9a* and *Stp23-8b* for CLV and *AGPsS-9*a alone for FLV had significant effects on these traits in different ways. There was an increase in CLV (mean value for the individual markers: 59.66 - 63.89) thereof associated with better chips quality, whereas the direction of effect was negative for FLV (67.36). Although FLV was negatively associated with the absence of *AGPsS-9a*, the mean FLV still persisted high score for processing purpose. The FLV and CLV mean values increased in the presence of Pain1-8c. Previous studies on the CHIPS-ALL population showed that *AGPsS-9a* (1) had a significant positive effect on chip quality; however, the effect was the opposite in the BNC breeding population. In the same study, the presence of three other markers improved the overall chip quality (Li et al., 2013). The absence of *Pain1-8c* was associated with lower DMC, SG, and SC in this study (Table 2). *AGPsS-9a* (-) in CHIPS-ALL and *AGPsS-9a* (+) in BNC breeding population overall improved the tuber starch content yet the marker did not produce a reproducible system for the selection and moreover, *AGPsS-9a* showed a minor effect in SKC population for SC in previous work (Li et al., 2013). Furthermore, the presence of the other three markers led to an increase in mean SC, and the findings were consistent among different populations, unlike the association of *StpL-3e* with SC in two consecutive years (positive in 2009 and negative in 2010) (Li et al., 2013). The question raised after screening different populations with these candidate molecular markers for processing traits concerned the reproducibility and applicability of these markers in other populations. This is expected because tuber quality traits are multigenic. Low reproducibility restricts the use of single markers that are selective for several tuber quality characteristics. As is known from other studies, marker combinations are considered to be more decisive for marker-assisted selection (Li et al., 2013).

This study screened the NOHU population using different marker combinations for all processing traits, and we investigated the outcomes showing significant associations (Table 3). The absence of *AGPsS-9a* and *Stp23-8b* markers had a significant effect on SC; however, the direction of the effect could not be tested

in our study, and the same response was obtained in *Stp23-8b* (0)/*StpL-3e* (0) for DMC, SG, and SC (Table 3). The available knowledge is very limited, and this makes it difficult to comment further on the findings; in a previous study, the presence of *Stp23-8b* and its combination with any of the markers presence improved SC (Li et al., 2013). In the NOHU population, the mean CLV value was higher score when the population was genotyped at 0/0 for *Stp23-8b* and *StpL-3e*. This is the only marker combination which exploited a potential for being a molecular marker for screening in our study. The association of previously defined marker combinations with different traits, *AGPsS-9a* (+)/ *Stp23-8b* (+) or *AGPsS-9a* (+)/ *Pain1-8c* (-/+) or *Pain1-8c* (+)/ *StpL-3e* (-) with chips quality; *AGPsS-9a* (+)/ *Stp23-8b*(+)/ *Pain1-8c* (-) with high level of starch content was not observed in the NOHU population (Li et al., 2013). The use of marker combinations rather than single markers in MAS studies is more reliable for screening processing traits in a population. Marker combinations are shown to have higher reproducibility compared to single markers. As Li et al. (2013) suggested, the optimal marker and its combination, unfortunately, might vary with the population and enviroment (Li et al., 2013). The screening for tuber quality traits may show inconsistent responses for individuals at the initial phases of a breeding process, as in the NOHU (our study) and in SKC population (Li et al., 2013). The findings of previous studies in different populations, therefore, require elaborate research on marker-trait associations.

Conclusion

This study aimed to screen the association between these four markers and tuber quality traits. The results showed that these markers and their combinations still have restrictions on the selection of processing populations in potato breeding programs. A similar situation was observed in the study by Li et al. (2013), and marker-trait associations were found not to be reproducible among different populations; therefore, these markers should be further screened in different and larger populations.

Acknowledgements

Table 3. Correlation of marker combinations with several tuber quality traits

Marker combination	Trait	Number of Genotype[a]	Mean[b]
AGPsS-9a (0)/Stp23-8b (0)	Starch content	13	*16.00
Stp23-8b (0)/StpL-3e (0)	Dry matter content	18	*20.41
	Specific gravity	18	*1.081
	Chips L value	13	*64.30↑
	Starch content	18	*15.82

[a]Number of genotypes showing either 0/1 banding pattern
[b]Statistical significance by ANOVA, *$P \leq 0.05$

Christina Gebhardt for providing positive/negative controls from their studies. We greatly appreciate Prof. Dr. Sevgi Caliskan for her valuable contributions and we also thank Dr. Ayten Kubra Yagiz, Cehibe Tarim and İlknur Tindas for their help during the work.

Author Contribution

CY: Investigation, Data Curation, Writing, and Editing; UD, MEÇ: Supervision, Conceptualization, Data Curation, Writing, and Editing

Conflict of Interest

The authors declare that they have no conflict of interest.

References

Anonymous. (2017). The European Cultivated Potato Database. https://www.europotato.org/. Accessed 4 May 2023.

Ballicora, M. A., Iglesias, A. A., & Preiss, J. (2004). ADP-glucose pyrophosphorylase: a regulatory enzyme for plant starch synthesis. *Photosynthesis Research*, 79(1), 1-24. https://doi.org/10.1023/B:PRES.0000011916.67519.58.

Bradshaw, J. E., Hackett, C. A., Pande, B., Waugh, R., & Bryan, G. J. (2008). QTL mapping of yield, agronomic and quality traits in tetraploid potato (*Solanum tuberosum* subsp. *tuberosum*). *Theoretical and Applied Genetics*, 116(2), 193-211. https://doi.org/10.1007/s00122-007-0659-1.

Cottrell, J. E., Duffus, C. M., Paterson, L., Mackay, G. R., Allison, M. J., & Bain, H. (1993). The effect of storage temperature on reducing sugar concentration and the activities of three amylolytic enzymes in tubers of the cultivated potato, *Solanum tuberosum* L. *Potato Research*, 36(2), 107-117. https://doi.org/10.1007/BF02358725.

D'hoop, B. B., Keizer, P. L., Paulo, M. J., Visser, R. G., van Eeuwijk, F. A., & van Eck, H. J. (2014). Identification of agronomically important QTL in tetraploid potato cultivars using a marker–trait association analysis. *Theoretical and Applied Genetics*, 127, 731-748. https://doi.org/10.1007/s00122-013-2254-y.

Freyre, R., & Douches, D. S. (1994). Development of a model for marker-assisted selection of specific gravity in diploid potato across environments. *Crop Science*, 34(5), 1361-1368. https://doi.org/10.2135/cropsci1994.0011183X003400050040x.

Friedman, M., & Levin, C. E. (2009). Analysis and biological activities of potato glycoalkaloids, calystegine alkaloids, phenolic compounds, and anthocyanins. In Advances in potato chemistry and technology, Academic Press.

Haase, N. U. (2003). Estimation of dry matter and starch concentration in potatoes by determination of under-water weight and near infrared spectroscopy. *Potato Research*, 46(3), 117-127. https://doi.org/10.1007/BF02736081.

Li, L., Paulo, M. J., Strahwald, J., Lübeck, J., Hofferbert, H. R., Tacke, E., Junghans, H., Wunder, J., Draffehn, A., van Eeuwijk, F., & Gebhardt C. (2008). Natural DNA variation at candidate loci is associated with potato chip color, tuber starch content, yield and starch yield. *Theoretical and Applied Genetics*, 116(8), 1167-1181. https://doi.org/10.1007/s00122-008-0746-y.

Li, L., Tacke, E., Hofferbert, H. R., Lübeck, J., Strahwald, J., Draffehn, A. M., Walkemeier, B., & Gebhardt C. (2013). Validation of candidate gene markers for marker-assisted selection of potato cultivars with improved tuber quality. *Theoretical and Applied Genetics*, 126(4), 1039-1052. https://doi.org/10.1007%2Fs00122-012-2035-z.

Lisińska, G., Pęksa, A., Kita, A., Rytel, E., & Tajner-Czopek, A. (2009). The quality of potato for processing and consumption. *Food*, 3(2), 99-104.

Manrique-Carpintero, N. C., Coombs, J. J., Cui, Y., Veilleux, R. E., Buell, C. R., & Douches, D. (2015). Genetic map and QTL analysis of agronomic traits in a diploid potato population using single nucleotide polymorphism markers. *Crop Science*, 55(6), 2566-2579. https://doi.org/10.2135/cropsci2014.10.0745.

Mestdagh, F., De Wilde, T., Castelein, P., Németh, O., Van Peteghem, C., & De Meulenaer, B. (2008). Impact of the reducing sugars on the relationship between acrylamide and Maillard browning in French fries. *European Food Research and Technology*, 227, 69-76. https://doi.org/10.1007/s00217-007-0694-9.

Milczarek, D., Przetakiewicz, A., Kamiński, P., & Flis, B. (2014). Early selection of potato clones with the *H1 resistance gene*-the relation of nematode resistance to quality characteristics. *Czech Journal of Genetics and Plant Breeding*, 50(4), 278-284. https://doi.org/10.17221/114/2014-CJGPB.

Rodriguez-Saona, L. E., & Wrolstad, R. E. (1997). Influence of potato composition on chip color quality. *American Potato Journal*, 74, 87-106. https://doi.org/10.1007/BF02851555.

Roe, M. A., Faulks, R. M., & Belsten, J. L. (1990). Role of reducing sugars and amino acids in fry colour of chips from potatoes grown under different nitrogen regimes. *Journal of the Science of Food and Agriculture*, 52(2), 207-214. https://doi.org/10.1002/jsfa.2740520207.

Schönhals, E. M., Ding, J., Ritter, E., Paulo, M. J., Cara, N., Tacke, E., Reinhard Hofferbert, H., Lübeck, J., Strahwald, J., & Gebhardt, C. (2017). Physical mapping of QTL for tuber yield, starch content and

starch yield in tetraploid potato (*Solanum tuberosum* L.) by means of genome wide genotyping by sequencing and the 8.3 K SolCAP SNP array. *BMC Genomics*, *18*(1), 1-20. https://doi.org/10.1186/s12864-017-3979-9.

Schönhals, E. M., Ortega, F., Barandalla, L., Aragones, A., Ruiz de Galarreta, J. I., Liao, J. C., Sanetomo, R., Walkemeier, B., Tacke, E., Ritter, E., & Gebhardt, C. (2016). Identification and reproducibility of diagnostic DNA markers for tuber starch and yield optimization in a novel association mapping population of potato (*Solanum tuberosum* L.). *Theorotical and Applied Genetics*, *129*, 767-785. https://doi.org/10.1007/s00122-016-2665-7.

Schreiber, L., Nader-Nieto, A. C., Schönhals, E. M., Walkemeier, B., & Gebhardt, C. (2014). SNPs in genes functional in starch-sugar interconversion associate with natural variation of tuber starch and sugar content of potato (*Solanum tuberosum* L.). *G3-Genes Genomes and Genetics*, *4*(10), 1797-1811.
https://doi.org/10.1534/g3.114.012377.

Sharma, S. K., MacKenzie, K., McLean, K., Dale, F., Daniels, S., & Bryan, G. J. (2018). Linkage disequilibrium and evaluation of genome-wide association mapping models in tetraploid potato. *G3-Genes Genomes and Genetics*, *8*(10), 3185-3202.
https://doi.org/ 10.1534/g3.118.200377.

Sobol, Z., Jakubowski, T., & Nawara, P. (2020). The effect of UV-C stimulation of potato tubers and soaking of potato strips in water on color and analyzed color by CIE L* a* b. *Sustainability*, *12*(8), 3487. https://doi.org/10.3390/su12083487.

Sołtys-Kalina, D., Szajko, K., Wasilewicz-Flis, I., Mańkowski, D., Marczewski, W., & Śliwka, J. (2020). Quantitative trait loci for starch-corrected chip color after harvest, cold storage and after reconditioning mapped in diploid potato. *Molecular Genetics and Genomics*, *295*(1), 209-219.
 https://doi.org/10.1007/s00438-019-01616-1.

Sverrisdóttir, E., Byrne, S., Sundmark, E. H. R., Johnsen, H. Ø., Kirk, H. G., Asp, T., Janss, L., & Nielsen, K. L. (2017). Genomic prediction of starch content and chipping quality in tetraploid potato using genotyping-by-sequencing. *Theoretical and Applied Genetics*, *130*(10), 2091-2108. https://doi.org/10.1007/s00122-017-2944-y.

Urbany, C., Stich, B., Schmidt, L., Simon, L., Berding, H., Junghans, H., Niehoff, K. H., Braun, A., Tacke, E., Hofferbert, H. R., Lübeck, J., Strahwald, J., & Gebhardt, C. (2011). Association genetics in *Solanum tuberosum* provides new insights into potato tuber bruising and enzymatic tissue discoloration. *BMC Genetics*, *12*(1), 1-14. https://doi.org/10.1186/1471-2164-12-7.

Yavuz, C. (2016). Patateste sanayilik çeşit ıslahında markör yardımlı seleksiyonun uygulama olanakları. Master Dissertation. Niğde: Niğde Omer Halisdemir University.

BIOTECH STUDIES

RESEARCH PAPER

Aspergillus oryzae as a host for SARS-CoV-2 RBD and NTD expression

Elif Karaman[1] [iD]**, Serdar Uysal[1],*** [iD]

[1] Beykoz Institute of Life Sciences and Biotechnology, Bezmialem Vakif University, Istanbul 34820, Turkiye

Abstract

The COVID-19 pandemic has increased demand for effective diagnostics, and extensive research has been conducted on the N-terminal domain (NTD) and the receptor-binding domain (RBD) of the SARS-CoV-2 spike glycoprotein, which are critical for viral binding. This study focuses on the expression of NTD and RBD in *pyrG* auxotrophic *Aspergillus oryzae* for the first time. Recombinant NTD and RBD were expressed as glucoamylase-fusion proteins and purified using metal affinity chromatography. Size-exclusion chromatography was used to confirm the correct folding and purity of the recombinant proteins. Employing an enzyme-linked immunosorbent assay, the binding ability of the fusion proteins to human anti-IgG antibodies in serum samples was evaluated. The results indicated a significant and concentration-dependent interaction, affirming the functionality of the NTD and RBD fusion proteins and establishing their efficacy in antigen-antibody interactions. This study not only elucidates the usage potential of the fusion proteins in immunoassays but also addresses the suitability of the *A. oryzae* expression system as a biotechnological platform to produce SARS-CoV-2 proteins. Furthermore, this study lays the foundation for scalable and cost-effective mass production of effective NTD and RBD proteins in *A. oryzae*, opening up a new era of COVID-19 research, vaccine development, and immunoassay design.

Introduction

Coronavirus disease 2019 (COVID-19) poses a serious threat to human health as a pandemic disease. One of the most significant characteristics of COVID-19 is its ability to spread quickly from the beginning to produce a variety of variant forms that have impacted millions of people worldwide (Hassanin et al., 2021; Tay et al., 2020). As a result, rapid solution recommendations are becoming increasingly important in the diagnosis and treatment of pandemic diseases.

SARS-CoV-2, the COVID-19 virus, penetrates host cells via epithelial cells and interacts with the angiotensin-converting enzyme-2 (ACE2) receptor of the host respiratory system (Lan et al., 2020; Walls et al., 2020). The virus has high pathogenicity with its single-stranded, enclosed, positive-sense RNA genome size of 30 kb. It encodes four structural proteins: spike glycoprotein (S), envelope glycoprotein, membrane glycoprotein, and nucleocapsid, which are responsible for infection initiation, assembly, release, and packing, respectively (Hassanin et al., 2021; Zhu et al., 2020). S protein consists of two subunits: S1 and S2. The N-terminal region (NTD) (aa 14–305) of the S1 subunit is followed by a receptor binding domain (RBD) (aa 319–591) (Balasubramaniyam et al., 2022; Cao et al., 2021; Huang et al., 2020; Wrapp et al., 2020).
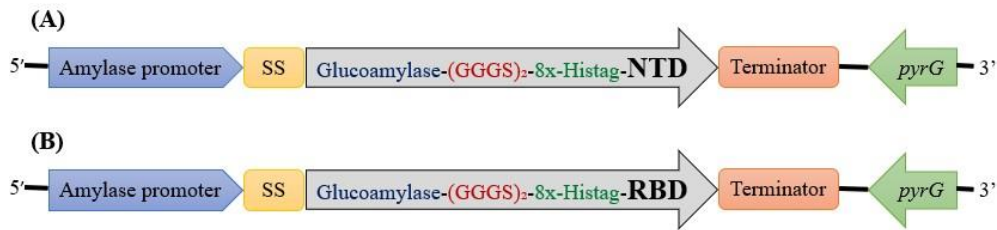
Figure 1. Representation of the linear expression vectors containing the amylase promoter, signal sequence (SS), gene-encoding fusion proteins, terminator, and *pyrG* gene for the transformation of *pyrG* auxotrophic *A. oryzae*. For Gla-NTD, the glucoamylase fusion protein is depicted as glucoamylase, linker (GGGS)$_2$, 8x-Histag, and gene-encoding NTD (A). For Gla-RBD, the glucoamylase fusion protein is depicted as glucoamylase, linker (GGGS)$_2$, 8x-Histag, and the gene-encoding RBD (B).

An easy-to-use, affordable, and straightforward immunoassay, useful diagnostic kits, and therapies, including vaccine development, are required in order to promptly combat COVID-19 cases. It has attempted the expression of SARS-CoV-2 proteins and their fragments in several expression systems for these purposes and has studied the efficacy of the expressed proteins as target antigens for COVID-19 detection in immunoassays (Conzentino et al., 2022; Márquez-Ipiña et al., 2021; Tozetto-Mendoza et al., 2021). Because the RBD of the S protein interacts directly with ACE2, it is the most crucial component to consider as a target (Cao et al., 2021; Shang et al., 2020; Zhu et al., 2020).

Aspergillus oryzae (*A. oryzae*) is a filamentous fungus used in fermentation technologies and has been given the GRAS (Generally Recognized as Safe) classification by the FDA. It is a safe microorganism for producing primary and secondary metabolites and industrial enzymes due to its high secretory capability (He et al., 2019). It is also a useful expression system due to its low-cost media, ability to produce complex proteins, and tolerance to various environmental conditions (Ntana et al., 2020).

In this study, the NTD and RBD of S protein were produced for the first time in *A. oryzae*, and their binding ability to detect anti-IgG antibodies in human serum was investigated utilizing a low-cost indirect enzyme-linked immunosorbent test (ELISA) as a straightforward immunoassay.

Materials and Methods

Materials

Chemicals and reagents used in this study were purchased from Sigma (MO, USA) and Biofroxx (Germany). The Gangnam-Stain Protein Ladder (24052) was purchased from Intron Biotechnology (South Korea). The plasmid midiprep kit (12143, Qiagen) was purchased from Qiagen (12143, Valencia, CA). 96-well ELISA plates were purchased from NEST (514201, Wuxi NEST Biotechnology Co., Ltd., China). The nickel resin (88221, HisPurTM Ni-NTA Resin), TMB ELISA Substrate (#34021), and 10K molecular weight cut-off (MWCO) of SnakeSkinTM Dialysis Tubing (68035) were purchased from Thermo Fisher Scientific (MA, USA). Amicon® Ultra-15 centrifugal filters (10K MWCO) were purchased from Merck Millipore (MA, USA). The Superdex 75 Increase

10/300 GL column was purchased from GE Healthcare (IL, USA). Restriction enzymes were purchased from New England Biolabs (MA, USA). The yatalase enzyme was purchased from Takara Bio Inc. (Japan).

Escherichia coli (E. coli) TOP10 (C404010) was purchased from Thermo Fisher Scientific (MA, USA). The *pyrG* auxotrophic *A. oryzae* strain was obtained in our previous study (Karaman et al., 2023) by using *A. oryzae* RIB40 (42149), which was purchased from the American Type Culture Collection (VA, USA).

Construction of expression vectors

In this study, the NTD and RBD regions of SARS-CoV-2 were selected for expression in the *pyrG* auxotrophic *A. oryzae*. The amino acid sequences of NTD (aa 14–305) and RBD (319–591 aa) were obtained from the NCBI database (accession number UBE87647.1). The DNA sequences encoding NTD and RBD were codon-optimized, and their constructs were separately prepared as fusions into the glucoamylase gene. For purification, a linker site consisting of two consecutive GGGS amino acid sequences and an 8x-Histag was inserted between the glucoamylase and the protein of interest. The nucleotide sequences were synthesized at GenScript Biotech PTE. LTD. (NJ, USA) and inserted into the separate expression vectors under the control of the amylase promoter (Figure 1).

Transformation of expression vectors into *pyrG* auxotrophic *A. oryzae*

The expression vectors were amplified by transforming into chemically component *E. coli.* 1% tryptone, 0.5% yeast extract, and 1% NaCl supplemented with 100 µg/mL ampicillin were used as growth medium for the bacteria. The amplified expression vectors were isolated with the plasmid midiprep kit and linearized for *A. oryzae* transformation by using *HindIII* and *EcoRI* restriction enzymes.

The transformation was carried out according to Sakai et al. (2012). Briefly, the *pyrG* auxotrophic *A. oryzae* was grown in a medium containing 2% dextrin, 1% polypeptone, 0.5% yeast extract, 0.5% KH$_2$PO$_4$, 0.05% MgSO$_4$.7H$_2$O (pH 5.5), 20 mM uridine, and 0.2% uracil at 30 °C and 180 rpm. After overnight incubation, mycelia were incubated in a lysis solution containing 50 mM malate buffer, 0.6 M (NH$_4$)$_2$SO$_4$, and 1% yatalase (pH 5.5) at 30 °C and 80 rpm for 4 h. The obtained

spheroplasts were washed with a solution containing 1.2 M sorbitol and 50 mM $CaCl_2$. Following that, spheroplasts and the linearized expression vectors belonging to glucoamylase fusion NTD (Gla-NTD) and glucoamylase fusion RBD (Gla-RBD) were combined in the presence of Polyethylene glycol 4000 and spread on minimal media consisting of 0.2% $NaNO_3$, 0.1% K_2HPO_4, 0.05% $MgSO_4.7H_2O$, 0.05% KCl, 0.001% $FeSO_4.7H_2O$, 3% sucrose, 5% NaCl, and %2 agar (pH 5.5). For the control group, no DNA was added to spheroplasts. Incubation was carried out at 30 °C and 180 rpm for 5-7 days.

Expression of recombinant Gla-NTD and Gla-RBD proteins

Transformant *A. oryzae* colonies were inoculated into 15 mL of growth medium containing 2% dextrin, 1% polypeptone, 0.5% yeast extract, 0.5% KH_2PO_4, and 0.05% $MgSO_4.7H_2O$ (pH 5.5) and incubated overnight at 30 °C and 180 rpm. Following that, culture suspensions were diluted in 75 mL of growth medium containing 4% dextrin, 1% polypeptone, 0.5% yeast extract, 0.5% KH_2PO_4, and 0.05% $MgSO_4.7H_2O$ (pH 5.5) at a ratio of 1:10. Incubation was performed at 30 °C and 180 rpm for 7 days. Supernatant samples taken from cultures were analyzed by sodium dodecyl sulfate - polyacrylamide gel electrophoresis (SDS-PAGE) with 12% gels.

Purification of recombinant Gla-NTD and Gla-RBD proteins

Expression cultures were filtered through Whatman filter paper to obtain a medium containing the recombinant Gla-NTD and Gla-RBD proteins secreted by *A. oryzae*. Following collection of the culture medium, recombinant 8x-Histagged Gla-NTD and Gla-RBD proteins were purified by metal affinity chromatography under native conditions. In this method, the harvested medium was loaded into a nickel-nitrilotriacetic acid (Ni-NTA) affinity column containing HisPur™ Ni-NTA resin, and then the column was washed with 50 mM NaH_2PO_4 and 500 mM NaCl (pH 7.4). Elution was performed with elution buffer containing 50 mM NaH_2PO_4, 300 mM NaCl, and 200 mM imidazole (pH 7.4). The eluted fractions were dialyzed against phosphate-buffered saline (PBS) buffer containing 137 mM NaCl, 2.7 mM KCl, 10 mM Na_2HPO_4, and 1.8 mM KH_2PO_4 (pH 7.4) for the removal of imidazole. After being dialyzed, samples were concentrated using an Amicon® Ultra-15 centrifugal concentration filter. Samples were analyzed on SDS-PAGE.

The ImageJ 1.53t tool (National Institutes of Health, USA, Version 1.53t) was used to perform densitometric analysis of total protein. A Bradford assay was performed to determine the concentration of Gla-NTD and Gla-RBD proteins at 595 nm using bovine serum albumin as a protein standard.

Size exclusion chromatographic analysis of recombinant Gla-NTD and Gla-RBD proteins

The concentrated recombinant Gla-NTD and Gla-RBD proteins were applied to a Superdex 75 Increase 10/300 GL size exclusion chromatography column coupled to an HPLC system (AKTA Pure Chromatography System) to check the purity (Cytiva, USA). PBS buffer was prepared according to the manufacturer's instructions and used as equilibration, wash, and elution buffers. The elution was performed at a linear flow rate of 0.5 mL/min.

In vitro functionality assay by indirect ELISA

Indirect ELISA was used to evaluate the binding ability of recombinant Gla-NTD and Gla-RBD proteins to anti-IgG antibodies in human serum samples obtained from COVID-19 patients. Flat-bottomed 96-well ELISA plates were coated with Gla-NTD and Gla-RBD, separately. Final concentrations of recombinant proteins were adjusted to 10 µg/mL in a coating buffer containing 50 mM carbonate (pH 9.6). Blank wells were coated with only coating buffer. Non-fusion glucoamylase expressed in *A. oryzae* and an irrelevant recombinant protein expressed in *A. oryzae* were coated on wells as negative controls. For positive control, recombinant RBD protein expressed in *Pichia pastoris* (*P. pastoris*) was coated in positive wells. Plates were incubated overnight at 4 °C. After incubation, plates were washed with 200 µL of PBS-T (PBS buffer supplemented with 0.05% Tween-20). The plates were blocked with 200 µL of PBS-T containing 5% skim milk for 2 h at room temperature. Following that, 100 µL of human serum samples were diluted in PBS-T containing 5% skim milk in a 1:500 ratio and applied to the plates.

After being incubated at 37 °C for 1 h, the plates were washed with 200 µL of PBS-T three times. HRP-conjugated anti-human IgG antibody was diluted by 1:10.000 in PBS-T containing 5% skim milk and added to the wells. After 1 h of incubation at 37 °C, the plates were washed with 200 µL of PBS-T three times. For detection, 100 µL of TMB ELISA substrate was added and incubated at room temperature for 30 min in the dark. The reaction was terminated with 500 µL of 1 M H_2SO_4. Absorption was read at 450 nm using a Biotek microplate reader. Furthermore, different concentrations (20, 10, and 2.5 ng/L) of expressed Gla-NTD and Gla-RBD proteins were evaluated in an ELISA against human serum samples to investigate their binding capacity. All the acquired data for these recombinant Gla-NTD and Gla-RBD proteins was statistically examined using the Kruskal-Wallis H test.

Results and Discussion

Expression of Gla-NTD and Gla-RBD in *A. oryzae*

The *pyrG* gene locus was introduced into the *pyrG* auxotrophic *A. oryzae* genome by gene replacement using expression vectors containing Gla-NTD and Gla-RBD. Following transformation, multiple transformed colonies were selected from transformant plates and subjected to an expression test in a small flask volume.
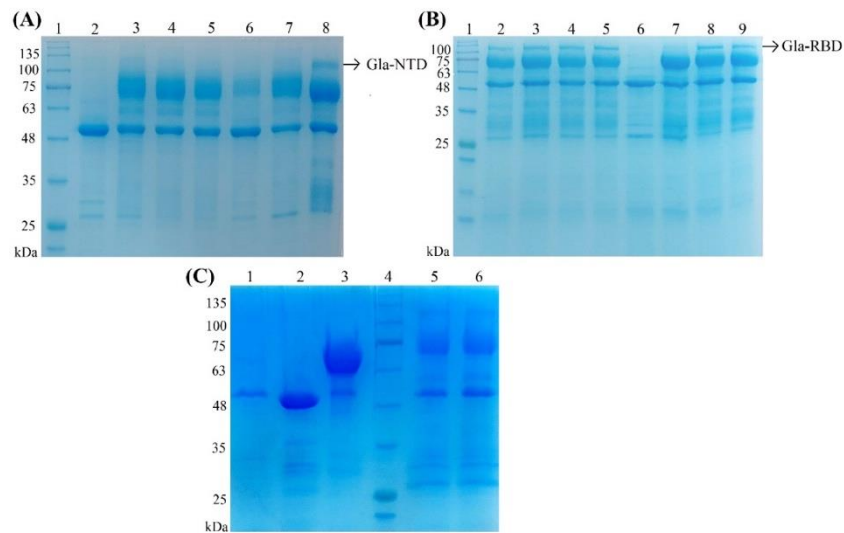
Figure 2. Sodium dodecyl sulfate - polyacrylamide gel electrophoresis (SDS-PAGE) analysis of expressed Gla-NTD and Gla-RBD proteins in *A. oryzae*. **(A)** Protein expression test of multiple transformed colonies on a small scale for Gla-NTD. Lane 1: Gangnam-Stain Protein Ladder. Lane 2–7: The colonies not expressing recombinant protein. Lane 8: The colony expressing Gla-NTD. **(B)** Protein expression test of multiple transformed colonies on a small scale for Gla-RBD. Lane 1: Gangnam-Stain Protein Ladder. Lanes 2–5, 8, and 9: colonies expressing Gla-RBD. Lanes 6 and 7: the colonies not expressing recombinant protein. **(C)** The comparison of the mock control and the colonies expressing glucoamylase, amylase, and fusion proteins. Lanes are as follows: mock transfection control (Lane 1), colony-expressing amylase (Lane 2), colony-expressing glucoamylase (Lane 3), colony-expressing Gla-RBD protein (Lane 5), and colony-expressing Gla-NTD protein (Lane 6). Gangnam-Stain Protein Ladder is located in Lane 4.

SDS-PAGE analysis of the culture samples after 7 days of incubation revealed that the expression of Gla-NTD fusion and Gla-RBD proteins was successfully maintained in *A. oryzae* (Figure 2). The recombinant colony expressing the Gla-NTD protein is shown in Figure 2A, and the recombinant colonies expressing the Gla-RBD protein are shown in Figure 2B. The recombinant Gla-NTD and Gla-RBD proteins were shown as bands measuring approximately 110 kDa in the SDS-PAGE investigation. Figure 2C compares differences in colonies expressing fusion proteins to the mock transfection control, the colonies expressing amylase and glucoamylase. Consequently, *A. oryzae* was able to express and secrete the recombinant Gla-NTD and Gla-RBD fusion proteins into the culture medium, as illustrated in Figure 2.

Bacterial expression systems in heterologous protein production offer advantages like simplicity, affordability, quick generation times, and scalability (He et al., 2021). Tantiwiwat et al. (2023) evaluated the potential of the *E. coli* expression system for RBD production to be used in neutralizing antibody detection kits, showing comparable results to the glycosylated RBD expressed in mammalian cells. Although the *E. coli* expression system is preferred for its advantages in recombinant SARS-CoV-2 protein production (Conzentino et al., 2021, 2022; Gao et al., 2022), the lack of post-translational modification makes it challenging, particularly for native RBDs, which are glycosylated proteins with eight cysteines that cause improper folding during production (Balasubramaniyam et al., 2022; He et al., 2021; Li et al., 2003; Tripathi et al., 2016).

In order to prevent the formation of inclusion bodies in *E. coli*, various strategies were used, including enzyme-assisted expression to produce RBD with comparable binding capacity to mammalian-produced RBD (Kim et al., 2022) and fusion protein in tandem with a carrier peptide (Brindha et al., 2022; McGuire et al., 2022). Fitzgerald et al. (2021) addressed the solubilization challenges of *E. coli*-expressed spike protein fragments, including RBD, through denaturation and refolding. Prahlad et al. (2021) employed a cytoplasmic disulfide bond formation system to overcome inclusion bodies and to avoid denaturing and refolding steps because of the reductive environment of the *E. coli* cytoplasm. However, mammalian-expressed RBD generally exhibits stronger immunogenicity and binding affinity than *E. coli*-expressed RBD (Maffei et al., 2021; Merkuleva et al., 2022).

A. oryzae possesses a robust secretion mechanism that allows for large-scale protein production. It has been utilized successfully as an expression system for expressing heterologous proteins derived from higher eukaryotes (He et al., 2019; Ntana et al., 2020). In our study, we employed the *pyrG* auxotrophic *A. oryzae* for the first time to produce recombinant glucoamylase fusion NTD and RBD proteins by utilizing its advantage in heterologous protein production, which includes complex protein production at the industrial level.

Purification of recombinant Gla-NTD and Gla-RBD proteins

Following harvesting and filtering the expression culture medium, the recombinant proteins were purified under native conditions. The amount of
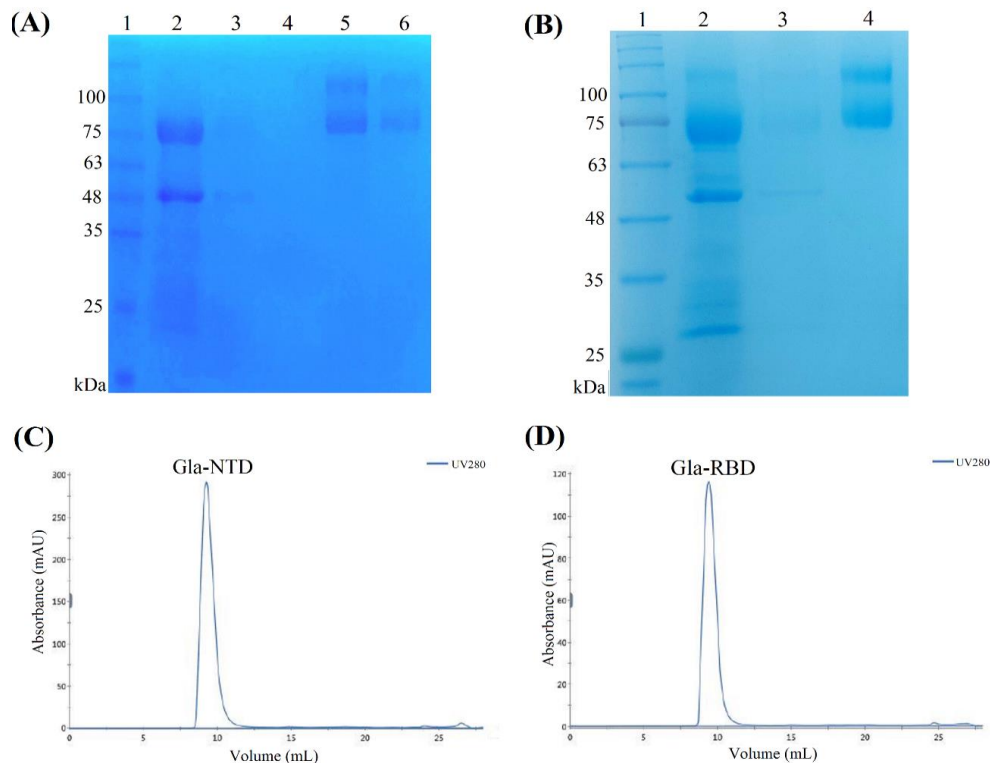
Figure 3. Purification of expressed Gla-NTD and Gla-RBD proteins. **(A)** Purification of His-tagged Gla-NTD by using the Ni-NTA column. Lane 1: Gangnam-Stain Protein Ladder. Lane 2: The culture medium of the colony expressing the Gla-NTD. Lanes 3–4: The wash solutions collected from the Ni-NTA column. Lanes 5–6: The eluted sample containing Gla-NTD. **(B)** Purification of His-tagged Gla-RBD by using the Ni-NTA column. Lane 1: Gangnam-Stain Protein Ladder. Lane 2: The culture medium of the colony expressing the Gla-RBD. Lane 3: The wash solution collected from the Ni-NTA column. Lane 4: The eluted sample containing Gla-RBD. **(C) (D)** Chromatograms of size exclusion chromatography purification using a Superdex 75 Increase 10/300 GL column. The peaks indicate the purified Gla-NTD **(C)** and Gla-RBD **(D)**.

recombinant His-tagged protein attached to the nickel resin was increased by co-incubating the sample and the resin for 1 h before purification. Following purification, the eluted samples were analyzed. SDS-PAGE analysis indicated the existence of protein bands with a molecular weight of approximately 110 kDa (Figures 3A and 3B). As expected, Gla-RBD has a slightly lower molecular weight than Gla-NTD (Figures A–B).

Maffei et al. (2021) investigated the differences between native and recombinant RBD expressed in *E. coli*, insect cells, and human HEK-293 cells. According to Maffei et al. (2021), RBD was expressed in soluble form in insect cells (6.5 mg/L) and mammalian cells (1.8 mg/mL), while *E. coli*-expressed RBD (2.5 mg/L) was recovered from inclusion bodies using a denaturing/refolding strategy. Chen et al. (2022) purified a stable and monomeric recombinant RBD protein from *P. pastoris* with a yield of 493 mg/L via hydrophobic interaction and anion exchange chromatography. In our study, size exclusion chromatography experiments indicated that *A. oryzae*-expressed Gla-NTD and Gla-RBD fusion proteins are stable and correctly folded. Following size exclusion chromatography (Figures 3C and 3D), the fractions containing Gla-NTD and Gla-RBD were concentrated. Consequently, the purified recombinant Gla-NTD protein yield was determined to be 14 mg/L, while the purified recombinant Gla-RBD protein yield was

determined to be 12 mg/L. Although the *E. coli* expression system offers cost-effective high-yield production than other expression systems, its use for complex proteins can be hindered by requiring refolding. On the other hand, despite the advantages of insect and mammalian expression systems in the production of complex proteins, their utilization in industrial production poses drawbacks due to their associated high costs and time-intensive production processes. *P. pastoris*, like *A. oryzae*, is commonly utilized in fermentation technology and has been demonstrated to produce RBD suitable for industrial production (Chen et al., 2022). In our study, we have demonstrated the feasibility of producing functional Gla-NTD and Gla-RBD proteins in *A. oryzae*, implying potential for industrial-scale production. This approach also allows us to circumvent the limitations associated with other expression systems.

The binding ability of Gla-NTD and Gla-RBD proteins

Indirect ELISA was performed using human sera obtained from patients suffering from COVID-19 to assess the binding ability of recombinant Gla-NTD and Gla-RBD proteins and to validate their in vitro functionality. Non-fusion glucoamylase-expressed *A. oryzae* culture mediums and irrelevant recombinant protein-expressed *A. oryzae* culture mediums were employed as negative control groups in order to
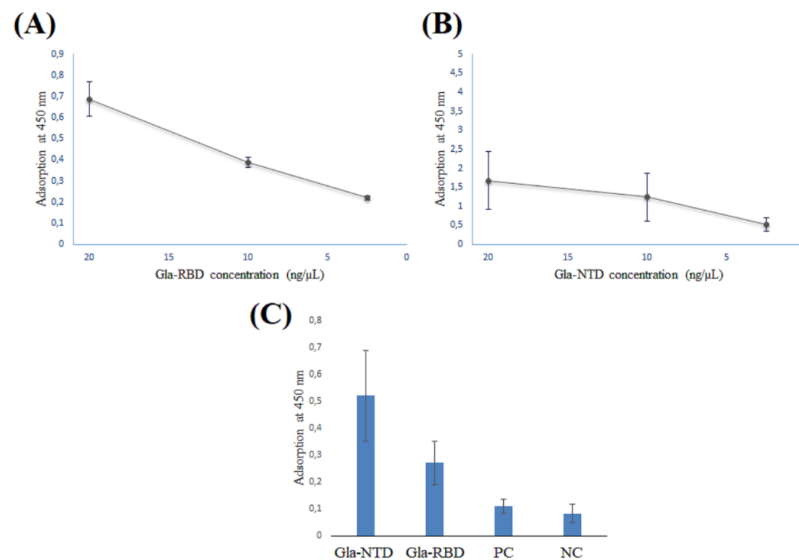
Figure 4. ELISA assays for purified recombinant Gla-RBD **(A)** and Gla-NTD **(B)** proteins compared to *P. pastoris*-expressed RBD and irrelevant recombinant protein **(C)**. The binding of the Gla-RBD (P = 0.011) and Gla-NTD (P = 0.006) proteins to human serum antibodies was detected using an HRP-conjugated anti-human IgG HRP antibody. Absorbance was measured at 450 nm, and bars indicate standard deviations. PC: positive control; recombinant RBD expressed in *P. pastoris*; NC: negative control; irrelevant protein.

investigate non-specific binding. Checkerboard titrations were used to evaluate the optimal concentration of recombinant Gla-NTD and Gla-RBD proteins as well as the ideal dilution ratio of human serum samples. For the ELISA, *P. pastoris*-expressed RBD, which was verified for its binding affinity of ACE2 homolog peptides (Azar et al., 2023), was utilized as a positive control group to confirm the binding ability of human anti-IgG antibodies to recombinant Gla-NTD and Gla-RBD.

ELISA was also used to qualitatively assess the IgG detection performance of recombinant fusion proteins in serum samples. The findings indicated that recombinant Gla-NTD (P = 0.006) and Gla-RBD (P = 0.011) proteins significantly bind to human anti-IgG antibodies in serum samples. As a result, the Gla-NTD and Gla-RBD proteins have correctly folded structures, allowing them to serve as antigen-antibody interactions. Furthermore, the data revealed a proportional relationship between recombinant fusion protein concentration and binding capacity (Figure 4).

The selection of the antigen exhibiting a stronger association with virus neutralization is critical to the efficacy of an immunoassay (McAndrews et al., 2020). The most dependable and commonly used technique for identifying antibodies produced against a particular antigen is ELISA (Bastos et al., 2020). While the specificity of antigen-based methods typically reaches around 100%, their sensitivity tends to fluctuate between 30% and 80% (Márquez-Ipiña et al., 2021). Studies on nucleoprotein-based ELISA assays for SARS-CoV-2 detection demonstrated sensitivity and cost-effectiveness in the detection of anti-IgG antibodies in serum samples (Tozetto-Mendoza et al., 2021). Additionally, RBD is an appropriate target antigen for developing serologic immunoassays. Márquez-Ipiña et

al. (2021) investigated the binding ability of *E. coli*-expressed RBD in ELISA assays utilizing human sera exposed and non-exposed to SARS-CoV-2. In their study conducted for *E. coli*-expressed RBD, the binding affinity was determined to be approximately 75%. However, owing to its rapid applicability and cost-effectiveness, the immunoassay offers substantial advantages on a large scale compared to techniques reliant on reverse transcription and polymerase chain reaction. In our study, the binding abilities of *A. oryzae*-expressed Gla-NTD and Gla-RBD proteins were investigated in human serum using a low-cost ELISA as a straightforward and reliable immunoassay. The research has demonstrated that recombinant Gla-NTD and Gla-RBD proteins exhibit significant and concentration-dependent binding to human anti-IgG antibodies in serum samples.

RBD can be expressed in *P. pastoris* as a vaccine agent with comparable yields and immunization results to *E. coli* (Chuck et al., 2009; Liu et al., 2022; Mi et al., 2022; Pino et al., 2021; Xing et al., 2022; Zang et al., 2021). Kalyoncu et al. (2023) utilized a fermentation system to produce RBD in *P. pastoris*, achieving over 1 g/L yield with a high immune response. As a potential vaccine agent, Chen et al. (2022) assessed the immunogenicity of *P. pastoris*-expressed RBD in mice. Notwithstanding that the RBD expressed in *P. pastoris* possesses high mannose-glycan-type glycosylation, it is able to stimulate immunization in mice just as the RBD is expressed in mammalian cells (Argentinian Anti-Covid Consortium, 2020). On the other hand, the results of our investigation indicate that *A. oryzae* can be used as a biotechnological platform to produce NTD and RBD fusion proteins. Because of its low cost of handling, easily applicable purification process from the gene to the recombinant protein, and ease of scale-up to obtain high protein titers in fermentation, *A. oryzae* is an

attractive tool for the production of SARS-CoV-2 antigens to be used in protein-based subunit vaccines.

Conclusion

The mass manufacture of functional NTD and RBD proteins provides an improvement in the development in COVID-19 research, diagnostics, and treatment. The solubility and functionality of RBD are the main problems in the case of its expression in *E. coli* (Argentinian Anti-Covid Consortium, 2020; Chen et al., 2005). In the mammalian expression system, the low final yield of transient transfection is a limiting issue for serologic assays (Esposito et al., 2020). *A. oryzae* is a useful biotechnological platform for producing functional Gla-NTD and Gla-RBD proteins on a large scale without the requirement for cell lysis or laborious purification procedures. In this study, for the first time, *pyrG* auxotrophic *A. oryzae* was used as a robust platform to produce heterologous glucoamylase-fused NTD and RBD proteins of the S protein of SARS-CoV-2. The ELISA assay results, employed to investigate the binding capabilities of recombinant fusion proteins to anti-human IgG antibodies in serum, have validated the functions of *A. oryzae*-expressed Gla-NTD and Gla-RBD. This study could pave the way for the efficient, affordable, and high-level production of various viral antigens in *A. oryzae* in future investigations.

Ethical Statement

The institutional review board approval for the study was granted by the Bezmialem Vakif University Institutional Review Board and by the Turkish Ministry of Health, and all procedures were in accordance with the approval. The subject had given informed consent for their samples to be stored and used for serological testing in the future.

Author Contributions

EK: Project Administration, Investigation, Methodology, Visualization, Validation, Formal Analysis, Resources, Writing -original draft, Writing-review, and editing; SU: Conceptualization; Supervision, Methodology, Resources, Writing-review, and editing.

Conflict of Interest

The authors declare that they have no known competing financial or non-financial, professional, or personal conflicts that could have appeared to influence the work reported in this paper.

Acknowledgements

References

Argentinian AntiCovid Consortium. (2020). Structural and functional comparison of SARS-CoV-2-spike receptor binding domain produced in *Pichia pastoris* and mammalian cells. *Nature Scientific Reports, 10*(1), 21779. https://doi.org/10.1038/s41598-020-78711-6

Azar, L. M., Öncel, M. M., Karaman, E., Soysal, L. F., Fatima, A., Choi, S. B., Eyupoglu, A. E., Erman, B., Khan, A. M., & Uysal, S. (2023). Human ACE2 orthologous peptide sequences show better binding affinity to SARS-CoV-2 RBD domain: Implications for drug design. *Computational and Structural Biotechnology Journal*, *21*, 4096-4109. https://doi.org/10.1016/j.csbj.2023.07.022

Balasubramaniyam, A., Ryan, E., Brown, D., Hamza, T., Harrison, W., Gan, M., Sankhala, R. S., Chen, W., Martinez, E. J., Jensen, J. L., Dussupt, V., Mendez-Rivera, L., Mayer, S., King, J., Michael, N. L., Regules, J., Krebs, S., Rao, M., Matyas, G. R., Joyce, M. G., Batchelor, A. H., Gromowski, G. D., & Dutta, S. (2022). Unglycosylated soluble SARS-CoV-2 receptor binding domain (RBD) produced in *E.coli* combined with the army liposomal formulation containing QS21 (ALFQ) elicits neutralizing antibodies against mismatched variants. *Vaccines*, *11*(1), 42. https://doi.org/10.3390/vaccines11010042

Bastos, M. L., Tavaziva, G., Abidi, S. K., Campbell, J. R., Haraoui, L. P., Johnston, J. C., Lan, Z., Law, S., MacLean, E., Trajman, A., Menzies, D., Benedetti, A., & Khan, F. A. (2020). Diagnostic accuracy of serological tests for COVID-19: Systematic review and meta-analysis. *BMJ*, *370*, 2516. https://doi.org/10.1136/bmj.m2516

Brindha, S., & Kuroda, Y. (2022). A multi-disulfide receptor-binding domain (RBD) of the SARS-CoV-2 spike protein expressed in *E. coli* using a SEP-tag produces antisera interacting with the mammalian cell expressed spike (S1) protein. *International Journal of Molecular Sciences*, *23*(3), 1703. https://doi.org/10.3390/ijms23031703

Cao, W., Dong, C., Kim, S., Hou, D., Tai, W., Du, L., Im, W., & Zhang, X. F. (2021). Biomechanical characterization of SARS-CoV-2 spike RBD and human ACE2 protein-protein interaction. *Biophysical Journal*, *120*, 1011–1019. https://doi.org/10.1016/j.bpj.2021.02.007

Chen, J., Miao, L., Li, J., Li, Y., Zhu, Q., Zhou, C., Fang, H., & Chen, H. P. (2005). Receptor-binding domain of SARS-CoV spike protein: Soluble expression in *E. coli*, purification and functional characterization. *World Journal of Gastroenterology, 11*(39), 6159-6164. https://doi.org/10.3748/wjg.v11.i39.6159

Chen, W. H., Pollet, J., Strych, U., Lee, J., Liu, Z., Kundu, R. T., Versteeg, L., Villar, M. J., Adhikari, R., Wei, J., Poveda, C., Keegan, B., Bailey, A. O., Chen, Y., Gillespie, P. M., Kimata, J. T., Zhan, B., Hotez, P.J., & Bottazzi, M. E. (2022). Yeast-expressed recombinant SARS-CoV-2 receptor binding domain RBD203-N1 as a COVID-19 protein vaccine candidate. *Protein Expression and Purification*, *190*, 106003. https://doi.org/10.1016/j.pep.2021.106003

Chuck, C. P., Wong, C. H., Chow, L. M., Fung, K. P., Waye, M. M., & Tsui, S. K. (2009). Expression of SARS-coronavirus spike glycoprotein in *Pichia pastoris*. *Virus Genes, 38*(1), 1-9.
https://doi.org/10.1007/s11262-008-0292-3

Conzentino, M. S., Forchhammer, K., Souza, E. M., Pedrosa, F. O., Nogueira, M. B., Raboni, S. M., Rego, F. G. M., Zanette, D. L., Aoki, M. N., Nardin, J. M., Fornazari, B., Morales, H. M. P., Celedon, P. A. F., Lima, C. V. P., Mattar, S. B., Lin, V. H., Morello, L. G., Marchini, F. K., Reis, R. A., & Huergo, L. F. (2021). Antigen production and development of an indirect ELISA based on the nucleocapsid protein to detect human SARS-CoV-2 seroconversion. *Brazilian Journal of Microbiology*, *52*, 2069-2073.
https://doi.org/10.1007/s42770-021-00556-6

Conzentino, M. S., Gonçalves, A. C., Paula, N. M., Rego, F. G., Zanette, D. L., Aoki, M. N., Nardin, J. M., & Huergo, L. F. (2022). A magnetic bead immunoassay to detect high affinity human IgG reactive to SARS-CoV-2 Spike S1 RBD produced in *Escherichia coli*. *Brazilian Journal of Microbiology*, *53*(3), 1263-1269.
https://doi.org/10.1007/s42770-022-00753-x

Esposito, D., Mehalko, J., Drew, M., Snead, K., Wall, V., Taylor, T., Frank, P., Denson, J-P., Hong, M., Gulten, G., Sadtler, K., Messing, S., & Gillette, W. (2020). Optimizing high-yield production of SARS-CoV-2 soluble spike trimers for serology assays. *Protein Expression and Purification*, *174*, 105686.
https://doi.org/10.1016/j.pep.2020.105686

Fitzgerald, G. A., Komarov, A., Kaznadzey, A., Mazo, I., & Kireeva, M. L. (2021). Expression of SARS-CoV-2 surface glycoprotein fragment 319–640 in *E. coli*, and its refolding and purification. *Protein Expression and Purification*, *183*, 105861.
https://doi.org/10.1016/j.pep.2021.105861

Gao, X., Peng, S., Mei, S., Liang, K., Khan, M. S. I., Vong, E. G., & Zhan, J. (2022). Expression and functional identification of recombinant SARS-CoV-2 receptor binding domain (RBD) from *E. coli* system. *Preparative Biochemistry & Biotechnology*, *52*(3), 318-324.
https://doi.org/10.1080/10826068.2021.1941106

Hassanin, A. A., Raza, S. H., Ujjan, J. A., Alrashidi, A. A., Sitohy, B. M., Al-surhanee, A. A., Saad, A. M., Al-Hazani, T. M., Atallah, O. O., Al Syaad, K. M., Ahmed, A. E., Swelum, A. A., El-Saadony, M. T. & Sitohy, M. Z. (2021). Emergence, evolution, and vaccine production approaches of SARS-CoV-2 virus: Benefits of getting vaccinated and common questions. *Saudi Journal of Biological Sciences*, *9*(4), 1981-1997.
https://doi.org/10.1016/j.sjbs.2021.12.020

He, B., Tu, Y., Jiang, C., Zhang, Z., Li, Y., & Zeng, B. (2019). Functional genomics of *Aspergillus oryzae*: Strategies and progress. *Microorganisms*, *7*(103), 1-13.
https://doi.org/10.3390/microorganisms7040103

He, Y., Qi, J., Xiao, L., Shen, L., Yu, W., & Hu, T. (2021). Purification and characterization of the receptor-binding domain of SARS-CoV-2 spike protein from *Escherichia coli*. *Engineering in Life Sciences*, *21*(6), 453-460.
https://doi.org/10.1002/elsc.202000106

Huang, Y.; Yang, C.; Xu, X.; Xu, W., & Liu, S. (2020). Structural and functional properties of SARS-CoV-2 spike protein: Potential antivirus drug development for COVID-19. *Acta Pharmacologica Sinica*, *41*, 1141–1149.
https://doi.org/10.1038/s41401-020-0485-4

Kalyoncu, S., Yilmaz, S., Kuyucu, A. Z., Sayili, D., Mert, O., Soyturk, H., Gullu, S., Akinturk, H., Citak, E., Arslan, M., Taskinarda, M. G., Tarman, I. O., Yilmazer Altun, G., Ozer, C., Orkut, R., Demirtas, A., Tilmensagir, I., Keles, U., Ulker, C., Aralan, G., Mercan, Y., Ozkan, M., Caglar, H. O., Arik, G., Ucar, M. C., Yildirim, M., Canavar Yildirim, T., Karadag, D., Bal, E., Erdogan, A., Senturk, S., Uzar, S., Enul, H., Adiay, C., Sarac, F., Ekiz, A. T., Abaci, I., Aksoy, O., Polat, H. U., Tekin, S., Dimitrov, S., Ozkul, A., Wingender, G., Gursel, I., Ozturk, M., & Inan, M. (2023). Process development for an effective COVID-19 vaccine candidate harboring recombinant SARS-CoV-2 delta plus receptor binding domain produced by *Pichia pastoris*. *Nature Scientific Reports*, *13*(1), 5224.
https://doi.org/10.1038/s41598-023-32021-9

Karaman, E., Eyüpoğlu, A. E., Mahmoudi Azar, L., & Uysal, S. (2023). Large-scale production of anti-RNase A VHH expressed in *pyrG* auxotrophic *Aspergillus oryzae*. *Current Issues Molecular Biology*, *45*(6), 4778-4795.
https://doi.org/10.3390/cimb45060304

Kim, W. S., Kim, J. H., Lee, J., Ka, S. Y., Chae, H. D., Jung, I., Jung, S. T., & Na, J. H. (2022). Functional expression of the recombinant spike receptor binding domain of SARS-CoV-2 Omicron in the periplasm of *Escherichia coli*. *Bioengineering*, *9*(11), 670.
https://doi.org/10.3390/bioengineering9110670

Lan, J., Ge, J., Yu, J., Shan, S., Zhou, H., Fan, S., Zhang, Q., Shi, X., Wang, Q., Zhang, L., & Wang, X. (2020). Structure of the SARS-CoV-2 spike receptor-binding domain bound to the ACE2 receptor. *Nature, 581*(7807), 215-220.
https://doi.org/10.1038/s41586-020-2180-5

Li, W., Moore, M. J., Vasilieva, N. J., Sui, J., Wong, S. K., Berne, M. A., Somasundaran, M., Sullivan, J. L., Luzuriaga, K., Greenough, T. C. Choe, H., & Farzan, M. (2003). Angiotensin-converting enzyme 2 is a functional receptor for the SARS coronavirus. *Nature*, *426*, 450–454.
https://doi.org/10.1038/nature02145

Liu, B., Yin, Y., Liu, Y., Wang, T., Sun, P., Ou, Y., Gong, X., Hou, X., Zhang, J., Ren, H., Luo, S., Ke, Q., Yao, Y., Xu, J., & Wu, J. (2022). A vaccine based on the receptor-binding domain of the spike protein expressed in glycoengineered *Pichia pastoris* targeting SARS-CoV-2 stimulates neutralizing and protective antibody responses. *Engineering*, *13*, 107-115.
https://doi.org/10.1016/j.eng.2021.06.012 14

Maffei, M., Montemiglio, L. C., Vitagliano, G., Fedele, L., Sellathurai, S., Bucci, F., Compagnone, M., Chiarini, V., Exertier, C., Muzi, A., Roscilli, G., Vallone, B., & Marra, E. (2021). The nuts and bolts of SARS-CoV-2 spike receptor-binding domain heterologous expression. *Biomolecules*, *11*(12), 1812.
https://doi.org/10.3390/biom11121812

Márquez-Ipiña, A. R., González-González, E., Rodríguez-Sánchez, I. P., Lara-Mayorga, I. M., Mejía-Manzano, L. A., Sánchez-Salazar, M. G., González-Valdez, J. G., Ortiz-Lopez, R., Rojas-Martinez, A., Santiago, G. T., & Alvarez, M. M. (2021). Serological test to determine exposure to SARS-CoV-2: ELISA based on the receptor-binding domain of the spike protein (S-RBD$_{N318-V510}$) expressed in *Escherichia coli*. *Diagnostics*, *11*(2), 271.
https://doi.org/10.3390/diagnostics11020271

McAndrews, K. M., Dowlatshahi, D. P., Dai, J., Becker, L. M., Hensel, J., Snowden, L. M., Leveille, J. M., Brunner, M. R.,

Holden, K. W., Hopkins, N. S., Harris, A. M., Kumpati, J., Whitt, M. A., Lee, J. J., Ostrosky-Zeichner, L. L., Papanna, R., LeBleu, V. S., Allison, J. P., & Kalluri, R. (2020). Heterogeneous antibodies against SARS-CoV-2 spike receptor binding domain and nucleocapsid with implications for COVID-19 immunity. *JCI Insight*, *5*(18). https://doi.org/10.1172/jci.insight.142386

McGuire, B. E., Mela, J. E., Thompson, V. C., Cucksey, L. R., Stevens, C. E., McWhinnie, R. L., Winkler, D. F. H., Pelech, S., & Nano, F. E. (2022). *Escherichia coli* recombinant expression of SARS-CoV-2 protein fragments. *Microbial Cell Factories*, *21*(1), 1-13. https://doi.org/10.1186/s12934-022-01753-0

Merkuleva, I. A., Shcherbakov, D. N., Borgoyakova, M. B., Shanshin, D. V., Rudometov, A. P., Karpenko, L. I., Belenkaya, S. V., Isaeva, A. A., Nesmeyanova, V. S., Kazachinskaia, E. I., Volosnikova, E. A., Esina, T. I., Zaykovskaya, A. V., Pyankov, O. V., Borisevich, S. S., Shelemba, A. A., Chikaev, A. N., & Ilyichev, A. A. (2022). Comparative immunogenicity of the recombinant receptor-binding domain of protein S SARS-CoV-2 obtained in prokaryotic and mammalian expression systems. *Vaccines*, *10*(1), 96. https://doi.org/10.3390/vaccines10010096

Mi, T., Wang, T., Xu, H., Sun, P., Hou, X., Zhang, X., Ke, Q., Liu, J., Hu, S., Wu, J., & Liu, B. (2022). Kappa-RBD produced by glycoengineered *Pichia pastoris* elicited high neutralizing antibody titers against pseudoviruses of SARS-CoV-2 variants. *Virology*, *569*, 56-63. https://doi.org/10.1016/j.virol.2022.03.001

Ntana, F., Mortensen, U.H., Sarazin, C., & Figge, R. (2020). *Aspergillus*: A powerful protein production platform. *Catalysts*, *10*(9), 1064; https://doi.org/10.3390/catal10091064

Pino, M., Abid, T., Pereira Ribeiro, S., Edara, V. V., Floyd, K., Smith, J. C., Latif, M. B., Pacheco-Sanchez, G., Dutta, D., Wang, S., Gumber, S., Kirejczyk, S., Cohen, J., Stammen, R. L., Jean, S. M., Wood, J. S., Connor-Stroud, F., Pollet, J., Chen, W., Wei, J., Zhan, B., Lee, J., Liu, Z., Strych, U., Shenvi, N., Easley, K., Weiskopf, D., Sette, A., Pollara, J., Mielke, D., Gao, H., Eisel, N., Lebranche, C. C., Shen, X., Ferrari, G., Tomaras, G. D., Montefiori, D. C., Sekaly, R. P., Vanderford, T. H., Tomai, M. A., Fox, c. B., Suthar, M. S., Kozlowski, P. A., Hotez, P. J., Paiardini, M., Bottazzi, M. E., & Kasturi, S. P. (2021). A yeast-expressed RBD-based SARS-CoV-2 vaccine formulated with 3M-052-alum adjuvant promotes protective efficacy in non-human primates. *Science Immunology*, *6*(61), eabh3634. https://doi.org/10.1126/sciimmunol.abh3634

Prahlad, J., Struble, L. R., Lutz, W. E., Wallin, S. A., Khurana, S., Schnaubelt, A., Broadhurst, M. J., Bayles, K. W., & Borgstahl, G. E. (2021). CyDisCo production of functional recombinant SARS-CoV-2 spike receptor binding domain. *Protein Science*, *30*(9), 1983-1990. https://doi.org/10.1002/pro.4152

Sakai, K., Kinoshita, H., & Nihira, T. (2012). Heterologous expression system in *Aspergillus oryzae* for fungal biosynthetic gene clusters of secondary metabolites. *Applied Microbiology and Biotechnology*, *93*(5), 2011-2022. https://doi.org/10.1007/s00253-011-3657-9

Shang, J., Ye, G., Shi, K., Wan, Y., Luo, C., Aihara, H., Geng, Q., Auerbach, A., & Fang, L. (2020). Structural basis of receptor recognition by SARS-CoV-2. *Nature, 581*(7807), 221-224. https://doi.org/10.1038/s41586-020-2179-y

Tantiwiwat, T., Thaiprayoon, A., Siriatcharanon, A. K., Tachaapaikoon, C., Plongthongkum, N., & Waraho-Zhmayev, D. (2023). Utilization of receptor-binding domain of SARS-CoV-2 spike protein expressed in *Escherichia coli* for the development of neutralizing antibody assay. *Molecular Biotechnology*, *65*(4), 598-611. https://doi.org/10.1007/s12033-022-00563-4

Tay, M. Z., Poh, C. M., Rénia, L., MacAry , P. A., & Ng, L. F. (2020). The trinity of COVID-19: immunity, inflammation and intervention. *Nature Reviews Immunology, 20*(6), 363-374. https://doi.org/10.1038/s41577-020-0311-8

Tozetto-Mendoza, T. R., Kanunfre, K. A., Vilas-Boas, L. S., Espinoza, E. P. S., Paião, H. G. O., Rocha, M. C., de Paula, A. V., de Oliveira, M., S., Zampelli, D. B., Vieira Jr., J. M., Buss, L., Costa, S., F., Sabino, E. C., Witkin, S. S., Okay, T. S., & Mendes-Correa, M. C. (2021). Nucleoprotein-based ELISA for detection of SARS-COV-2 IgG antibodies: Could an old assay be suitable for serodiagnosis of the new coronavirus?. *Journal of Virological Methods*, *290*, 114064. https://doi.org/10.1016/j.jviromet.2021.114064

Tripathi, N.K. (2016). Production and purification of recombinant proteins from *Escherichia coli*. *Chem Bio Eng Reviews, 3*, 116–133. https://doi.org/10.1002/cben.201600002

Walls, A. C., Park, Y. J., Tortorici, M. A., Wall, A., McGuire, A. T., & Veesler, D. (2020). Structure, function, and antigenicity of the SARS-CoV-2 spike glycoprotein. *Cell*, *181*(2), 281-292. https://doi.org/10.1016/j.cell.2020.02.058

Wrapp, D., Wang, N., Corbett, K.S., Goldsmith, J.A., Hsieh, C., Abiona, O., Graham, B.S., & McLellan, J.S. (2020). Cryo-EM structure of the 2019-nCoV spike in the prefusion conformation. *Science*, *367*, 1260–1263. https://doi.org/10.1126/science.abb2507

Xing, H., Zhu, L., Wang, P., Zhao, G., Zhou, Z., Yang, Y., Zou, H., & Yan, X. (2022). Display of receptor-binding domain of SARS-CoV-2 spike protein variants on the *Saccharomyces cerevisiae* cell surface. *Frontiers in Immunology*, *13*, 935573. https://doi.org/10.3389/fimmu.2022.935573

Zang, J., Zhu, Y., Zhou, Y., Gu, C., Yi, Y., Wang, S., Xu, S., Hu, G., Du, S., Yin, Y., Wang, Y., Yang, Y., Zhang, X., Wang, H., Yin, F., Zhang, C., Deng, Q., Xie, Y., & Huang, Z. (2021). Yeast-produced RBD-based recombinant protein vaccines elicit broadly neutralizing antibodies and durable protective immunity against SARS-CoV-2 infection. *Cell Discovery*, *7*(1), 71. https://doi.org/10.1038/s41421-021-00315-9

Zhu, G., Zhu, C., Zhu, Y., & Sun, F. (2020). Minireview of progress in the structural study of SARS-CoV-2 proteins. *Current Research in Microbial Sciences, 1*, 53-61. https://doi.org/10.1016/j.crmicr.2020.06.003

BIOTECH STUDIES

RESEARCH PAPER

The developmental stage is a critical parameter for accurate assessment of the drug-induced liver injury (DILI) potentials of drugs with the zebrafish larval liver model

Gulcin Cakan-Akdogan[1,2]* , Cigdem Bilgi[1,3]

[1]Izmir Biomedicine and Genome Center, 35340, Izmir, Türkiye
[2]Department of Medical Biology, Faculty of Medicine, Dokuz Eylul University, 35340, Izmir, Türkiye
[3]Istanbul University-Cerrahpasa, Faculty of Pharmacy, Department of Pharmacognosy, Istanbul Türkiye

Abstract

Prediction of drug-induced liver injury (DILI) potential of drugs is one of the most challenging issues of drug development. Zebrafish larvae provide an *in vivo* and robust test platform. Due to the ease of handling developing larvae between 2 - 5 days post fertilization (dpf) has been extensively used as a DILI test model. However, the liver is not fully functional at this stage. Here, the importance of larval liver maturation was tested by applying selected known DILI-rank drugs to liver reporter zebrafish between 2-5 dpf and 5-7 dpf. Acetaminophen (most-DILI) treatment caused a significant dose-dependent reduction in liver size only at the early stage. Isoniazid (most-DILI) administration after liver maturation induced hepatomegaly, while it induced liver size reduction between 2-5 dpf. Chlorambucil (less-DILI) treatment induced opposing effects on liver size, in the two stages tested. A non-DILI agent chloramphenicol did not induce any liver size change in either larval stage. Clinical observations were better reproduced when isoniazid and chlorambucil were administered after liver maturation. Our findings show that often-overlooked liver maturity status is a critical parameter for the evaluation of DILI.

Introduction

Drug-induced liver injury (DILI) is a term describing liver damage observed after administration of various drugs, herbal products, and dietary supplements (Garcia-Cortes et al., 2020). Currently, the diagnosis of DILI is challenging due to the lack of specific biomarkers and therefore, DILI is a diagnosis of exclusion (Iruzubieta et al., 2015). Serum transaminase levels, alanine aminotransferase (ALT), aspartate aminotransferase (AST), and total serum bilirubin levels (TSB) are assessed to detect DILI using some calculations and score tables such as Roussel Uclaf Causality Assessment Method-

RUCAM (Andrade & Robles-Díaz, 2020). Even though these methods are in clinical guidelines for the diagnosis of DILI, reliability and sensitivity are not high enough for early detection and diagnosis (Robles-Díaz et al., 2016). Drug-induced hepatotoxicity is not always dose-dependent and predictable, and the severity of DILI may depend on individual factors. DILI remains one of the most challenging issues in the discovery and pre/post-marketing stages of drug development (Andrade et al., 2019). Zebrafish larva due to it being time and cost-effective, has attracted interest as an *in vivo* model for

prediction of a drug candidate's hepatotoxicity potential (Jagtap et al., 2022). The rapid maturation of the liver within 5 days post fertilization (dpf), transparency of the larvae, easy application of test compounds, and the possibility for medium-throughput live imaging are among attractive features of zebrafish (Chu & Sadler, 2009; Katoch & Patial, 2021; Vliegenthart et al., 2014). Different features of DILI can be screened with the help of numerous transgenic reporter zebrafish lines. Among these, the most widely used method is the liver size measurement in transgenic larva that expresses fluorescent protein in hepatocytes (Choi et al., 2014; Lin et al., 2019; Nguyen et al., 2017; Park et al., 2022; X. Zhang et al., 2014). Several studies confirmed that drug detoxification enzymes are conserved in zebrafish, and drugs are processed in zebrafish liver (Sato et al., 2023). Early zebrafish between 2-5 dpf are highly preferred for hepatotoxicity studies, this is a stage during which liver specification and maturation take place (Cassar et al., 2019; Chu & Sadler, 2009). While important drug-metabolizing enzymes such as Cytochrome p450 enzymes (CYPs) are expressed early on in extrahepatic tissues, the maturation of the larval liver is typically completed by the end of 5 dpf (Goldstone et al., 2010; Nawaji et al., 2020). Therefore, we hypothesized that the drug-induced liver toxicity observed before 5 dpf is partly due to interference with developmental processes, and the use of larvae with fully functional liver may provide a more direct hepatotoxicity assessment.

This study aims to investigate the effect of larval liver maturation status on liver damage. To this end, FDA-approved drugs with different DILI concern classifications were applied to zebrafish between 2-5 dpf and 5-7 dpf, and DILI potentials were evaluated with liver size changes.

Materials and Methods

Chemicals and reagents

Acetaminophen (APAP) (Santa Cruz Biotechnology, Inc., Dallas, TX, USA), chloramphenicol (CHLP) (Bioshop Canada Inc., Burlington, Ontario, Canada), isoniazid (INH) (Goldbio Technology, St. Louis, MO, USA), chlorambucil (CHB) (Sigma-Aldrich, St. Louis, MO, USA), dimethyl sulfoxide (DMSO) (Sigma-Aldrich, St. Louis, MO, USA) and ethanol (Sigma-Aldrich, St. Louis, MO, USA) were of analytical grade. Low melting point agarose and tricaine methanosulfate (MS-222) were purchased from Sigma (Sigma-Aldrich, St. Louis, MO, USA).

Preparation of drug solutions

APAP and INH were dissolved in deionized water. CHB and CHLP were dissolved in DMSO and 95% ethanol, respectively. Working solutions were prepared freshly by diluting in E3 medium (15 mM NaCl, 0.5 mM KCl, 1 mM $MgSO_4$, 1 mM $CaCl_2$, 0.15 mM KH_2PO_4, 0.05 mM Na_2HPO_4, 0.7 mM $NaHCO_3$, 0.5% methylene blue,

pH 7.5). The final doses applied were 1.25 mM - 10 mM for APAP, 1.25 mM - 10 mM for INH, 25 μM - 100 μM for CHB, and 0.25 mM - 2 mM for CHLP. Control groups were treated with E3 for APAP and INH, with 1% DMSO for CHB, and 0.5% Ethanol for CHLP. DMSO did not induce any systemic toxicity according to the previous study and did not cause any liver size change in our setup (Cornet et al., 2017).

Zebrafish treatments

All adult zebrafish were maintained under standard conditions. Embryos were obtained by crossing *fabp10a:mCherry* transgenics with AB+/+ wild-type fish and incubated in E3 at 28 °C at Izmir Biomedicine and Genome Center (IBG) zebrafish facility. All experiments were conducted according to the national regulations. The protocols were approved by IBG Animal Experimentation Local Ethics Committee by protocol no 2021-005. 10 larvae per well were maintained in 1 mL of medium, in 24-well plates for treatments. Medium was refreshed and larvae were monitored daily. The experiment was repeated two times with similar findings. One set of experiment results were presented in the figures.

Liver size measurements and statistical analysis

Larvae were anesthetized and embedded in low melting point agarose for imaging (Lecaudey et al., 2008). Liver images were captured with a fluorescent stereomicroscope (Olympus SZX16, XC50 camera). The liver area was measured with Fiji software. For each group 10 individual samples were measured, the average value was plotted, and standard deviation was used as the error bar. Statistical significance was calculated with one-way ANOVA, and significance was annotated: $*P<0.05$, $**P<0.01$, $***P<0.001$.

Results

DILI-concern categories of selected drugs were determined according to the DILIrank database published by the Food and Drug Administration (FDA) (Chen et al., 2011). Most-DILI agents APAP and INH, less-DILI agent CHB, and non-DILI agent CHLP were tested. DILI was evaluated based on liver size change in *fabp10a:mcherry* liver reporter zebrafish transgenic larvae. The drugs were administered to zebrafish larvae between 2-5 or 5-7 dpf.

Acetaminophen induced liver size reduction only at 2-5 dpf stage

APAP is a commonly used drug known for its analgesic and antipyretic effects and accepted as the model drug for dose-dependent, direct DILI studies (Klotz, 2012; Vliegenthart et al., 2014). While several studies employed zebrafish embryos and early larvae younger than 5 dpf showed that APAP induces hepatotoxicity in the zebrafish model, none of the previous studies tested larvae with fully functional liver

(Guo et al., 2015; North et al., 2010; X. Zhang et al., 2014).

Here, previously reported hepatoxic doses (2 mM - 10 mM) of APAP were tested (North et al., 2010). 1.25 mM APAP did not cause any visible morphological changes or liver size change when applied between 2-5 dpf or 5-7 dpf. 10 mM APAP caused lethality when applied between 2-5 dpf. 2.5 mM APAP caused changes in melanocyte pattern, and 5 mM APAP caused smaller eyes and defects in pigmentation, which are previously reported phenotypes (Figure 1A) (Sato et al., 2023). However, the same concentrations of APAP did not induce any morphological or pigmentation defects when applied between 5-7 dpf (Figure 1B). 2.5 mM and 5 mM APAP induced a dose-dependent and significant liver size reduction when applied between 2-5 dpf. On the other hand, when APAP was applied after maturation of liver, between 5-7 dpf, no change in liver size was detected (Figure 1C and 1D).

Figure 1. Morphology and liver size of acetaminophen (APAP) treated larvae. Whole body lateral images of controls and APAP treated larvae at the end of treatment applied between A) 2-5 dpf, B) 5-7 dpf. C) Average liver area ± std measured at the end of treatment, n=10 for each group. D) Representative liver images of *fabp10a:mCherry* transgenic fish. Scale bars A, B) 1 mm, D) 200 μm.

Isoniazid induced liver enlargement only at 5-7 dpf stage

INH is a widely used first-line drug for the treatment of tuberculosis. Unlike APAP, INH is known to cause idiosyncratic DILI (iDILI), which is more difficult to detect in preclinical test models (Chan & Benet, 2017).

It was demonstrated that the administration of 10 mM INH between 3-4 dpf resulted in liver size decrease (Jagtap et al., 2022). Another study reported induction of apoptosis upon exposure to 6 mM INH between 4-5 dpf (Higuchi et al., 2021). Here, 1.25 mM - 10 mM INH were applied between 2-5 dpf and 5-7 dpf. When applied between 2-5 dpf, 1.25 mM and 5 mM INH did not cause any morphological defects or apparent phenotypes, whereas 10 mM INH caused a significant

reduction of larval body size (Figure 2A). When applied between 5-7 dpf, 1.25 mM INH did not cause any defect, while 10 mM was lethal. In this group, 2.5 mM INH caused the darkening of the liver, and 5 mM INH caused darkening of the head and liver as well as bending of the larval body (Figure 2B). The effect of INH treatment on liver size was different in tested two stages. While lower doses did not induce any change of liver size, 10 mM INH caused a significant decrease in liver size when applied before 5 dpf (Figure 2C, D). In contrast, INH caused a significant increase in liver size when applied between 5-7 dpf, at doses of 2.5 mM or 5 mM (Figure 2C, D).

Figure 2. Morphology and liver size of isoniazid (INH) treated larvae. Whole body lateral images of controls and INH treated larvae at the end of treatment applied between A) 2-5 dpf, B) 5-7 dpf. C) Average liver area ± std measured at the end of treatment, n=10 for each group. D) Representative liver images of *fabp10a:mCherry* transgenic fish. Scale bars A, B) 1 mm, D) 200 μm.

Chlorambucil induced liver enlargement only at 2-5 dpf stage

CHB is one of the best-tolerated oral alkylating agents prescribed for the treatment of chronic leukaemia and lyphomas as well as ovarian and breast cancers (Sienkiewicz et al., 2005). CHB is classified as a less-DILI drug which can still lead to moderate-to-serious clinical DILI manifestations (Patel, 2000; Patel et al., 2000). Clinical cases reported mild hepatomegaly or hepatosplenomegaly after CHB administration (Kyle et al., 2000; Skoutelis, 2000). CHB hepatotoxicity on zebrafish liver has not been studied previously. Microinjection of CHB (6 mM, 40 nL) into the yolk sac of 2 dpf zebrafish larvae resulted in 60% lethality, and body deformation was observed in survivors (Akdogan et al., 2022), while blastula treated with 10 μM - 50 μM of CHB exhibited delayed epiboly (Nakayama et al., 2021).

Here, CHB was applied at 25 μM, 50 μM, and 100 μM concentrations. When 25 μM - 50 μM CHB was applied between 2-5 dpf, no morphological change was observed in larvae. 100 μM CHB caused a systemic effect

resulting in a reduction in the larval body length, smaller craniofacial region, and eye size (Figure 3A). When applied between 5-7 dpf; 25 µM caused mild darkening of the liver, 50 µM caused darkening of the liver and bending of the larval body, while 100 µM CHB was lethal (Figure 3B). When administered between 2-5 dpf 50 µM CHB caused liver enlargement. While 100 µM CHB-treated larvae were much smaller than controls, average liver size was similar to untreated healthy controls, which indicated liver size increase when compared to body size (Figure 3A, B, D). In contrast, when applied between 5-7 dpf, 50 µM CHB caused a small reduction in liver size, while 100 µM drug caused lethality (Figure 3).
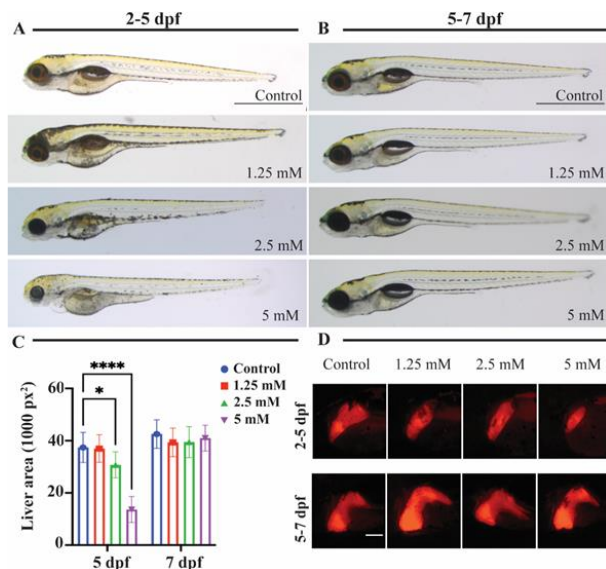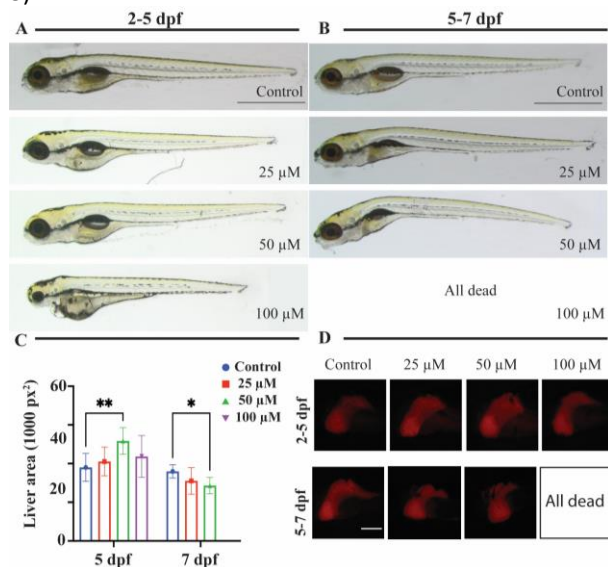

Figure 3. Morphology and liver size of chlorambucil (CHB) treated larvae. Whole body lateral images of controls and CHB treated larvae at the end of treatment applied between **A)** 2-5 dpf, **B)** 5-7 dpf. **C)** Average liver area ± std measured at the end of treatment, n=10 for each group. **D)** Representative liver images of *fabp10a:mCherry* transgenic fish. Scale bars **A, B)** 1 mm, **D)** 200 µm.

Chloramphenicol did not cause liver size change

Chloramphenicol (CHLP) is an effective broad-spectrum antibiotic against meningeal pathogens, but its use is limited due to safety concerns such as hematological problems, neurotoxicity, and hypersensitivity reactions (Feder Jr, 1986; Singhal et al., 2020). CHLP was used here as a negative control since FDA-DILI rank dataset categorizes it as a non-DILI agent. Ali et al. (2012) reported LC_{50} values of 1.62 mM or 23.36 mM when applied to zebrafish between 1-5 dpf for different durations. Sublethal concentrations were verified in our preliminary studies and the drug was applied within a range of 0.25 mM - 2 mM. CHLP was well tolerated by zebrafish between 2-5 dpf, and no morphological changes were observed (Figure 4A). Similarly, larvae between 5-7 dpf tolerated CHLP well. While a minor darkening of the liver was observed at higher doses, the larvae looked healthy and normal (Figure 4B). Average liver sizes remained unchanged in

all groups, and livers looked normal under stereomicroscope (Figure 4C, D).
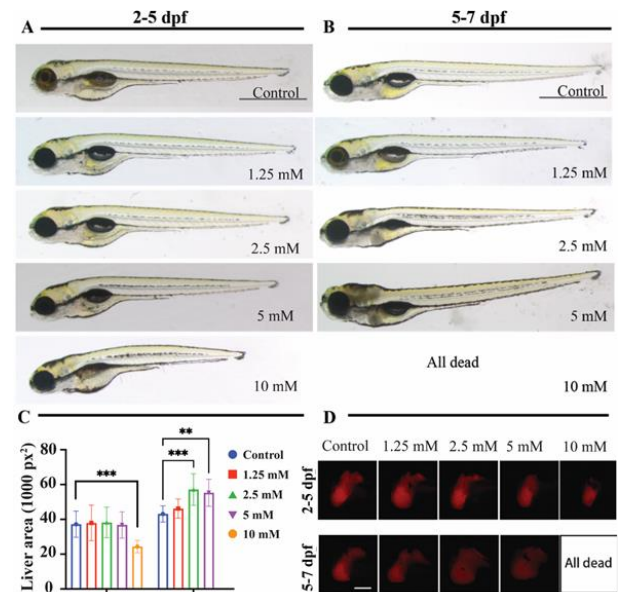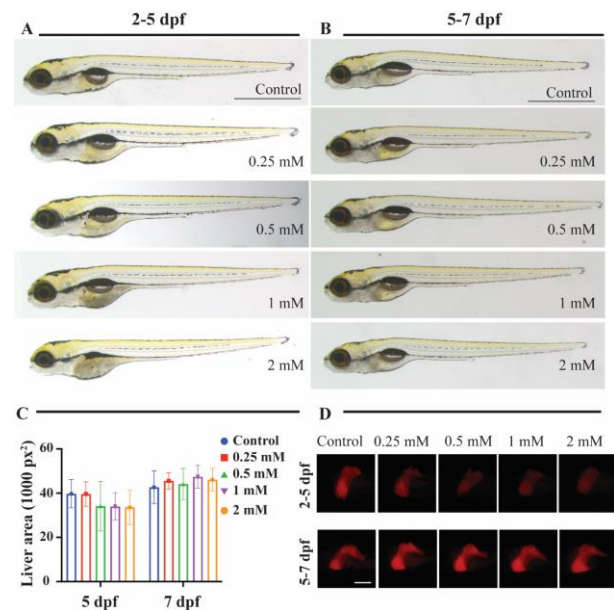

Figure 4. Morphology and liver size of chloramphenicol (CHLP) treated larvae. Whole body lateral images of controls and CHLP treated larvae at the end of treatment applied between A) 2-5 dpf, B) 5-7 dpf. C) Average liver area ± std measured at the end of treatment, n=10 for each group. D) Representative liver images of *fabp10a:mCherry* transgenic fish. Scale bars A, B) 1 mm, D) 200 µm.

Discussion

Drug metabolism in the liver converts the drug molecules into more polar and soluble forms that can be excreted and this can occur in three phases: modification (phase I), conjugation (phase II), and transported mediated elimination (phase III) (Almazroo et. al, 2017). The zebrafish liver is accepted to gain function as of 4 dpf but levels of most drug metabolising enzymes increase at day five or later (Chu & Sadler, 2009; Cakan-Akdogan et. al, 2023). Although zebrafish has been increasingly used as a hepatoxicity screening tool, majority of the studies use early larvae (younger than 5 dpf), a stage in which the liver is still developing (Vliegenthart et. al, 2014). Here, the importance of stage for hepatotoxicity assessment was investigated by comparing affects of selected drugs in early developing larvae and 5 dpf larvae with a fully functional liver. Interestingly, hepatotoxicity potentials and the liver size phenotypes varied according to the stage and drug applied.

The first selected drug was APAP, a most-DILI agent, which has been extensively studied in zebrafish in early larvae and adult stages. Liver size reduction caused by 2.5 mM - 5 mM APAP before 5 dpf reported here is in line with previous findings (North et al., 2010). However, to our knowledge, exposure of larvae to APAP after full development of the liver is performed for the first time in this study. Interestingly, 5 mM APAP did not induce liver size change in larvae older than 5 dpf. These

findings suggest that the enhanced tolerance of zebrafish towards APAP after completing liver development may be associated with the rapid increase in glutathione levels or more effective functioning of alternative detoxification pathways, such as glucuronidation and sulfation. Supporting this hypothesis, the glutathione-*S*-transferase levels of zebrafish larvae increase gradually between 3-5 dpf, followed by a dramatic increase after 5 dpf (Tierbach et al., 2018).

The second tested drug, INH (most-DILI) was chosen as a model drug for iDILI in this study. Previous studies reported that INH induces apoptosis and a liver size reduction in early larvae (Higuchi et al., 2021; Y. Zhang et al., 2019). Interestingly, we showed that the liver size reduction is only observed at a dose when the overall larval size is also reduced, hence it is likely not liver-specific. On the other hand, larvae treated with INH after the liver is functional (5-7 dpf) had hepatomegaly without any apparent toxicity in the rest of the larval body. Hepatomegaly is a known clinical manifestation of liver injury induced by INH administration (Nanton et al., 2004; Shah et al., 2016; Wolf & Lavine, 2000). To our knowledge, this is the first study demonstrating INH induced hepatomegaly in the zebrafish model. Our findings indicate that the utilization of zebrafish larvae older than 5 dpf may represent a preferable approach for modeling INH-induced DILI effects in zebrafish. The hepatotoxicity of INH is suggested to be either due to the bioactivation of the acetyl hydrazine metabolite generated during the metabolism of INH or due to the protein adducts formed by INH, which in turn trigger an immune response (Metushi et al., 2016). Hepatomegaly, liver enlargement, is known to involve five underlying mechanisms: inflammation, inappropriate storage, infiltration, vascular congestion, and biliary obstruction (Wolf & Lavine, 2000). Since all these functions are active only after 5 dpf in zebrafish, the observation of liver enlargement is expected only at stages older than 5 dpf in agreement with our results.

The third test drug CHB is a less-DILI agent, which was not previously studied in the zebrafish liver toxicity model. A consistent trend of hepatomegaly was observed at all tested concentrations of CHB during the 2-5 dpf period. In contrast, when applied after 5 dpf, CHB exposure resulted in liver damage and a reduction in liver size. Notably, hepatomegaly is rarely reported in patients. Therefore, examination of CHB effects in both stages reflected possible clinical manifestations in the fish larval model. The 5-7 dpf larval stage proved to be better for studying CHB-induced hepatotoxicity. Hepatotoxicity caused by CHB is not very common, and the mechanisms of the toxicity are not well described. The toxicity detected in the zebrafish DILI model reported here supports the sensitivity of the test model.

The fourth test drug CHLP is a non-DILI agent that was selected as a negative control. As expected, CHLP did not affect the liver size in larvae of 2-5 dpf or 5-7 dpf. Our findings further demonstrate the suitability of CHLP

as a negative control in the liver size-based toxicity screening studies conducted on the zebrafish larvae.

In the present study, we revealed that DILI potentials of drugs significantly change depending on the stage of treatment in zebrafish (Figure 5). The toxic effects of APAP were found to be more prevalent in the developing liver, whereas the functional liver was more tolerant to APAP. On the other hand, the functional larval liver (between 5-7 dpf) was affected more by CHB treatment. Interestingly, iDILI agent INH-induced hepatomegaly was reproduced only in the larvae older than 5 dpf. On the other hand, non-DILI CHLP did not induce liver size change in either stage.
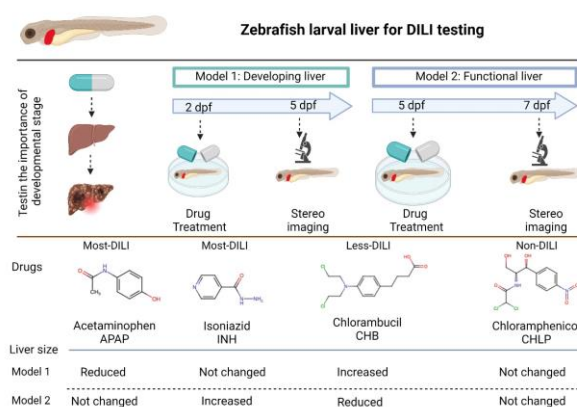
Figure 5. Graphical representation of study design and findings.

Conclusion

We found that the developmental stage of the zebrafish is critical for reproducing the clinical hepatotoxicity effects of drugs. Although zebrafish up to 5 dpf has been almost exclusively used for DILI testing, this study is the first to show that maturity status of larval liver is a critical factor affecting the test outcome. Researchers are advised not to overlook the importance of the zebrafish stage in drug-induced liver injury studies. This difference is likely to be due to difference in expression levels of drug detoxicification enzymes in tested stages. Testing of a wider collection of drugs in both developmental stages, together with metabolite and gene expression profiling may provide a better understanding of the underlying mechanisms.

Ethical Statement

Experimental procedure was approved by IBG Local Ethics Committe with 2021-005 protocol number.

Funding Information

Author Contributions

Conflict of Interest

The author(s) declare that they have no known competing financial or non-financial, professional, or personal conflicts that could have appeared to influence the work reported in this paper.

Acknowledgements

References

Akdogan, Y., Sozer, S. C., Akyol, C., Basol, M., Karakoyun, C., & Cakan-Akdogan, G. (2022). Synthesis of albumin nanoparticles in a water-miscible ionic liquid system, and their applications for chlorambucil delivery to cancer cells. *Journal of Molecular Liquids*, *367*, 120575. https://doi.org/10.1016/-j.molliq.2022.120575

Ali, S., Champagne, D. L., & Richardson, M. K. (2012). Behavioral profiling of zebrafish embryos exposed to a panel of 60 water-soluble compounds. *Behavioural Brain Research*, *228*(2), 272–283. https://doi.org//0.1016//j.bbr.2011.11.020

Almazroo, O. A., Miah, M. K., & Venkataramanan, R. (2017). Drug metabolism in the liver. *Clinics in liver disease*, *21*(1), 1-20. https://doi.org/10.1016/j.cld.2016.08.001

Andrade, R. J., Chalasani, N., Björnsson, E. S., Suzuki, A., Kullak-Ublick, G. A., Watkins, P. B., Devarbhavi, H., Merz, M., Lucena, M. I., & Kaplowitz, N. (2019). Drug-induced liver injury. *Nature Reviews Disease Primers*, *5*(1), 58. https://doi.org/10.1038/s41572-019-0105-0

Andrade, R. J., & Robles-Díaz, M. (2020). Diagnostic and prognostic assessment of suspected drug-induced liver injury in clinical practice. *Liver International*, *40*(1), 6–17. https://doi.org/10.1111/liv.14271

Cassar, S., Adatto, I., Freeman, J. L., Gamse, J. T., Iturria, I., Lawrence, C., Muriana, A., Peterson, R. T., Van Cruchten, S., & Zon, L. I. (2019). Use of zebrafish in drug discovery toxicology. *Chemical Research in Toxicology*, *33*(1), 95–118. https://doi.org/10.1021/acs.chemrestox.9b00335

Cakan-Akdogan, G., Aftab, A. M., Cinar, M. C., Abdelhalim, K. A., & Konu, O. (2023). Zebrafish as a model for drug induced liver injury: state of the art and beyond. *Exploration of Digestive Diseases*, *2*(2), 44-55. https://doi.org/10.37349/edd.2023.00017

Chan, R., & Benet, L. Z. (2017). Evaluation of DILI predictive hypotheses in early drug development. *Chemical Research in Toxicology*, *30*(4), 1017–1029. https://doi.org/10.1021/acs.chemrestox.7b00025

Chen, M., Vijay, V., Shi, Q., Liu, Z., Fang, H., & Tong, W. (2011). FDA-approved drug labeling for the study of drug-induced liver injury. *Drug Discovery Today*, *16*(15–16), 697–703. https://doi.org/10.1016/j.drudis.2011.05.007

Choi, T., Ninov, N., Stainier, D. Y. R., & Shin, D. (2014). Extensive conversion of hepatic biliary epithelial cells to hepatocytes after near total loss of hepatocytes in zebrafish. *Gastroenterology*, *146*(3), 776–788. https://doi.org/10.1053/j.gastro.2013.10.019

Chu, J., & Sadler, K. C. (2009). New school in liver development: lessons from zebrafish. *Hepatology*, *50*(5), 1656–1663. https://doi.org/10.1002/hep.23157

Cornet, C., Calzolari, S., Miñana-Prieto, R., Dyballa, S., Van Doornmalen, E., Rutjes, H., Savy, T., D'Amico, D., & Terriente, J. (2017). ZeGlobalTox: an innovative approach to address organ drug toxicity using zebrafish. *International Journal of Molecular Sciences*, *18*(4), 864. https://doi.org/10.3390/ijms18040864

Feder Jr, H. M. (1986). Chloramphenicol: what we have learned in the last decade. *Southern Medical Journal*, *79*(9), 1129–1134.

Garcia-Cortes, M., Robles-Diaz, M., Stephens, C., Ortega-Alonso, A., Lucena, M. I., & Andrade, R. J. (2020). Drug induced liver injury: an update. *Archives of Toxicology*, *94*, 3381–3407. https://doi.org/10.1007/s00204-020-02885-1

Goldstone, J. V, McArthur, A. G., Kubota, A., Zanette, J., Parente, T., Jönsson, M. E., Nelson, D. R., & Stegeman, J. J. (2010). Identification and developmental expression of the full complement of *Cytochrome P450* genes in Zebrafish. BMC Genomics, 11(1), 1–21. https://doi.org/10.1186/1471-2164-11-643

Guo, Q., Yang, W., Xiao, B., Zhang, H., Lei, X., Ou, H., Qin, R., & Jin, R. (2015). Study on early biomarkers of zebrafish liver injury induced by acetaminophen. Toxin Reviews, 34(1), 28–36. https://doi.org/10.3109/15569543.2014.986282

Higuchi, A., Wakai, E., Tada, T., Koiwa, J., Adachi, Y., Shiromizu, T., Goto, H., Tanaka, T., & Nishimura, Y. (2021). Generation of a Transgenic Zebrafish Line for In Vivo Assessment of Hepatic Apoptosis. *Pharmaceuticals*, *14*(11), 1117. https://doi.org/10.3390/ph14111117

Iruzubieta, P., Arias-Loste, M. T., Barbier-Torres, L., Martinez-Chantar, M. L., & Crespo, J. (2015). The need for biomarkers in diagnosis and prognosis of drug-induced liver disease: does metabolomics have any role? *BioMed Research International, 2015*(1), 386186. https://doi.org/10.1155/2015/386186

Jagtap, U., Basu, S., Lokhande, L., Bharti, N., & Sachidanandan, C. (2022). BML-257, a Small Molecule that Protects against Drug-Induced Liver Injury in Zebrafish. Chemical Research in Toxicology, 35(8), 1393–1399. https://doi.org/10.1021/acs.chemrestox.2c00100

Katoch, S., & Patial, V. (2021). Zebrafish: An emerging model system to study liver diseases and related drug discovery. *Journal of Applied Toxicology*, *41*(1), 33–51. https://doi.org/10.1002/jat.4031

Klotz, U. (2012). Paracetamol (acetaminophen)–a popular and widely used nonopioid analgesic. *Arzneimittelforschung*, *62*(08), 355–359. https://doi.org/10.1055/s-0032-1321785

Kyle, R. A., Greipp, P. R., Gertz, M. A., Witzig, T. E., Lust, J. A., Lacy, M. Q., & Therneau, T. M. (2000). Waldenström's

macroglobulinaemia: a prospective study comparing daily with intermittent oral chlorambucil. *British Journal of Haematology*, 108(4), 737–742. https://doi.org/10.1046/j.1365-2141.2000.01918.x

Lecaudey, V., Cakan-Akdogan, G., Norton, W. H. J., & Gilmour, D. (2008). Dynamic Fgf signaling couples morphogenesis and migration in the zebrafish lateral line primordium. *Development*, 135(16): 2695–2705. https://doi.org/10.1242/dev.025981

Lin, H.-S., Huang, Y.L., Wang, Y.-R. S., Hsiao, E., Hsu, T.A., Shiao, H.Y., Jiaang, W.T., Sampurna, B.P., Lin, K.H., & Wu, M.S. (2019). Identification of novel anti-liver cancer small molecules with better therapeutic index than sorafenib via zebrafish drug screening platform. *Cancers*, 11(6), 739. https://doi.org/739. 10.3390/cancers11060739

Metushi, I., Uetrecht, J., & Phillips, E. (2016). Mechanism of isoniazid-induced hepatotoxicity: then and now. *British Journal of Clinical Pharmacology*, 81(6), 1030–1036. https://doi.org/10.1111/bcp.12885

Nakayama, J., Tan, L., Li, Y., Goh, B. C., Wang, S., Makinoshima, H., & Gong, Z. (2021). A zebrafish embryo screen utilizing gastrulation identifies the HTR2C inhibitor pizotifen as a suppressor of EMT-mediated metastasis. *Elife*, 10, e70151. https://doi.org/10.7554/eLife.70151

Nanton, S. E., Bu-Ghanim, M., Ponnambalam, A., Nathan, R., & Fisher, S. E. (2004). Isoniazid induced fulminant hepatic failure in a teenager: 971. *American College of Gastroenterology*, 99, S319.

Nawaji, T., Yamashita, N., Umeda, H., Zhang, S., Mizoguchi, N., Seki, M., Kitazawa, T., & Teraoka, H. (2020). *Cytochrome P450* expression and chemical metabolic activity before full liver development in zebrafish. *Pharmaceuticals*, 13(12), 456. https://doi.org/10.3390/ph13120456

Nguyen, X.-B., Kislyuk, S., Pham, D.-H., Kecskés, A., Maes, J., Cabooter, D., Annaert, P., De Witte, P., & Ny, A. (2017). Cell imaging counting as a novel ex vivo approach for investigating drug-induced hepatotoxicity in zebrafish larvae. *International Journal of Molecular Sciences*, 18(2), 356. https://doi.org/10.3390/ijms18020356

North, T. E., Babu, I. R., Vedder, L. M., Lord, A. M., Wishnok, J. S., Tannenbaum, S. R., Zon, L. I., & Goessling, W. (2010). PGE2-regulated wnt signaling and N-acetylcysteine are synergistically hepatoprotective in zebrafish acetaminophen injury. *Proceedings of the National Academy of Sciences*, 107(40), 17315–17320. https://doi.org/10.1073/pnas.1008209107

Park, Y. M., Dahlem, C., Meyer, M. R., Kiemer, A. K., Müller, R., & Herrmann, J. (2022). Induction of Liver Size Reduction in Zebrafish Larvae by the Emerging Synthetic Cannabinoid 4F-MDMB-BINACA and Its Impact on Drug Metabolism. Molecules, 27(4), 1290. https://doi.org/10.3390/molecules27041290

Patel, S. P. (2000). First report of liver failure: case report. Reactions, 818, 9. https://doi.org/10.2165/00128415-200008180-00016

Patel, S. P., Nast, C. C., & Adler, S. G. (2000). Chlorambucil-induced acute hepatic failure in a patient with membranous nephropathy. *American Journal of Kidney Diseases*, 36(2), 401–404. https://doi.org/10.1053/ajkd.2000.8995

Robles-Díaz, M., Medina-Caliz, I., Stephens, C., Andrade, R. J., & Lucena, M. I. (2016). Biomarkers in DILI: one more step forward. *Frontiers in Pharmacology*, 7, 267. https://doi.org/10.3389/fphar.2016.00267

Sato, Y., Dong, W., Nakamura, T., Mizoguchi, N., Nawaji, T., Nishikawa, M., Onaga, T., Ikushiro, S., Kobayashi, M., & Teraoka, H. (2023). Transgenic Zebrafish Expressing Rat *Cytochrome P450 2E1* (*CYP2E1*): Augmentation of Acetaminophen-Induced Toxicity in the Liver and Retina. *International Journal of Molecular Sciences*, 24(4), 4013. https://doi.org/10.3390/ijms24044013

Shah, R., Ankale, P., Sinha, K., Iyer, A., & Jayalakshmi, T. K. (2016). Isoniazid induced lupus presenting as oral mucosal ulcers with pancytopenia. *Journal of Clinical and Diagnostic Research*, 10(10), OD03. https://doi.org/10.7860/JCDR/2016/22543.8629

Sienkiewicz, P., Bielawski, K., Bielawska, A., & Pałka, J. (2005). Inhibition of collagen and DNA biosynthesis by a novel amidine analogue of chlorambucil is accompanied by deregulation of β1-integrin and IGF-I receptor signaling in MDA-MB 231 cells. *Environmental Toxicology and Pharmacology*, 20(1), 118–124. https://doi.org/10.1016/j.etap.2004.11.001

Singhal, K.K., Mukim, M.D., Dubey, C.K., & Nagar, J.C. (2020). An Updated Review on Pharmacology and Toxicities Related to Chloramphenicol. *Asian Journal of Pharmaceutical Research and Development, 8*(4), 104–109. https://doi.org/10.22270/ajprd.v8i4.671

Skoutelis, A. (2000). Chlorambucil/methylprednisolone. *Reactions*, 811, 22. https://doi.org/10.2165/00128415-200008110-00011

Tierbach, A., Groh, K. J., Schönenberger, R., Schirmer, K., & Suter, M. J.-F. (2018). Glutathione S-transferase protein expression in different life stages of zebrafish (Danio rerio). *Toxicological Sciences*, 162(2), 702–712. https://doi.org/10.1093/toxsci/kfx293

Vliegenthart, A. D. B., Tucker, C. S., Del Pozo, J., & Dear, J. W. (2014). Zebrafish as model organisms for studying drug-induced liver injury. *British Journal of Clinical Pharmacology*, 78(6), 1217–1227. https://doi.org/10.1111/bcp.12408

Wolf, A. D., & Lavine, J. E. (2000). Hepatomegaly in neonates and children. *Pediatrics in Review*, 21(9), 303–310. https://doi.org/10.1542/pir.21-9-303

Zhang, X., Li, C., & Gong, Z. (2014). Development of a convenient in vivo hepatotoxin assay using a transgenic zebrafish line with liver-specific *DsRed* expression. *PloS One*, 9(3), e91874. https://doi.org/10.1371/journal.pone.0091874

Zhang, Y., Cen, J., Jia, Z., Hsiao, C.-D., Xia, Q., Wang, X., Chen, X., Wang, R., Jiang, Z., & Zhang, L. (2019). Hepatotoxicity induced by isoniazid-lipopolysaccharide through endoplasmic reticulum stress, autophagy, and apoptosis pathways in zebrafish. *Antimicrobial Agents and Chemotherapy*, 63(5), e01639-18. https://doi.org/10.1128/aac.01639-18

BIOTECH STUDIES

R E S E A R C H   P A P E R

Effects of turmeric meal supplementations on performance, carcass traits, and meat antioxidant enzymes of broilers fed diets containing monosodium glutamate

Olumuyiwa Joseph Olarotimi (iD)

Department of Animal Science, Faculty of Agriculture, Adekunle Ajasin University, P.M.B. 001, Akungba-Akoko, Nigeria

Abstract

The use of monosodium glutamate (MSG) as a potential taste enhancer in poultry nutrition is discouraged due to its perceived adverse effects. Hence, this study evaluated the impacts of turmeric powder (TP) on performance and some meat qualities of chickens fed MSG. Three hundred broilers were divided into four diets: T_1 (control), T_2 (1.25 g MSG/kg), T_3 (1.25 g MSG/kg and 1.25 g TP/kg), and T_4 (1.25 g MSG/kg and 2.50 g TP/kg). Results indicated increased ($P<0.05$) feed intake with a decrease ($P<0.05$) in weight gain resulting in poor feed conversion ratio ($P<0.05$) in T_2. However, inclusions of TP positively enhanced ($P<0.05$) these parameters in T_3 and T_4. Carcass characteristics did not differ significantly ($P>0.05$) between T_1 and T_2 but were improved ($P<0.05$) in T_3 and T_4. Organ weights were higher ($P<0.05$) in T_2 but were restored ($P<0.05$) in T_3 and T_4. While meat CAT and GSH-Px decreased ($P<0.05$), and MDA and cholesterol increased ($P<0.05$) in T_2, significant reversal of these trends was observed in T_3 and T_4. Hence, the inclusion of MSG without TP led to compromised performance, carcass, organ weights, and meat antioxidant enzymes in T_2 while they were ameliorated in T_3 and T_4.

Introduction

Several factors influence the feed consumption of broiler chickens, consequently impacting nutrient intake levels, production efficiency, and the profitability of the enterprise. While various factors affect feed intake, farmers often overlook the role of feed palatability. The palatability of feed largely depends on the ingredients used, with unappealing smells and tastes leading to reduced intake and diminished returns on investment (Maroof et al., 2017). Moreover, non-conventional feedstuffs, although cheaper and easily accessible, are generally less preferred by chickens (Ababor et al., 2023).

Factors like spoilage due to the rancidity of fats and oils, sugar molding, and protein putrefaction, commonly found in long-term stored feed, can also adversely affect feed palatability. Deteriorating feed quality leads to the development of aversive flavors and odors for the birds (Windisch et al., 2008). To address these challenges and improve productivity, farmers may consider using feed additives like monosodium glutamate (MSG) to enhance feed palatability (Khalil & Khedr, 2016). MSG is renowned for intensifying the savory flavor of food, as natural glutamate does in various cuisines (Ikeda, 2002). Several studies have highlighted the positive impact of MSG on feed intake and animal performance. For instance, Osman & Mohammed (2021) observed a statistically significant increase in both feed consumption and body mass gain in broilers when

subjected to 5 g/L concentration of MSG. Gbore et al. (2016) observed that MSG had favorable effects on feed intake, body weight gains, and feed conversion ratio in female rabbits. Similarly, Rezaei et al. (2022) found a significant increase in piglet weight growth when gilts were fed a diet containing 1.15% MSG.

Nevertheless, it has been hypothesised that the overconsumption of MSG in livestock diets may have detrimental impacts on the overall health and welfare of farm animals (Zanfirescu et al., 2019). According to Olarotimi (2020), it was suggested that the excessive incorporation of MSG at levels exceeding 0.5g/kg in the diet of broilers resulted in the development of oxidative stress and a decline in overall antioxidant capacity. The use of excessive amounts of MSG has been associated with alterations in antioxidant systems and renal indicators, as suggested by Paul et al. (2012). According to Sharma et al. (2013), there was a considerable increase in the serum electrolyte levels of rats that were administered high quantities of MSG, as compared to the control group. According to the findings of Olarotimi et al. (2020), it was observed that the inclusion of MSG at a concentration of 1.00 g/kg diet and higher resulted in a decrease in both daily sperm production and efficiency in cocks. Consequently, the researchers concluded that a high level of MSG in the diets of male chickens has the potential to considerably diminish their reproductive capabilities.

To counteract the potential negative effects of MSG, incorporating antioxidants as feed additives has emerged as a promising strategy. The use of organic antioxidants, particularly phyto-additives like turmeric (Curcuma longa), has gained significant research attention (Kermanshahi & Riasi, 2006; Olarotimi, 2018). Turmeric has been recognized for its various properties, including being an antimicrobial, anti-inflammatory, and antioxidant agent. It contains essential minerals and antioxidants, which contribute to its potential as a beneficial feed additive for broiler chickens (Adegoke et al., 2018; Youssef et al., 2014). Thus, the aim of this study was to evaluate the effects of incorporating turmeric meals in the diets of broiler chickens fed high dietary MSG, focusing on their performance and meat antioxidative enzymes.

Materials and Methods

Experimental materials, site, design, and animals

Turmeric powder was obtained by first sourcing fresh turmeric rhizomes from the local market, and they were thoroughly washed with clean water to remove any extraneous materials and then drained. Thereafter, the rhizomes were grated and air-dried under a shade for a week. After they were thoroughly dried, they were milled to produce turmeric powder (TP). The MSG used was procured from the nearest departmental store. The study was conducted at the Poultry Unit, Teaching and Research Farm of Adekunle Ajasin University, Akungba Akoko, Nigeria, after obtaining approval from the University's Research and Ethics Committee for the ethical use and care of animals. Ethics Reference No: AAUA/FA/ANS/014/2024. Three hundred (300) day-old, mixed sex Arbor-acre broiler chicks were purchased from a dependable hatchery. Their weights were captured and documented before they were randomly assigned to four treatment groups labeled as T1, T2, T3, and T4. These groups received diets containing different quantities of MSG and TP per kilogram of food: (0.00 g MSG and TP), (1.25 g MSG), (1.25 g MSG and 1.25 g TP), and (1.25 g MSG and 2.50 g TP) respectively. Each of the four treatment groups was replicated five times, with each replication consisting of 15 birds. Throughout the six-week experiment, the chicks were provided with starter and finisher diets (Table 1) and had unrestricted access to fresh water for the whole experimental weeks.

Table 1. Gross composition of the basal diet for the experimental birds

Ingredients(kg)	Starter (1 to 3 weeks)	Finisher (4 to 6 weeks)
Maize	47	57
Corn bran	10	10
Rice bran	5	5
Soybean meal	15	15
Groundnut cake	15	5
Fish meal	5	5
Bone meal	1.2	1.1
Limestone	0.8	1.1
Lysine	0.3	0.2
Methoinine	0.25	0.15
Salt	0.2	0.2
Vitamin-Mineral Premix	0.25	0.25
Total	**100**	**100**
Calculated Nutrients		
ME (Kcal/Kg)	2975.04	3054.24
Crude Protein (%)	23.01	19.31
Fat	5.34	5.16
Calcium (%)	1.1	1.15
Phosphorus (%)	0.49	0.46
Lysine (%)	1.35	1.12
Methionine (%)	0.62	0.49
Crude Fibre (%)	4.17	3.94

Experimental data collection

The body weight gain (BWG) and feed intake (FI) were documented on a weekly basis. The weekly feed conversion ratio (FCR) was estimated as follows:

FCR = FI/BWG

At the end of the feeding trial, 25 birds per treatment (5 birds per replicate) were selected randomly and humanely sacrificed. The weights of the eviscerated organs such as the lungs, gizzard, heart, kidneys, and liver were captured and recorded using a sensitive laboratory weighing balance. The dressing percentage as the percentage ratio of the live weight to that of the dressed weight of the birds determined. The intestinal microflora population was determined according to Engberg et al. (2004) and Tsiouris et al. (2020). Briefly, the intestinal contents were extracted into a sterile 15-mL container and subsequently homogenized in 9 mL of sterile PBS (Phosphate Buffered

Solution). Serial tenfold dilutions ranging from 10^3 to 10^7 were then prepared. Lactobacilli enumeration was conducted using De Man–Rogosa–Sharpe (MRS) agar, with plates incubated anaerobically at 37 °C for 48 h to calculate lactic acid bacteria counts. Total anaerobic bacteria were enumerated using Plate Count Agar (PCA) and anaerobic incubation at 37 °C for 48 h, with anaerobiosis achieved by placing the inoculated plates in a jar. The anaerobic environment was generated using Anaerocult® and confirmed using Anaerotest®. Lactose-negative bacteria were counted on MacConkey agar, with colonies appearing as red and colorless after aerobic incubation at 38°C for 24 h. Furthermore, breast meats were sampled after dressing and evisceration to determine the antioxidant enzymes of the meat. The meat catalase, glutathione peroxidase, and cholesterol activities were determined as described by Farman & Hadwan (2021) and reported by Olarotimi et al. (2022). Briefly, the samples were packaged aerobically in oxygen-permeable bags and stored in a freezer at -18°C for a duration of 20 days. Subsequently, the extent of lipid oxidation in the meat was assessed using the thiobarbituric acid (TBA) assay method. Catalase activity in the meat was determined by monitoring the reduction in absorbance at 240 nm, indicative of hydrogen peroxide (H_2O_2) consumption. Glutathione peroxidase activity was determined by spectrophotometric monitoring of $NADPH^+$ oxidation at a wavelength of 340 nm. The total cholesterol concentration of the meat was determined by colorimetric method and the values were read at the absorbance of 550 nm.

Statistical analysis

Data collected were subjected to One-Way Analysis of Variance (ANOVA) using SAS (2008, software version 9.2). Significant differences between the treatment means were compared using Tukey's Honestly Significant Difference (HSD) option of the same software at 5% level of significance.

Results and Discussion

Performance of broilers fed diets containing Monosodium Glutamate and turmeric powder

The outcomes from the evaluation of broilers that were provided with diets containing varying amounts of MSG and TP are shown in Table 2. Throughout the trial stages, notable decreases ($P<0.05$) were observed in the body weight gains (BWG) of the birds on T_2 compared to those on the control diet (T1). Conversely, the inclusion of 1.25 and 2.5 g TP/kg diet led to significant ($P<0.05$) improvements in the BWG during both experimental phases and overall, in contrast to the broilers on T_1 and T_2. Notably, the birds on a diet T_4 exhibited the most favorable BWG. Similarly, the starter, finisher, and overall total feed intake (TFI) among the birds fed with 1.25 g MSG/kg diet alone (T_2) were significantly ($P<0.05$) higher than the TFI recorded among the birds on the control diet. Conversely, the TFI observed among birds fed diets with varying amounts of TP were significantly ($P<0.05$) lower than those on T_2. Birds on diet T_4 demonstrated lower TFI compared to those on T_3, although the difference was not statistically significant ($P>0.05$). However, both diets T_3 and T_4 displayed significantly ($P<0.05$) higher TFI when compared to the control diet.

Regarding the feed conversion ratio (FCR), broilers on diet T_2 showed the least significant ($P<0.05$) values as against the FCR by birds on diets T_1, T_3 and T_4 respectively at the starter and finisher phases as well as the overall. The FCR values among the birds on diets T_3 and T_4 were statistically similar ($P>0.05$) to those of the control diet during both the starter and finisher phases of the experiment. However, the FCR recorded among the birds on diet T_3 during the overall phase was significantly higher ($P<0.05$) than the values obtained for the birds fed diet T_4 and the control diet.

Performance metrics, including BWG, TFI, and FCR, are commonly employed to assess the effectiveness and profitability of poultry farming. The noticeable increase in TFI among the birds fed MSG during all experimental

Table 2. Performance of broilers fed diets containing MSG and turmeric powder

Parameters	T_1	T_2	T_3	T_4	SEM	P-value
Starter Phase (1 to 21 days)						
Initial Body Weight (g/bird)	35.00	34.20	33.60	33.20	0.54	0.31
Body Weight Gain (g/bird)	650[b]	619[c]	668[a]	673[a]	38.7	0.02
Feed Intake (g/bird)	1510[c]	1830[a]	1620[b]	1550[b]	58.7	0.02
Feed Conversion Ratio	2.32[b]	2.96[a]	2.43[b]	2.30[b]	0.16	0.01
Finisher Phase (22 to 42 days)						
Body Weight Gain (g/bird)	1510[b]	1480[c]	1640[a]	1670[a]	111	0.03
Total Feed Intake (g/bird)	3220[c]	3670[a]	3580[b]	3540[b]	180	0.01
Feed Conversion Ratio	2.13[b]	2.48[a]	2.18[b]	2.12[b]	0.19	0.01
Overall (1 to 42 days)						
Body Weight Gain (g/bird)	2160[c]	2099[d]	2308[b]	2343[a]	106	0.01
Total Feed Intake (g/bird)	4730[d]	5500[a]	5200[b]	5090[c]	189	0.02
Feed Conversion Ratio	2.19[c]	2.62[a]	2.25[b]	2.17[c]	0.12	0.01

Values are means and SEM (Standard Error of Means). Means in a row without a common superscript letter differ significantly ($P<0.05$). Diets: T_1 (control), T_2 (1.25 g MSG/kg), T_3 (1.25 g MSG/kg and 1.25 g TP/kg), and T_4 (1.25 g MSG/kg and 2.50 g TP/kg).

stages suggested that the incorporation of MSG up to 1.25 g/kg in broiler diets, as implemented in this study, is an effective nutritional tactic for enhancing the taste of poultry feed. This finding further corroborated earlier research, which consistently highlighted the positive effects of MSG on the FI and BWG of livestock (Gbore et al., 2016; Olarotimi & Adu, 2022; Osman & Mohammed, 2021; Zhelyazkov, 2018).

However, despite the increased TFI recorded in this study, the significant decrease observed in the BWG among the broilers on diet T_2 suggested that a high MSG inclusion in broiler diets might impede BWG. This is in line with the assertions of Kondoh & Toril (2008) that a high MSG inclusion rate in diets could induce stress, leading to heightened energy expenditure and subsequently reduced BWG in animals. Similarly, Yamazaki et al. (2011) observed diminished body weight in rats fed a high MSG diet, despite an increase in FI, attributing it to reduced growth and sex hormone activity or decreased fat content and deposition.

Furthermore, the inclusion of 1.25 and 2.50 g TP/kg diet proved to be effective in enhancing the BWG of broilers on diets T_3 and T_4, with a corresponding reduction in TFI compared to birds on diet T_2. Additionally, the FCR of birds on diets containing TP was better than those of birds fed a diet without TP. The positive impact of TP on broilers fed a high MSG inclusion could be attributed to its rich reservoir of bioactive compounds. Previous studies reported improved growth performance in broiler chickens fed a diet with 0.2 g/kg TP (Rajput et al., 2013). Kafi et al. (2017) also documented improved BWG, FI, and FCR in broilers supplemented with 0.75% turmeric. The results aligned with Durrani et al. (2006), who noted increased BWG and FCR with a significant reduction in FI in broilers fed 0.5% TP.

The significant enhancement in body weight observed throughout all experimental stages at the TP inclusion levels utilized in our study may be attributed to the antioxidant activity of turmeric, capable of stimulating protein synthesis by the animal's enzymatic system. The substantial reduction in FI among broilers fed MSG with TP, compared to those fed only MSG, concurred with Emadi & Kermanshahi (2007), who reported a significant reduction effect of turmeric on FI alongside corresponding BWG. Earlier reports also documented the best FCR among birds fed TP (Durrani et al., 2006, Raghdad & Al-Jaleel 2012), attributing this to the enhanced dietary efficiency among broilers fed TP at the levels used in this study.

Carcass traits, relative organ weights, and intestinal microflora of broilers fed MSG and TP

The data on carcass attributes, relative organ weights, and intestinal microflora of the birds fed MSG alongside varying amounts of TP are presented in Table 3. The results of the current study indicated no significant difference (*P>0.05*) in the final live weights (FLW), dressed weights (DW), and dressed percentages (DP) of the birds on both T_1 and T_2. Nevertheless, significant (*P<0.05*) increases were noted in FLW, DW, and DP among the birds on diets T_3 and T_4 compared to birds on both T_1 and T_2, with T_4 showing the most significant increase. The relative weights of the hearts, livers, bile, and lungs of the birds on T_2 were found to be notably (*P>0.05*) higher than those recorded among the control birds, as well as T_3 and T_4 when compared. The gizzard, proventriculus, and spleen as well as intestinal microflora of the birds across all treatments were not significantly affected (*P>0.05*).

The absence of significant differences recorded for FLW, DW, and DP among broilers fed diet T_2 indicated that the inclusion of MSG at 1.25 g/kg diet did not enhance the carcass characteristics of broiler chickens. Increased carcass breast meat quantity and decreased abdominal fat are among the critical factors used to assess the profitability of broiler production (Adetunji et al., 2019). However, the fortification of these MSG-treated diets with 1.25 and 2.5 g TP/kg diet demonstrated the potential of TP in enhancing the overall meat quality of broiler chickens, countering the limiting effects of MSG on carcass and meat quality. The significant increases observed in the FLW, DW, and DP was evidence of the positive effects of turmeric powder

Table 3. Carcass traits, relative organ weights and intestinal microflora of broilers fed MSG and turmeric powder

Parameters	T_1	T_2	T_3	T_4	SEM	P-value
Carcass Characteristics						
Final Live Weight (g/bird)	2195.00[b]	2133.30[b]	2341.60[a]	2376.2[a]	122	0.01
Dressed Weight (g/bird)	1950[c]	1907[c]	2150[b]	2200[a]	109	0.01
Dressed Percentage (%)	88.84[b]	89.39[b]	91.82[a]	92.58[a]	4.18	0.02
Relative Organ Weights						
Heart	2.39[b]	3.93[a]	2.51[b]	2.22[b]	0.18	0.01
Liver and Bile	11.30[b]	17.00[a]	11.90[b]	11.10[b]	0.71	0.01
Gizzard and Proventriculus	16.80	16.70	16.57	16.30	0.83	0.11
Lungs	4.16[ab]	4.54[a]	3.70[b]	4.11[ab]	0.20	0.01
Spleen	0.87	0.76	0.78	0.76	0.03	0.34
Intestinal Microflora						
Aerobic Bacteria	7.57	7.78	7.30	7.74	0.37	0.28
Lactobicillus	7.44	7.59	7.56	8.37	0.37	0.13
Lactose Negative	6.90	6.39	6.87	7.30	0.23	0.30

Values are means and SEM (Standard Error of Means). Means in a row without a common superscript letter differ significantly (*P<0.05*). Diets: T_1 (control), T_2 (1.25 g MSG/kg), T_3 (1.25 g MSG/kg and 1.25 g TP/kg), and T_4 (1.25 g MSG/kg and 2.50 g TP/kg).

on enhancing carcass traits. Our findings were in complete agreement with the findings of Raghdad & Al-Jaleel (2012), who reported a substantial increase in the dressing yield of chickens fed diets supplemented with turmeric.

The observed elevation in the relative organ weights of the heart, lungs, liver, and bile among the broilers fed a diet containing 1.25 g MSG/kg diet indicated the hypertrophic effects of high MSG inclusion in broiler diets on the vital organs of broiler chickens, which could potentially lead to serious health challenges for the animals. For instance, the hypertrophy of the heart signifies an increased thickness of the heart muscle, which typically predisposes affected animals to cardiovascular damage. El Malik & Sabahelkhier (2019) and Okon et al. (2013) previously reported a significant increase in the tissue weight of the heart in rats fed elevated levels of MSG. Additionally, the hepatotoxic effects of MSG have been previously emphasized (Dharita et al., 2023). The enlarged liver and bile weights observed among broilers fed a diet containing 1.25 g MSG/kg diet confirmed the hepatotoxic potential of MSG, particularly when administered at high levels and for an extended duration. Banerjee et al. (2021) explained that liver hypertrophy occurs due to the dilatation of the central hepatic vein with lysed erythrocytes and distorted hepatocytes, caused by impaired membrane permeability resulting from high MSG inclusion.

However, the ameliorative effects of TP at the two inclusion levels used in the present study were clearly evident. The antioxidant and anti-inflammatory properties of turmeric may have been responsible for the significant reduction in the weights of the lungs, heart, liver, and bile among broilers on diets T_3 and T_4, making them comparable to the values recorded for broilers on the control diet. The decreased lung, liver, and heart relative weights of birds fed TP indicated the nephroprotective, hepatoprotective, and anti-inflammatory properties of TP, demonstrating its restorative effects when used as dietary supplements in broilers fed diets containing MSG for improved palatability. MSG has been proven to generate reactive oxygen species (ROS), causing oxidative stress (Olarotmi, 2020, Olarotimi & Adu, 2022). Turmeric, on the other hand, is a known phyto-additive that contains natural antioxidants (Olarotimi, 2018). It is capable of scavenging the ROS generated by high MSG inclusion, thus safeguarding the vital organs of the body against oxidative stress. Since the dietary incorporation of phytogens in broiler diets has been reported to reduce cholesterol levels in meat and liver (Oloruntola et al., 2018), the reduced cholesterol concentration in the liver of the broilers on diets T_3 and T_4 in this study may explain the lower weights of the liver compared to the liver weights of birds on diet T_2. Consumers of meat from broilers fed TP would also benefit from its anti-cholesterolemic effects, resulting in the production of leaner meat and potentially protecting humans from the risks of hypercholesterolemia, atherosclerosis, and coronary heart diseases (Shen et al., 2019). The proper functioning of the gastrointestinal tract (GIT) and the composition of the gut microbial population are crucial for effective nutrient absorption, immune system development, and resilience against diseases in chickens. Changes in the composition of the GIT microbial community can negatively impact feed efficiency, productivity, and overall health outcomes for poultry (Shang et al., 2018). From this study, the gut integrity of the broilers was maintained, as the inclusions of MSG and TP did not individually or synergistically alter the intestinal microflora counts of the birds. The role of non-pathogenic intestinal bacteria in inhibiting pathogen proliferation, enhancing growth performance, and reducing morbidity and mortality in poultry cannot be overstated (Abd El-Hack et al., 2022).

Meat antioxidant status and cholesterol of broilers fed MSG and turmeric powder

Figures 1 to 4 depict the meat antioxidant enzymes and cholesterol levels of broilers fed diets with a high inclusion of MSG, both with and without the addition of turmeric powder. The current study revealed that the meat catalase (CAT) (Figure 1) and glutathione peroxidase (GSH-Px) (Figure 2) activities in the meat from broilers fed T_2 were significantly ($P<0.05$) reduced compared to the values recorded among the control birds for the same parameters. However, the inclusion of both 1.25 and 2.50 g TP/kg diet significantly ($P<0.05$) increased the antioxidant enzyme activities of the meat among broilers on diets T_3 and T_4, respectively, when compared with birds on T_2, with significantly higher values recorded among the broilers on diet T_4 for both parameters. Furthermore, the concentrations of meat malondialdehyde (MDA) (Figure 3), and cholesterol (Figure 4) were found to be significantly ($P<0.05$) higher among the broilers on diet T_2 compared to birds from other diets, respectively. Although the inclusion of 1.25 g TP/kg diet significantly reduced the values of these parameters among broilers on T_3, it still remained higher ($P<0.05$) than the values recorded among the birds on the control diet for the same parameters. Notably, doubling the inclusion of TP in diet T_4 significantly ($P<0.05$) further decreased the meat MDA and cholesterol concentrations to a level comparable ($P>0.05$) with the values recorded on the control diet.
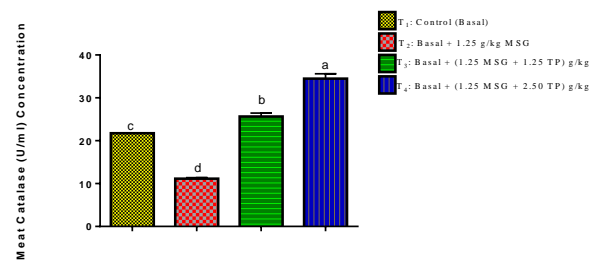

Figure 1. Meat catalase of broilers fed MSG and turmeric powder.

It is evident that the inclusion of MSG at 1.25 g/kg diet in broilers' diet compromised the oxidative stability of the meat as well as its cholesterol concentrations. The meat CAT and GSH-Px were noticeably depressed among the broilers fed diet T_2, while the MDA and meat cholesterol were significantly elevated. The primary function of antioxidative enzymes in meat is to preserve it against oxidative decomposition (Gbore et al., 2021). Cellular damage controlled by the absorption of superoxide and hydrogen peroxide occurs in meat whenever there is a reduction in the activities of antioxidative enzymes and an increase in MDA and meat cholesterol. This study suggests that the high inclusion of MSG promotes higher meat lipid peroxidation and cholesterol deposition due to the significantly higher meat MDA and cholesterol concentrations observed among broilers fed diet containing MSG. Adetunji et al. (2019) previously proposed that the inclusion of MSG up to 1.00 g/kg in broiler diets did not compromise meat quality parameters such MDA and antioxidative enzymes. The lipid peroxidation and antioxidant capacity of meat are typically indirectly linked (Gbore et al., 2021), highlighting the reason for an increase in lipid peroxidation of the breast meat in response to reduced antioxidative enzyme activities among the broilers fed MSG. Consequently, this implies a deterioration in meat quality among the birds fed MSG, posing significant health risks to humans as lipid peroxidation favors implies morbidity (Gbore et al., 2021).
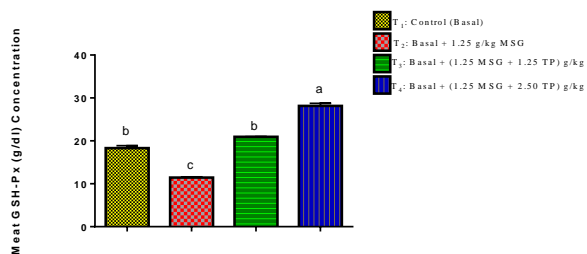

Figure 2. Meat glutathione peroxidase of broilers fed MSG and turmeric powder.

Noteworthy is the ameliorative role of the inclusion of TP at 1.25 and 2.5 g/kg diet in this study, clearly restoring the quality of the meat from the broilers, as observed among the birds fed diets T_3 and T_4, respectively. The restorative effect of TP observed on meat antioxidative enzymes of broilers fed diets T_3 and T_4 suggests that turmeric has a complementary effect on the concentrations of catalase and glutathione peroxidase, resulting in improved meat antioxidant status of the birds. From this study, it can be deduced that the ameliorative effects of turmeric are quantity-dependent, as better enhancement of the meat antioxidant enzymes was recorded among the broilers on diet T_4. The results also confirmed the cholesterolemic potentials of MSG as well as the anticholesterolemic effects of turmeric. The presence of curcumins in turmeric is responsible for its antioxidant activities and its capability to stimulate superoxide

dismutase, catalase, and glutathione peroxidase activities, as well as its anticholesterolemic property (Olarotimi, 2018). Earlier studies have also reported the tendency of phytogens to mitigate meat lipid peroxidation (Gbore et al., 2021; Oloruntola et al., 2018). The apparent reduction in meat cholesterol concentration in response to an increasing level of TP further strengthens the anticholesterolemic effects of turmeric.
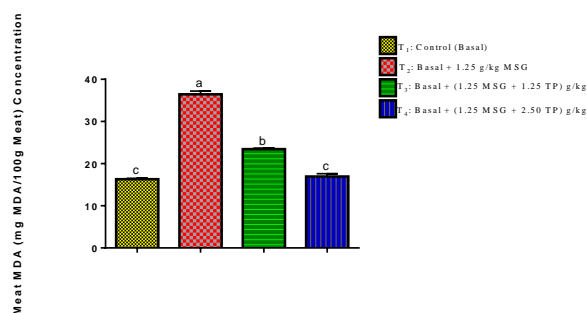
Figure 3. Meat malondialdehyde of broilers fed MSG and turmeric powder.

Overall, incorporating MSG at 1.25 g/kg diet in broilers' diets enhanced feed palatability, resulting in increased feed intake but without corresponding body weight gain and improvement in feed conversion ratio. There was no enhancement in the dressed weight and dressed weight percentage of the broilers. Furthermore, the inclusion of MSG appeared to potentially compromise the integrity of internal organs, including the heart, lungs, liver and bile. The study also indicated a significant reduction in meat catalase and glutathione peroxidase levels, accompanied by notable increases in lipid peroxidation and cholesterol. However, the incorporation of TP at 1.25 and 2.5 g/kg diet played a restorative role by enhancing the performance and carcass traits, along with the enhancement of the antioxidative enzymes of the meat.
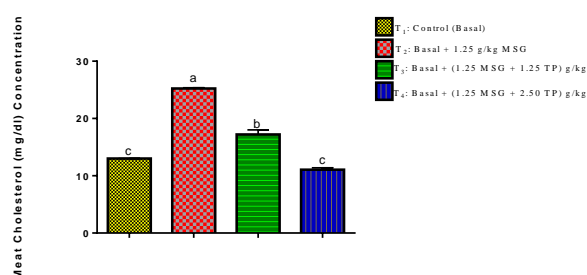
Figure 4. Meat cholesterol of broilers fed MSG and turmeric powder.

Conclusion

In conclusion, the findings of this study shed light on the effects of incorporating MSG and TP in broiler diets. While MSG at 1.25 g/kg diet enhanced feed palatability, it did not translate into improvements in body weight gain or feed conversion ratio. Moreover, it

appeared to have adverse effects on the integrity of internal organs and meat quality parameters. Conversely, the inclusion of TP at 1.25 and 2.5 g/kg diet showed promising results, enhancing performance, carcass traits, and antioxidative enzymes in meat. Of particular note, diets containing 2.50 g/kg TP demonstrated the most favorable outcomes. Based on these findings, it is recommended to feed broilers with a diet containing 1.25 g/kg MSG alongside 2.50 g/kg TP inclusion to optimize broiler production.

Ethical Statement

The entire procedure complied with the guidelines for the Care and Use of Laboratory Animals, and the experimental protocol was approved by institution's Animal Research Ethics Committee. Ethics Reference No: AAUA/FA/ANS/4759/2023.

Acknowledgements

References

Ababor, S., Tamiru, M., Alkhtib, A., Wamatu, J., Kuyu, C. G., Teka, T. A., Terefe, L. A. & Burton, E. (2023). The use of biologically converted agricultural byproducts in chicken nutrition. *Sustainability*, *15(19),* 14562. https://doi.org/10.3390/su151914562

Abd El-Hack, M.E., El-Saadony, M.T., Salem, H.M., El-Tahan, A.M., Soliman, M.M., Youssef, G.B.A., Taha, A.E., Soliman, S.M., Ahmed, A.E., El-Kott, A.F., Al Syaad, K.M., & Swelum, A.A. (2022). Alternatives to antibiotics for organic poultry production: types, modes of action and impacts on bird's health and production. *Poultry science*, *101(4),* 101696. https://doi.org/10.1016/j.psj.2022.101696

Adegoke, A.V., Abimbola, M.A., Sanwo, K.A., Egbeyale, L.T., Abiona, J.A., Oso, A.O. & Iposu, S.O. (2018). Performance and blood biochemistry profile of broiler chickens fed dietary turmeric (*Curcuma longa*) powder and cayenne pepper (*Capsicum frutescens*) powders as antioxidants. *Veterinary and Animal Science*, *6*, 95–102. https://doi.org/10.1016/j.vas.2018.07.005

Adetunji, A.O., Olarotimi, O.J., Adu, O.A., Oladeji, I.S. & Onibi, G.E. (2019). Meat quality and consumer acceptability of broiler chickens fed different levels of monosodium glutamate (MSG). *Journal of Poultry Research, 16 (1),* 1-6. https://doi.org/10.34233/jpr.483081

Banerjee, A., Mukherjee, S. & Maji, B. K. (2021). Worldwide flavor enhancer monosodium glutamate combined with high lipid diet provokes metabolic alterations and systemic anomalies: An overview. *Toxicology reports*, *8*, 938–961. https://doi.org/10.1016/j.toxrep.2021.04.009

Dharita M.J., Varsha T.D., Shyamla R.K., Harshada B.P. & Pallavi M.M. (2023). Effect of monosodium glutamate on hepatotoxicity and nephrotoxicity: A mini review. *World Journal of Biology Pharmacy and Health Sciences, 15(1),* 152–159. https://doi.org/10.30574/wjbphs.2023.15.1.0318

El Malik, A. & Sabahelkhier, M.K. (2019). Changes in lipid profile and heart tissues of wistar rats induce by using monosodium glutamate as food additive. *International Journal of Biochemistry and Physiology, 4(1),* 141-147. https://doi.org/10.23880/ijbp-16000147

Emadi, M. & Kermanshahi, H. (2007). Effect of turmeric rhizome powder on the activity of some blood enzymes in broiler chickens. *International Journal of Poultry Science*, 6, 48-51. https://doi.org/10.3923/ijps.2007.48.51

Engberg, R.M., Hedemann, M.S., Steenfeldt, S. & Jensen, B.B. (2004). Influence of whole wheat and xylanase on broiler performance and microbial composition and activity in the digestive tract. *Poultry Science,*. *83(6,* 925-38. https://10.1093/ps/83.6.925

Farman, A.A. & Hadwan, M.H. (2021). Simple kinetic method for assessing catalase activity in biological samples. *MethodsX*, *8*, 101434. https://doi.org/10.1016/j.mex.2021.101434

Gbore, F.A., Oloruntola, O.D., Adu, O.A., Olarotimi, O.J., Falowo, A.B. & Afolayan, E.O. (2021). Serum and meat antioxidative status of broiler chickens fed diets supplemented with garlic rhizome meal, moringa leaf meal and their composite. *Tropical Animal Health and Production, 53*, 26. https://doi.org/10.1007/s11250-020-02438-9

Gbore, F.A., Olumomi, O.R., Aworetan, I.M. & Gabriel-Ajobiewe, R.A.O. (2016). Oral administration of monosodium glutamate alters growth and blood parameters in female rabbits. *European Journal of Biological Research, 6 (3),* 218-225. https://doi.org/10.5281/zenodo.150297

Ikeda, K. (2002). New seasonings. *Chemical senses, 27(9),* 847-849. https://doi.org/10.1093/chemse/27.9.847

Kafi, A., Uddin, M.N., Uddin, M.J., Khan, M.M.H. & Haque, M.E. (2017). Effect of dietary supplementation of turmeric (*Curcuma longa*), ginger (*Zingiber officinale*) and their combination as feed additives on feed intake, growth performance and economics of broiler. *International Journal of Poultry Science, 16, 257-265.* https://doi.org/10.3923/ijps.2017.257.265

Kermanshahi, H. & Riasi, A. (2006). Effect of turmeric rhizome powder (Curcuma longa) and soluble NSP degrading enzyme on some blood parameters of laying hens. *International Journal of Poultry Science, 5,* 494–498. https://doi.org/10.3923/ijps.2006.494.498

Khalil, R.M. & Khedr, V. (2016). Curcumin protects against monosodium glutamate neurotoxicity and decreasing NMDA2B and mGluR5 expression in rat hippocampus. *Neurosignals, 24*, 81-87. https://doi.org/10.1159/000442614

Kondoh, T. & Torii, K. (2008). MSG intake suppresses weight gain, fat deposition, and plasma leptin in male Sprague-Dawley rats. *Physiology and Behaviour, 95,* 135-144. https://doi.org/10.1016/j.physbeh.2008.05.010

Maroof, K., Oka, T., Fujihara, M. & Bungo, T. (2017). Effect of supplemental japanese pepper seed on the palatability of feed in chicks. *The journal of poultry science, 54(4),* 278–281. https://doi.org/10.2141/jpsa.0160150

Okon, A.K., Jacks, T.W., Amaza, D.S., Peters, T.M. & Otong, E.S. (2013). The effect of monosodium glutamate (MSG) on the gross weight of the heart of albino rats. *Scholar Journal of Applied Medical Sciences, 1(2),* 44-47.

Olarotimi, O.J. & Adu, O.A. (2022). Growth performance, blood indices and hormonal responses of broiler chickens fed monosodium glutamate. *Iranian Journal of Applied Animal Science, 12(2),* 341-352.
https://dorl.net/dor/20.1001.1.2251628.2022.12.2.14.5

Olarotimi, O.J., Gbore, F.A., Adu, O.A., Oloruntola, O.D. & Falowo, A.B. (2022). Effects of ginger meal supplementation on performance and meat antioxidative enzymes of broilers fed monosodium glutamate. *Acta Fytotechnica et Zootechnica, 25(3),* 174–184.
https://doi.org/10.15414/afz.2022.25.03.174-184

Olarotimi, O.J. (2018). Turmeric (*Curcuma Longa*): An underutilized phytogenic additive in poultry nutrition. *Turkish Journal of Agriculture - Food Science and Technology, 6 (1),* 102-106.
https://doi.org/10.24925/turjaf.v6i1.102-106.1572

Olarotimi, O.J. (2020). Serum electrolyte balance and antioxidant status of broiler chickens fed diets containing varied levels of monosodium glutamate (MSG). Bulletin of the National Research Center, *44* (103).
https://doi.org/10.1186/s42269-020-00360-6

Olarotimi, O.J., Adu, O.A., Olarotimi, A.O. (2020). High level dietary inclusion of monosodium glutamate lowers daily sperm production and efficiency in cocks. *European Journal of Biological Research, 10(3),* 240-250.
https://doi.org/10.5281/zenodo.3969026

Oloruntola, O.D., Agbede, J.O., Ayodele, S.O. & Oloruntola, D.A. (2018). Neem, pawpaw, and bamboo leaf meal dietary supplementation in broiler chickens: Effect on performance and health status. *Journal of Food Biochemistry,* e12723.
https://doi.org/10.1111/jfbc.12723

Osman, I. & Mohammed, A. (2021). Assessing the efficacy of monosodium glutamate as a growth enhancer in broiler chicken production. *Asia Pacific Journal of Sustainable Agriculture, Food and Energy*, *9(2),* 29-37.
https://doi.org/10.36782/apjsafe.v9i2.104

Paul, M.V., Abhilash, M., Varghese, M.V., Alex, M. & Harikumaran, N.R. (2012). Protective effects of alpha-tocopherol against oxidative stress related to nephrotoxicity by monosodium glutamate in rats. *Toxicology Mechanisms and Methods, 22(8),* 625–630.,
https://doi.org/10.3109/15376516.2012.714008

Raghdad, A. & Al-Jaleel, A. (2012). Use of turmeric (*Curcuma longa*) on the performance and some physiological traits on the broiler diets. *The Iraqi Journal of Veterinary Medicine*, *36 (1),* 51-57.
https://doi.org/10.30539/iraqijvm.v36i1.548

Rajput, N., Muhammad, N., Yan, R., Zhong, X. & Wang, T. (2013) Effect of dietary supplementation of curcumin on growth performance, intestinal morphology and nutrients utilization of broiler chicks. *Journal of Poultry Science*, 50: 44–52.
https://doi.org/10.2141/jpsa.0120065

Rezaei, R., Gabriel, A. S. & Wu, G. (2022). Dietary supplementation with monosodium glutamate enhances milk production by lactating sows and the growth of suckling piglets. *Amino acids*, *54(7),* 1055–1068.
https://doi.org/10.1007/s00726-022-03147-3

SAS (Statistical Analysis System Institute) (2008). SAS/ STAT User's Guide: version 9.2 for windows, SAS Institute Inc., SAS Campus Drive, Cary, NC, USA.

Shang, Y., Kumar, S., Oakley, B., & Kim, W.K. (2018). Chicken gut microbiota: importance and detection technology. *Frontier in Veterinary Science, 23(5),* 254.
https://doi.org/10.3389/fvets.2018.00254

Sharma, A., Prasongwattana, V., Cha'on, U., Selmi, C., Hipkaeo, W., Boonnate, P., Pethlert, S., Titipungul, T., Intarawichian, P., Waraasawapati, S., Puapiroj, A., Sitprija, V., & Reungjui, S. (2013). Monosodium glutamate (MSG) consumption is associated with urolithiasis and urinary tract obstruction in rats. *PloS one*, *8*(9), e75546.
https://doi.org/10.1371/journal.pone.0075546

Shen, M., Xie, Z., Jia, M., Li, A., Han, H., Wang, T. & Zhang, L. (2019). Effect of bamboo leaf extract on antioxidant status and cholesterol metabolism in broiler chickens. *Animal, 9,* 699-711.
https://doi.org/10.3390/ani9090699

Tsiouris, V., Kontominas, M.G., Filioussis, G., Chalvatzi, S., Giannenas, I., Papadopoulos, G., Koutoulis, K., Fortomaris, P. & Georgopoulou, I. (2020). The effect of whey on performance, gut health and bone morphology parameters in broiler chicks. *Foods, 9 (5),* 588.
https://doi.org/10.3390/foods9050588

Windisch, W., Schedle, K., Plitzner, C. & Kroismayr, A. (2008). Use of phytogenic products as feed additives for swine and poultry. *Journal of Animal Science, 86,* 140-148.
https://doi.org/10.2527/jas.2007-0459

Yamazaki, R.K., Brito, G.A. & Coelho, I. (2011). Low fish oil intake improves insulin sensitivity, lipid profile and muscle metabolism on insulin resistant MSG obese rats. *Lipids Health and Diseses, 10,* 66-72.
https://doi.org/10.1186/1476-511X-10-66

Youssef, M.K.E., El-Newihi, A.M., Omar, S.M. & Ahmed, Z.S. (2014). Assessment of proximate chemical composition, nutritional status, fatty acid composition and antioxidants of curcumin (Zingiberaceae) and mustard seeds powders (Brassicaceae). *Food and Public Health, 4,* 286-292.
https://doi.org/10.5923/j.fph.20140406.05

Zanfirescu, A., Ungurianu, A., Tsatsakis, A. M., Niţulescu, G. M., Kouretas, D., Veskoukis, A., Tsoukalas, D., Engin, A. B., Aschner, M. & Margină, D. (2019). A review of the alleged health hazards of monosodium glutamate. *Comprehensive reviews in food science and food safety*, *18(4),* 1111–1134.
https://doi.org/10.1111/1541-4337.12448

Zhelyazkov, G. (2018). Effect of monosodium glutamate dietary supplementation on some productive traits of common carp (*Cyprinus carpio*) cultivated in net cages. *Agricultural Science and Technology, 10(3),* 204-207.
https://doi.org/10.15547/ast.2018.03.039

BIOTECH STUDIES

RESEARCH PAPER

The antioxidant and cytotoxicity capabilities of the total methanol leaf extract of *Camellia yokdonensis*

Thanh Chi Hoang [1] ⓘ, Trung Quan Nguyen[2] ⓘ, Thi Kim Ly Bui[1]* ⓘ

[1]Department of Medicine and Pharmacy, Thu Dau Mot University, Thu Dau Mot, Binh Duong 820000, Vietnam
[2]Faculty of Biology and Biotechnology, VNU University of Science, Vietnam National University, Ho Chi Minh City 72711, Vietnam

Abstract

Camellia yokdonensis was first described in 2006 and clarified as a Vietnamese endemic *Camellia*. *Camellia* species are often associated with strong biological activity and have high application potential. However, there is currently no research on the biological activity of *C. yokdonensis*. The experiment was performed using DPPH assay and PFRAP assay to investigate the antioxidant capacity of the leaf extract. Besides, a 72-hour cytotoxic assay experiment on cancer cells showed the toxicity of the extract. The results showed that *C. yokdonensis* leaf extract has the ability to reduce iron ions and scavenge DPPH free radicals with an EC50 of 19.37 ± 1.66 μg/mL. Anticancer activity was determined by IC50 values (μg/mL) on HCC-J5, A549, MCF-7, and K562 cells as 138.00 ± 11.60, 172.90 ± 22.31, 175.52 ± 16.70, and 48.82 ±12.59, respectively.

Introduction

Tea culture is popular in Asia countries; it has gone along with humans throughout history (Wang et al., 2022). Drinking tea is not only a culture or habit; it also brings many crucial benefits (Aboulwafa et al., 2019; Bakhriansyah, Sulaiman, & Fauzia, 2022). Many scientific reports showed the potent antioxidant effects of tea, which contribute to a healthy human life (Khan & Mukhtar, 2013). Tea leaves were used in folk remedies to treat human illnesses such as diarrhea, metabolic disorders, and cardiovascular diseases (Besra et al., 2003; Yang, Chen, & Wu, 2014). Tea extracts are essences with biological activity in modern medicine, typically as catechin derivatives (Chí et al., 2020). The tea family (Theaceae) gather many different individuals; some species are drinkable, and others may have toxins

(Li et al., 2022; Nguyet Hai Ninh et al., 2020). *Camellia* is a vital genus that contributes the most regarding the number of species and potential for exploitation and application (Nguyet Hai Ninh et al., 2020). Although many species are used as herbs in traditional medicine, *Camellia* species still require scientific evidence to be applied easily in orthodox medicine. *Camellia sinensis* is the most popular type of tea, and it has been exploited and scientifically researched. The potent antioxidant capacity of *C. sinensis* extracts has been reported (Chí et al., 2020). Besides, it is also famous for its anti-inflammatory and proliferation-inhibiting properties in many different types of cancer (Chattopadhyay et al., 2004; Chaudhary et al., 2023; Novilla et al., 2017). Regular use of tea helps prevent the commencement of

cancer effectively ([Boehm et al., 2009](#); [Yang et al., 2007](#)). However, tea research is still only conducted on common species such as *C. senensis*, *C. oleifera*, or *C. nitidissima*, and many other *Camellia* are still overlooked in research, especially local tea species. Recently, research on endemic tea species in Vietnam has shown the remarkable biological activity of endemic tea varieties, such as *C. cuongiana*, *C. quephongensis*, *C. tamdaoensis*, *C. tienii*; that indicating the potential of many untapped tea species ([Nga, Oanh, & Linh, 2023](#); [Nguyen et al., 2023](#)). Although it was first discovered in 2005 and described in 2006 in Yokdon National Park in Vietnam, studies on *Camellia yokdonensis* are still scarce. This endemic tea is rarely approached due to its distribution in deep forests, so mining is challenging. The locals call it "pink tea" because the flowers are in carmine. According to them, these types of "pink tea" often have the ability to improve health and treat digestive diseases. Studies on the activity will be necessary to evaluate the medicinal value and better conserve this rare tea species. This study aims to investigate two major biological activities of tea leaves: antioxidants and anticancer.

Materials and Methods

Sample preparation

The mature leaves from *Camellia yorkdonensis* were harvested in July, and the tea was identified and tagged with voucher 073022CYO. The leaves were doubly washed with distilled water before draining and drying at 40 °C. The dry powder was obtained by grounding the dried leaves; the tea powder and pure solvent methanol mixture were added 10 times the solvent volume into the powder. The extract was filtrated every 24 h of shaking, and the process took place 5 times. The pooled extract eliminated the solvent by using a rotary evaporator. The crude extract was dissolved by DMSO (Dimethyl sulfoxide, Sigma-Aldrich, USA) to concentrate the final stock of 400 mg/mL, abbreviated as CYE.

Cell lines and cell culturing

The lung, chronic myeloid leukaemia and breast cancer cells, A549, K562, and MCF7, were derived from ATCC (American Type Culture Collection, USA), and the hepatocellular carcinoma cells, HCC-J5, were derived from the Cell Culture Center of the National Taiwan University (Taipei, Taiwan). Cells were cultured in RPMI-1640 Medium (Sigma-Aldrich, USA) added with 10% Fetal bovine serum (FBS, Sigma-Aldrich, USA) and 1% antibiotic (Penicillin-Streptomycin (100U/mL), Sigma-Aldrich, USA). Cells were refreshed medium every 72 h, and the sub-culturing was carried out as 80% of the culturing surface was occupied by cells. The initial cell density was 10^5 cells/mL.

Free radical scavenging assay

The DPPH (2,2-Diphenyl-1-picrylhydrazyl, Sigma-Alrich, USA) reagent was used as a nitrogen-centered radical for analysis. The extract in different concentrations reacted with DPPH 0.3 mM at a ratio of 1:1 in the dark for 30 mins at 37°C. The absorbance of the reacted solution was measured at 517 nm. The percentage of trapped DPPH was computed following the formula:

%DPPH$_{scavenging}$ = [1- (OD$_{test}$ − OD$_{blank}$)/(OD$_{negative}$ − OD$_{blank}$)] × 100%.

Non-linear regression was performed with model Y=100*(X^{HillSlope})/[EC50^{HillSlope} + (X^{HillSlope})] to regress the half-maximal response dose (EC50).

Reducing power investigation

A volume of 1 mL of extract in different concentrations was diluted with 2.5 mL of 1X PBS solution and 2.5 mL of 1% K$_3$[Fe(CN)$_6$] solution. The solution was mixed in 15 s by using a vortexer, and the tubes were incubated in the dark at 50°C for 20 min. Then, the reaction was stopped with 2.5 mL of 10% trichloroacetic solution and incubated at room temperature for 10 min. 2.5 mL of the solution was diluted with 2.5 mL of water; 1 mL of 0.1% FeCl$_3$ solution was added. After mixing, the absorbance at 700 nm was measured ([Ly et al., 2019](#)).

Cytotoxicity evaluation

Cells were seeded into 96-well plates at a density of 10^5 cells/mL and then incubated for 24 h. The medium supplemented with extract in different concentrations was added into wells to reach the final volume of 200 μL and the extract's 0 to 400 μg/mL range. The evaluation lasted for 72 h before replacing the medium with a basal medium with 10% MTT (3-(4,5-Dimethylthiazol-2-yl)-2,5-Diphenyltetrazolium Bromide, Sigma-Aldrich, USA). After 4 h of incubation, the medium was removed, and the crystals were dissolved by 100 μL DMSO. The cell viability reflected as the absorbance at 490 nm; thus, the cell viability rate was declared as the percentage between the test well and the negative one (DMSO 0.01%). Non-linear regression was performed with model Y=100/(1+(IC50/X)^{HillSlope})to regress the half-maximal inhibitory dose (IC50).

Data analysis

The data accumulation was in triple. The data was stored in Microsoft Excel 365 and analyzed using GraphPad Prism version 9.0.0. The differences were determined by performing the one-way ANOVA and Turkey Post-hoc combination or Student's T-test with a confidence level of 95% (alpha value = 0.05).

Results and Discussion

CYE inhibits radical scavenging capacity

The CYE showed the ability to neutralize the DPPH, which was indicated in a dose-dependent impact. The reaction curves are shown in [Figure 1](#). In the presence of the CYE below 50 μg/mL, the more concentrated extract, the more DPPH was electronically received. At

50 µg/mL of the extract, the reaction reached a saturation state with about 80% scavenged DPPH. In addition, the curves of the two positive controls, vitamin C and Trolox were also described, and the curves were observed to be asymptotic to each other. The similarity and proximity to the two controls showed that the free radical scavenging ability of CYE extract was comparable to vitamin C or Trolox.
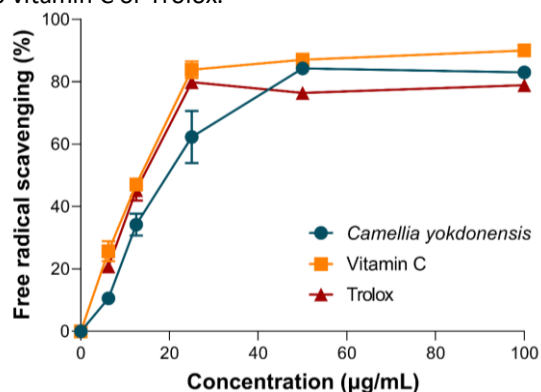

Figure 1. The DPPH scavenging effect of *C. yokdonensis* and positive controls (Vitamin C and Trolox).

Non-linear regression indicated the EC50 values of CYE, Trolox, and Vitamin C extracts on DPPH were 19.37 ± 1.66 µg/mL, 14.36 ± 2.71 µg/mL, and 12.22 ± 1.15 µg/mL, respectively (Figure 2). The lower the EC50 value, the stronger the antioxidant capacity of a compound. Therefore, Vitamin C and Trolox have a more remarkable ability to scavenge DPPH radicals than CYE (with lower EC50 values). However, CYE also demonstrates an excellent ability to scavenge DPPH radicals with an EC50 value of 19.37 ± 1.66 µg/mL, close to Trolox and Vitamin C, indicating that CYE still holds considerable antioxidant potential.
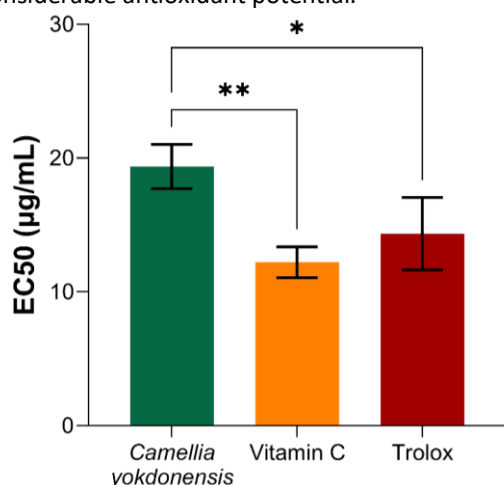

Figure 2. The EC50 values of *C. yokdonensis* and positive controls (Vitamin C and Trolox). *Note: p-value < 0.05 (*) and p-value <0.005 (**).*

There was a statistically significant difference in the activity of CYE compared to Trolox (P-value = 0.0455) and Vitamin C (P-value = 0.0099). However, the Vitamin C and Trolox tested were essences while CYE was a total extract, and the effect noted on the total extract was notable. Therefore, CYE has the potential for application in health protection products or as an antioxidant ingredient in the food and pharmaceutical industries. CYE can be developed into health care products or functional foods to enhance antioxidant capacity and protect the body from harmful free radicals. Additionally, further research on other antioxidant mechanisms could unlock its diverse potential applications in anti-aging and disease prevention industries.

Moreover, considering cost factors, natural origin, and long-term safety, CYE could be a potential alternative or complementary to standard antioxidants like Vitamin C and Trolox.

C. yokdonensis has not been reported to scavenge DPPH, but there have been reports of other members of the same genus. The phenolic leaf extract of *C. sinensis* reflects the EC50 on DPPH of 7.60 ± 0.48 µg/mL (Chí et al., 2020). The antioxidant ability was found to be under the influence of ambient conditions, such as collection time, collection position, weather conditions, and other factors. Some Indigenous tea species in Vietnam, living under the same geographical conditions as *C. yokdonensis*, have also demonstrated antioxidant capacity through their ability to neutralize DPPH free radicals, with the following EC50 values: *C. kissi* (EC50 = 10.85 ± 0.65 µg/mL), *C. longii* (EC50 = 60.5 ± 1.19 µg/mL), and *C. tamdaoensis* (EC50 = 9.00 ± 1.72 µg/mL) (Nga, Oanh, & Linh, 2023; Tran-Trung et al., 2023).

CYE reduces cation iron in solution

The ability to balance the oxidation potential is also considered through the process of donating and accepting electrons, in which electron donors are considered to have antioxidant properties (Lobo et al., 2010). Functional groups and unsaturated structures allow many phytochemicals to act as reducing agents in redox reactions (Chen et al., 2020; Eggler & Savinov, 2013). Hence, investigating the reducing power of compounds helps reflect their antioxidant capacity (Eggler & Savinov, 2013). Reducing Fe^{3+} to Fe^{2+} in solution reflects the CYE's reducing power. The results showed that the reduction process depends on the CYE concentration. Figure 3 shows a curve of the reducing power correlating the concentration of Vitamin C, Trolox, and CYE in the PFRAP assay. The results indicate that the reduction process of Fe^{3+} to Fe^{2+} in the solution is correlated with the concentration of Vitamin C, Trolox, and CYE in the PFRAP assay. At a concentration of 1.6 mg/mL, the absorbance of CYE is only 50% of that of Trolox and Vitamin C, suggesting that CYE has a lower antioxidant activity compared to the two reference substances at this lower concentration. However, when the concentration increases to 3.2 mg/mL, the absorbance becomes nearly equal for all three substances, indicating that at higher concentrations, the antioxidant activity of CYE increases significantly and becomes comparable to Trolox and Vitamin C. This suggests that CYE has good antioxidant potential but may require higher concentrations to achieve the same

effect as Trolox and Vitamin C. This antioxidant capacity could be related to the mechanism of action or the chemical composition of CYE, where certain compounds in the extract may need to reach a threshold concentration to exhibit their effects fully. Further research on CYE's chemical structure and mechanism of action could help optimize its use as a potential antioxidant.
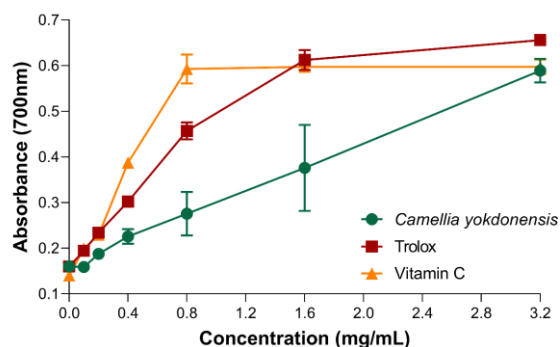

Figure 3. The reducing power of *C. yokdonensis* and positive controls (Vitamin C and Trolox).

CYE inhibits cancer cell proliferation

One popular research topic on *Camellia* is its ability to inhibit cancer cell proliferation. Studies show that *Camellia sinensis* extract has many inhibitory effects on cancer, such as breast, lung, liver, and other cancers (Esghaei et al., 2018; Koňariková et al., 2015; Mbuthia et al., 2017). Recently, Vietnamese endemic *Camellia* was indicated to express anticancer ability, namely *C. cuongiana*, *C. vuquangensis*, and *C. hatinhensis* (An et al., 2023; Linh et al., 2023). This study described the ability of *C. yokdonensis* to inhibit cancer cell proliferation for the first time. The results are illustrated in Figure 4.
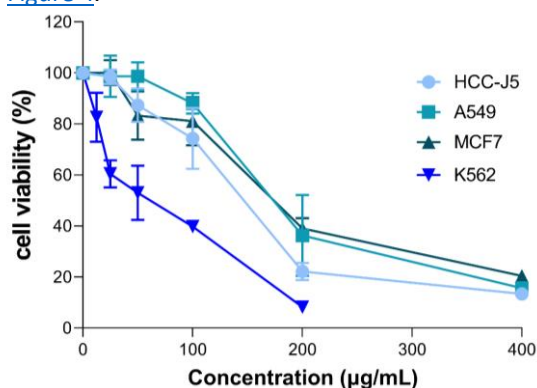

Figure 4. The cytotoxic effect of *C. yokdonensis* on cancer cell lines (HCC-J5, A549, MCF7, and K562).

The results indicate that the CYE extract inhibits the proliferation of tested cancer cells, including A549 (lung cancer), HCC-J5 (liver cancer), K562 (leukaemia), and MCF-7 (breast cancer). The inhibitory activity of CYE depends on the concentration of the extract, showing different levels of effectiveness across the various cell lines, which suggests a specific selectivity in the effects of this extract. At the highest tested concentration of 400 μg/mL, the survival rate of the cells decreased to about 20%, demonstrating a strong ability of CYE to

inhibit the growth of cancer cells (Figure 4). Notably, the IC50 value ranged from 48.82 ±12.59 μg/mL for K562 cells to 175.52 ± 16.70 μg/mL for MCF-7 (HCC-J5: 138.00 ± 11.6 μg/mL and A549: 172.90 ± 22.31) (Figure 5). Among these, CYE exhibited the most robust activity on the K562 cell line, with the lowest IC50 value (48.82 μg/mL), indicating its strong potential for application in leukaemia treatment. The activity is also notable on A549, HCC-J5, and MCF-7 cell lines but with higher IC50 values, suggesting that the inhibitory effects on these cell lines are weaker than K562.
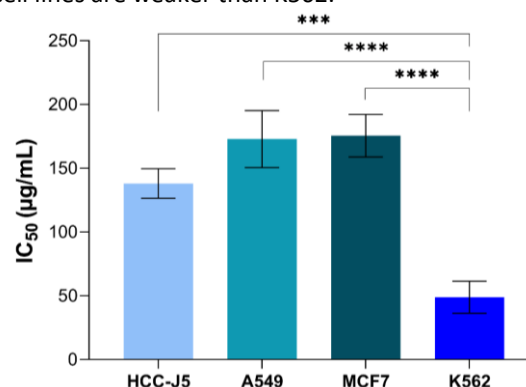
Figure 5. The IC50 values of *CYE* on cancer cell lines (HCC-J5, A549, MCF7, and K562). *Note: p-value < 0.0002 (***) and p-value <0.0001 (****).*

There was a difference in the impact of CYE on suspension cells being more effective than on adherent cells, P-value = 0.0007. From the IC50 value, plant extracts can be divided into different effective groups, and based on that, research can further develop (Indrayanto, Putra, & Suhud, 2021). The effect of CYE on K562 cells was moderately effective, while the impact on the rest was weak (Indrayanto, Putra, & Suhud, 2021). In previous reports, some of *Camellia* showed cytotoxic on several cancer cells, such as *C. cuongiana* on HCC-J5 and K562 (IC50 > 100 and IC50 = 72.26 ± 5.75 μg/mL), *C. kissi* on K562 (IC50 = 40,01 ± 3,12 μg/mL), *C. hatinhensis* on A549 and MCF-7 (IC50 = 76.26 ± 1.68 and 72.27 ± 1.71 μg/mL) (An et al., 2023; Linh et al., 2024; Linh et al., 2023). These results demonstrate the potential of CYE as a natural anticancer agent, particularly in the K562 cell line. However, due to the differences in effects among the various cell lines, further research into the active components of CYE, specific mechanisms of action, and testing in animal models and clinical settings will be necessary to determine its application potential in cancer treatment. CYE could become a promising candidate for the development of anticancer therapies, especially when combined with other methods to optimize treatment efficacy.

The development of anticancer research from extracts is important in the context that cancer is gradually increasing rapidly, and current treatment methods still have many challenges in terms of effectiveness and specificity. In 2022, there were about 20 million incidents of cancer, most concentrated in Asia, with 9.8 million cases; China was the country with

the highest number of cases, with 4.8 million cases. Lung, breast, liver cancer, and leukaemia, respectively, landed at the first, third, sixth, and 13th place in popularity (Bray et al., 2024). On the other hand, the first, third, fourth, and 10th positions were the peaks of the mentioned cancer types in terms of deaths (Bray et al., 2024). Thus far, the mechanism in action of the *Camellia* extracts on cancer cells has been investigated, such as BCR-ABL in K562, the P53 pathway in MCF-7, and Pi3K in HCT116, and it expressed the potential in cancer treatment research and applications (Chen, Chen, & Xu, 2013; Gao et al., 2020; Xuan et al., 2024).

The relationship between the antioxidant activity and the cancer cell inhibitory activity of CYE was considered to be closely related. The relationship was analyzed based on the DPPH scavenged rate and cell viability. The analysis results were recorded in the negative direction (Table 1), and the percentage of viable cells decreased as the amount of DPPH absorbed increased. The results suggested the supportive action of antioxidant and cytotoxicity effects of the *C. yokdonensis* extract. However, the connection between those impacts requires profound studies to be demystified. The evidence of the leaf extract's antioxidant and anticancer cell proliferation might positively support and contribute to the *C. yokdonensis* reservation, exploitation, and application.

Table 1. The correlation coefficient between the DPPH scavenging and anticancer effects of *C. yokdonensis*

Value	HCC-J5	A549	MCF-7	K562
Pearson r	-0,9255	-0,9386	-0,9044	-0,8509
P-value	0,1237	0,1121	0,1403	0,1761
Classification	Very strong correlation coefficient			

Conclusion

The antioxidant and anti-proliferative properties of the *C. yokdonensis* leaf extract are reported for the first time in this study, thereby enhancing the existing scientific knowledge surrounding this rare Camellia species. Given its combined antioxidant and anti-cancer activities, CYE presents a promising opportunity for the development of natural cancer therapies. Nevertheless, additional research is essential to elucidate the underlying mechanisms of action and to identify the bioactive compounds responsible for these effects.

Funding Information

Author Contributions

TCH: Design, Methodology, Writing-review and editing; TQN: Data Curation, Formal Analysis, Investigation and Writing-original draft; TKLB: Funding Acquisition, Project Administration.

Conflict of Interest

The author(s) declare that they have no known competing financial or non-financial, professional, or personal conflicts that could have appeared to influence the work reported in this paper.

References

Aboulwafa, M. M., Youssef, F. S., Gad, H. A., Altyar, A. E., Al-Azizi, M. M., & Ashour, M. L. (2019). A Comprehensive Insight on the Health Benefits and Phytoconstituents of Camellia sinensis and Recent Approaches for Its Quality Control. *Antioxidants (Basel)*, *8*(10). https://doi.org/10.3390/antiox8100455

An, N., Chau, D., Thi Huong, L., Khoa, V., Hung, N., Do, T., Trang, V., Dai, D., & Setzer, W. (2023). Lipid Peroxidation Inhibitory and Cytotoxic Activities of Two Camellia Species Growing Wild in Vietnam. *Pharmacognosy Magazine*, *19*, 097312962311584. https://doi.org/10.1177/09731296231158437

Bakhriansyah, M., Sulaiman, S. N., & Fauzia, R. (2022). The effect of Camellia sinensis tea on a decreased risk of anxiety for medical students at Universitas Lambung Mangkurat Indonesia. *Clinical Epidemiology and Global Health*, *17*, 101114. https://doi.org/10.1016/j.cegh.2022.101114

Besra, S. E., Gomes, A., Ganguly, D. K., & Vedasiromoni, J. R. (2003). Antidiarrhoeal activity of hot water extract of black tea (Camellia sinensis). *Phytotherapy Research*, *17*(4), 380-384. https://doi.org/10.1002/ptr.1171

Boehm, K., Borrelli, F., Ernst, E., Habacher, G., Hung, S. K., Milazzo, S., & Horneber, M. (2009). Green tea (Camellia sinensis) for the prevention of cancer. *Cochrane Database Syst Rev*, *2009*(3), Cd005004. https://doi.org/10.1002/14651858.CD005004.pub2

Bray, F., Laversanne, M., Sung, H., Ferlay, J., Siegel, R. L., Soerjomataram, I., & Jemal, A. (2024). Global cancer statistics 2022: GLOBOCAN estimates of incidence and mortality worldwide for 36 cancers in 185 countries. *CA: A Cancer Journal for Clinicians*, *n/a*(n/a). https://doi.org/10.3322/caac.21834

Chattopadhyay, P., Besra, S. E., Gomes, A., Das, M., Sur, P., Mitra, S., & Vedasiromoni, J. R. (2004). Anti-inflammatory activity of tea (Camellia sinensis) root extract. *Life Sciences*, *74*(15), 1839-1849. https://doi.org/10.1016/j.lfs.2003.07.053

Chaudhary, P., Mitra, D., Das Mohapatra, P. K., Oana Docea, A., Mon Myo, E., Janmeda, P., Martorell, M., Iriti, M., Ibrayeva, M., Sharifi-Rad, J., Santini, A., Romano, R., Calina, D., & Cho, W. C. (2023). Camellia sinensis: Insights on its molecular mechanisms of action towards nutraceutical, anticancer potential and other therapeutic applications. *Arabian Journal of Chemistry*, *16*(5), 104680. https://doi.org/10.1016/j.arabjc.2023.104680

Chen, J., Yang, J., Ma, L., Li, J., Shahzad, N., & Kim, C. K. (2020). Structure-antioxidant activity relationship of methoxy, phenolic hydroxyl, and carboxylic acid groups of phenolic acids. *Scientific Reports*, *10*(1), 2611. https://doi.org/10.1038/s41598-020-59451-z

Chen, L., Chen, J., & Xu, H. (2013). Sasanquasaponin from Camellia oleifera Abel. induces cell cycle arrest and apoptosis in human breast cancer MCF-7 cells. *Fitoterapia*, *84*, 123-129. https://doi.org/10.1016/j.fitote.2012.11.009

Chí, H. T., Hằng, B. M., Thương, N. T. L., & Lý, B. T. K. (2020). Khảo sát hoạt tính kháng oxi hóa của catechin chiết xuất từ lá trà xanh - Antioxidant activities of catechin extracted from green tea leaves. *Tạp chí khoa học - Đại học Thủ Dầu Một*, *49*, 71-79. https://doi.org/10.37550/tdmu.VJS/2020.06.097

Eggler, A. L., & Savinov, S. N. (2013). Chemical and biological mechanisms of phytochemical activation of Nrf2 and importance in disease prevention. *Recent Adv Phytochemistry*, *43*, 121-155. https://doi.org/10.1007/978-3-319-00581-2_7

Esghaei, M., Ghaffari, H., Rahimi Esboei, B., Ebrahimi Tapeh, Z., Bokharaei Salim, F., & Motevalian, M. (2018). Evaluation of Anticancer Activity of Camellia Sinensis in the Caco-2 Colorectal Cancer Cell Line. *Asian Pacific Journal of Cancer Prevention*, *19*(6), 1697-1701. https://doi.org/10.22034/apjcp.2018.19.6.1697

Gao, X., Li, X., Ho, C.-T., Lin, X., Zhang, Y., Li, B., & Chen, Z. (2020). Cocoa tea (Camellia ptilophylla) induces mitochondria-dependent apoptosis in HCT116 cells via ROS generation and PI3K/Akt signalling pathway. *Food Research International*, *129*, 108854. https://doi.org/10.1016/j.foodres.2019.108854

Indrayanto, G., Putra, G. S., & Suhud, F. (2021). Validation of in-vitro bioassay methods: Application in herbal drug research. *Profiles Drug Subst Excip Relat Methodol*, *46*, 273-307. https://doi.org/10.1016/bs.podrm.2020.07.005

Khan, N., & Mukhtar, H. (2013). Tea and health: studies in humans. *Current Pharmaceutical Design*, *19*(34), 6141-6147. https://doi.org/10.2174/1381612811319340008

Koňariková, K., Ježovičová, M., Keresteš, J., Gbelcová, H., Ďuračková, Z., & Žitňanová, I. (2015). Anticancer effect of black tea extract in human cancer cell lines. *Springer Plus*, *4*(1), 127. https://doi.org/10.1186/s40064-015-0871-4

Li, Z., Huang, Q., Zheng, Y., Zhang, Y., Li, X., Zhong, S., & Zeng, Z. (2022). Identification of the Toxic Compounds in Camellia oleifera Honey and Pollen to Honey Bees (Apis mellifera). *Journal of Agricultural and Food Chemistry*, *70*(41), 13176-13185. https://doi.org/10.1021/acs.jafc.2c04950

Linh, P. H., Ly, B. T. K., & Chi, H. T. (2024). Evaluation the Anti-leukemia effect of Methanol extracts of Camellia cuongiana on the K562 cell line. *Research Journal of Pharmacy and Technology*, *17*(2), 568-570. https://doi.org/10.52711/0974-360X.2024.00088

Linh, P. H., Lý, B. T. K., & Chí, H. T. (2023). Khảo sát hoạt tính Cao chiết Methanol từ Camellia Cuongiana Thu hái tại Vườn Quốc Gia Bidoup – Núi Bà Trên Tế bào Ung Thư biểu Mô Gan HCC-J5. *Tạp Chí Khoa học Và Công nghệ - Đại học Đà Nẵng*, *21*(5), 78-81.

Lobo, V., Patil, A., Phatak, A., & Chandra, N. (2010). Free radicals, antioxidants and functional foods: Impact on human health. *Pharmacognosy Reviews*, *4*(8), 118-126. https://doi.org/10.4103/0973-7847.70902

Ly, B., Quan, N., Dao, L., Nguyen, H., Lam, M., & Hoang, C. (2019). Evaluation of Antimicrobial, Antioxidant and Cytotoxic Activities of Dialium cochinchinensis Seed Extract. *Indian Journal of Pharmaceutical Sciences*, *81*(5), 975-980. https://doi.org/10.36468/pharmaceutical-sciences.594

Mbuthia, K. S., Mireji, P. O., Ngure, R. M., Stomeo, F., Kyallo, M., Muoki, C., & Wachira, F. N. (2017). Tea (Camellia sinensis) infusions ameliorate cancer in 4TI metastatic breast cancer model. *BMC Complementary and Alternative Medicine*, *17*(1), 202. https://doi.org/10.1186/s12906-017-1683-6

Nga, N. P., Oanh, N. T. K., & Linh, N. D. (2023). Evaluation of the antioxidant activity of two endemic golden Camellia species (Camellia tamdaoensis Ninh et Hakoda and Camellia tienii Ninh) in Vietnam. *TNU Journal of Science and Technology*, *228*(5), 333 - 340. https://doi.org/10.34238/tnu-jst.7010

Nguyen, T. H. D., Vu, D. C., Nguyet, N. T. M., Tran-Trung, H., Nguyen, L. L. P., & Baranyai, L. (2023). Evaluation of phenolics and bioactivities of Camellia quephongensis leaf extracts as affected by various extraction solvents. *Journal of Agriculture and Food Research*, *14*, 100914. https://doi.org/10.1016/j.jafr.2023.100914

Nguyet Hai Ninh, L., Van Dung, L., Nguyen Van, C., Pham Thi, T. D., Luu, T., & Pham, T. (2020). An updated checklist of Theaceae and a new species of Polyspora from Vietnam. *Taiwana*, *65*, 216-227. https://doi.org/10.6165/tai.2020.65.216

Novilla, A., Djamhuri, D. S., Nurhayati, B., Rihibiha, D. D., Afifah, E., & Widowati, W. (2017). Anti-inflammatory properties of oolong tea (Camellia sinensis) ethanol extract and epigallocatechin gallate in LPS-induced RAW 264.7 cells. *Asian Pacific Journal of Tropical Biomedicine*, *7*(11), 1005-1009. https://doi.org/10.1016/j.apjtb.2017.10.002

Tran-Trung, H., Nguyen, T. C., Dung, V. C., Ngoc, H. N., Nguyen, D. K., Vu, D. C., Van, S. D., Nguyen, Q. A. T., Nguyen, T. H. D., Tham, V. M., & Dau, X. D. (2023). Characterization and Evaluation of the In Vitro Antioxidant, α-Glucosidase Inhibitory Activities of Camellia longii Orel and Luu. (Theaceae) Flower Essential Oil and Extracts From Vietnam. *Natural Product Communications*, *18*(11), 1934578X231208348. https://doi.org/10.1177/1934578x231208348

Wang, C., Han, J., Pu, Y., & Wang, X. (2022). Tea (Camellia sinensis): A Review of Nutritional Composition, Potential Applications, and Omics Research. *Applied Sciences*, *12*(12), 5874. https://www.mdpi.com/2076-3417/12/12/5874

Xuan, N., Quan, N., Ly, B., & Thanh Chi, H. (2024). Induction of Apoptosis in BCR-ABL Fusion Associated Chronic Myeloid Leukemia Cells by Camellia kissiWall. (Theaceae) Extract. *European Journal of Biology*. https://doi.org/10.26650/EurJBiol.2024.1399845

Yang, C. S., Chen, G., & Wu, Q. (2014). Recent scientific studies of a traditional chinese medicine, tea, on prevention of chronic diseases. *Journal of Traditional and Complementary Medicine*, *4*(1), 17-23. https://doi.org/10.4103/2225-4110.124326

Yang, C. S., Lambert, J. D., Ju, J., Lu, G., & Sang, S. (2007). Tea and cancer prevention: molecular mechanisms and human relevance. *Toxicology and Applied Pharmacology*, *224*(3), 265-273. https://doi.org/10.1016/j.taap.2006.11.024

BIOTECH STUDIES

RESEARCH PAPER

Bench scale production of butyrohydroxamic acid using amidotransferase activity of amidase from whole resting cell *Bacillus* sp. APB-6.

Pankaj Kumari[1] ⬡, Mohinder Pal[2]* ⬡, Abhishek Thakur[1] ⬡, Duni Chand[1]* ⬡

[1]Department of Biotechnology, Multi Faculty Building (Phase-I), Gyan Path, HP University Campus, Summer Hill, Shimla 171 005 (HP), India

[2]Department of Biotechnology, Chandigarh College of Technology, Chandigarh Group of Colleges, Landran, Mohali 140307 (Punjab), India

Corresponding Author
Tel.: +91 701 831 55 90
E-mail:
mohinder.pal1@gmail.com
dunichand_2000@yahoo.com

Abstract

Butyrohydroxamic acid is a hydroxamic acid that has various biological and pharmacological applications. This study reports the bioconversion of butyramide and hydroxylamine to butyrohydroxamic acid with the help of amidase of Bacillus sp. APB-6, which has amidotransferase activity. Optimal conditions for the reaction were determined as 100/1200 mM butyramide/hydroxylamine ratio, incubation time 5 hr, pH 9.5, temperature 55°C, and resting cell concentration of 1.578 mg dcw ml-1. Under these conditions, the complete conversion of butyramide to butyrohydroxamic acid was attained in a 50 ml flask scale. The batch reaction was preferred over fed-batch reaction for scaling up the process to a 1 L scale, and the reaction time was reduced by 30 minutes. The final product yield was 10.23 g butyrohydroxamic acid with 95% purity, volumetric productivity of 2.273 g/L/h and 1.44 g/g/h catalytic productivity. The amidase used in this study showed high amidotransferase activity along with the industrially relevant process for the production of butyrohydroxamic acid. The NMR spectrum of the recovered product confirmed its identity as butyrohydroxamic acid.

Introduction

In recent years, there has been tremendous interest in the application of hydroxamic acids and their derivation. They have pharmacological and toxicological significance and have been shown to have various biological activities such as antimicrobial, antileukemic, antituberculous, and chemotherapeutic agents (Syed et al., 2020). Also, α-amino hydroxamic acid derivatives can effectively block the activity of metalloproteases, which are responsible for the tissue changes that facilitate tumor development and metastasis (Lin et al., 2022). Also, acetohydroxamic acid and

butyrohydroxamic acid have shown anti-human immunodeficiency and antimalarial activities (Adebayo et al., 2024; Wang et al., 2022; Končić et al., 2011). The chemical synthesis of hydroxamic acids usually involves the Angeli-Rimini reaction or Lossen rearrangement (Mountanea et al., 2023). However, these methods need many solvents and complex reaction conditions, such as nitrogen requirements, higher temperatures, and tedious steps that may produce undesired by-products (Wang et al., 2022). On the other hand, mild reaction conditions can be achieved with the use of

enzymes, and therefore find more applications as biochemicals.

The main determining factors for the effective application of enzyme-based bioprocesses to useful products are enzyme activity, substrate, and product tolerance (Victorino da Silva Amatto et al., 2022; Kanwar et al., 2024). Amidotransferases are of considerable industrial interest in bioconversion processes to make valuable hydroxamic acids. Researchers have exploited amidases with acyl transfer activities for the enzymatic conversion of amides to hydroxamic acid. (Wu et al., 2020; Sharma et al., 2022). Hydroxamic is synthesized by enzymes under mild conditions of pH, temperature, and pressure, resulting in a pure product. These bioprocesses are more advantageous than the current chemical processes, as they offer high specificity, high selectivity, and environmental friendliness (Boodhoo et al., 2022). To overcome the challenges of large-scale hydroxamic acid production, this study focuses on optimizing fermentation parameters for butyrohydroxamic production. Here, we described the amidotransferase activity of the amidase of *Bacillus* sp. APB-6 with high butyramide tolerance. We optimized the process at a 50 mL scale using fed-batch and batch reactions, and at a bench scale (1L), which can be further upscaled to industrial-level bioreactors. To the best of the literature knowledge, this is the first study exploiting bacterial amide for the batch-scale production of butyrohydroxamic acid from *Bacillus* sp. APB-6.

Materials and Methods

Reagents and chemicals

The amides were procured from Alfa Aesar (Heysham, UK) (A Johnson Matthey Company). All other chemicals, including the culture media and their components, were purchased from HiMedia (Mumbai, India).

Bacterial strain and growth parameters

The bacterial strain APB-6 was obtained from the Department of Biotechnology, Himachal Pradesh University, isolated in a previous study, and acquired accession number MTCC-7540 (Pandey et al. 2011). The strain was cultured in a modified nutrient broth as per described by Kumari and Chand (2017) and Kumari et al. (2017).

Amidotransferase assay

Amidotransferase activity was measured as per the previous method of Brammar and Clarke (1964). To prepare the standard curve, butyrohydroxamic acid was used in concentrations ranging from 80 mg to 340 mg. Amidotransferase activity was measured in terms of enzyme units (U), where one unit corresponded to the quantity of enzyme that released one micromole of product per min under standard reaction conditions (Kumari et al., 2017).

Analytical methods

Substrate and product were subjected to high-performance liquid chromatography (HPLC) for their quantitative estimation using the Waters HPLC system, which consisted of a reverse phase C18 column with 4.6 mm x 250 mm; 5 μm dimensions and a 515 series pump operated at 1 mL/min flow rate. The solvent system consists of 30% acetonitrile-water with 0.2% orthophosphoric acid. Absorbance was recorded at 200 nm using a photodiode array (PDA) detector. The standard curves were prepared for butyramide (20-200 mM), hydroxylamine (50-200 mM), and butyrohydroxamic acid (1-10 mM).

Effect of substrate molarity and enzyme concentration

The optimization of the conversion of butyramide to butyrohydroxamic acid was performed by varying the concentrations of butyramide (100 mM, 150 mM, and 200 mM) and resting cell (0.789-2.367 mg dcw/mL) as a catalyst and keeping the hydroxyl amine concentration constant (1200 mM). The reaction was conducted at 50 mL scale for 120 min at 55°C.

Time course for enzymatic reaction at variable temperatures

The temperature dependency of enzyme activity was studied by stopping the reaction at 2, 4, 6, and 8 hrs intervals at 50°C, 55°C, and 60°C variable temperatures. The enzymatic reaction was performed at a 50 mL scale with 1200 mM hydroxylamine. The product concentration (mM) was determined in HPLC by comparing it against the commercial standard of butyrohydroxamic acid.

Time course of butyramide conversion for increasing substrate concentration

To study the effect of butyramide concentration, a reaction was set using 50 mM-200 mM butyramide and 1200 mM hydroxyl amine. The reaction was conducted on a 50 mL scale at 55°C. The samples were analyzed hourly by HPLC for substrate and product concentrations.

Time course of butyramide conversion with a corresponding increase in the concentration of substrate and resting cell

Optimization of the reaction volume (50 mL) was performed by increasing the concentrations of substrate and resting cell proportionally from 100 mM; 2.104 mg dcw/mL to 150 mM; 3.156 mg dcw/mL and 200 mM; 4.206 mg dcw/mL. The reaction was analyzed by HPLC after 5 hrs for substrate and product concentrations.

Standardization of 50 mL scale fed-batch and batch reactions

A 50 mL scale batch reaction was performed with 0.2 M of glycine-NaOH having a pH of 9.5, 100 mM butyramide, 1200 mM hydroxylamine, and 1.578 mg dcw/mL resting cells at 55°C. The reaction was shaken

reciprocally in a water bath for 5 hrs and analyzed by HPLC for substrate and product concentrations.

To increase the molar conversion yield, a 50 mL scale fed-batch reaction was performed using 0.2 M Glycine-NaOH buffer with pH 9.5, 100 mM butyramide, and 1200 mM hydroxylamine along with resting cells (1.578 mg dcw/mL) at 55°C. Further, the flask containing the reaction was shaken reciprocally in the water bath and the substrates (butyramide 100 mM and hydroxylamine 1200 mM) were added every 5 hrs. Three additions were made and the product concentration was measured by HPLC before and after each addition.

Bench scale (1L) bioconversion of butyramide and hydroxylamine to butyrohydroxamic acid

Bench scale (1L) bioconversion was performed in a BIOFLO C-32 fermenter (New Brunswick Scientific, Edison, NJ, USA) with a 1.5 L capacity. The reaction conditions comprise 0.2 M glycine NaOH having 9.5 pH, 100 mM butyramide, 1200 mM hydroxylamine, and resting cells with 1.578 mg dcw/mL concentration at 55°C. Further, the substrates and resting cells were mixed well at 200 rpm. The reaction was conducted for 5 hrs, and at one-hour interval, samples were analyzed by HPLC for the concentration of substrate and product.

Downstream processing of the reaction mixture

The reaction mixture was then centrifuged at 10,000 g for 15 min at room temperature to remove the resting cells from the supernatant. After this, the supernatant was vacuum-dried in a lyophilizer to reduce its volume by half and then used for acid-base extraction. Further, the supernatant was acidified with 12.5 N HCl and resuspended in 20 mL of acetone. To eliminate the salts the solution was filtered using Whatman filter paper and the filtrate was evaporated to obtain a slightly white powder. The weight of the powder was measured to calculate the recovery percentage. The powder was analyzed by HPLC to check its purity (Fournand et al., 1997). For characterization, the purified product was dissolved in deuterated dimethyl sulfoxide and an NMR spectrum was obtained to confirm butyrohydroxamic acid (Figure 1).
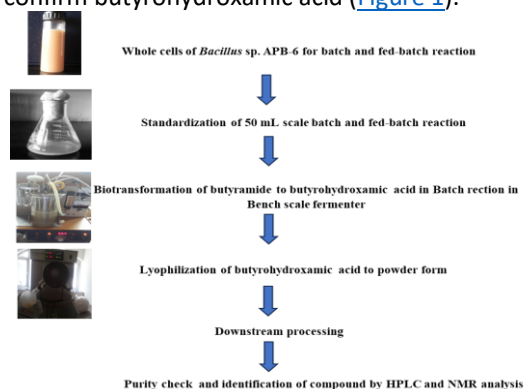
Figure 1. Schematic for bench scale biotransformation process of butyramide to butyrohydroxamic acid.

Results and Discussion

Effect of substrate molarity and enzyme concentration using resting cells

The conversion of butyramide to butyrohydroxamic acid was performed by varying the resting cell concentration and the butyramide concentration while keeping the hydroxylamine concentration constant (1200 mM). The conversion rate increased with the increase in cell concentration, and the highest conversion was achieved with 1.578 mg dcw for resting cells and 100 mM butyramide in 2 hrs (Figure 2).
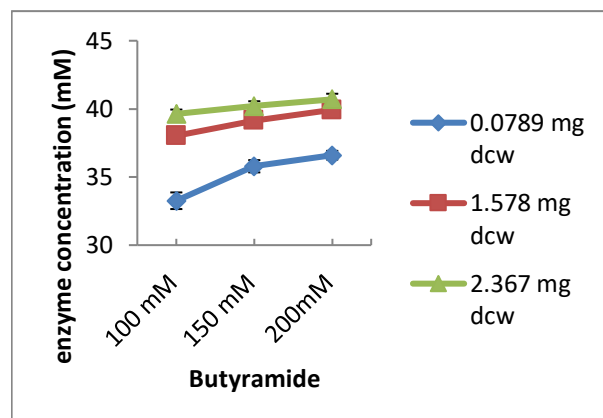
Figure 2. Effect of molarity of substrate and enzyme concentration on conversion of butyramide to butyrohydroxamic acid.

Therefore, these conditions were selected for the subsequent experiment. However, at 2.367 mg dcw/mL, the conversion of 100 mM substrate was only slightly higher (39.63%) than that at 1.578 mg dcw/mL (38.03%) in 2 hrs using resting cells. This suggests that the further addition of cells did not contribute to a significant increase in conversion. For the prevention of hydrolysis of the product and process cost-effectiveness, 1.578 mg dcw/mL was chosen for the subsequent experiment. These results were supported by Agarwal et al. (2013), who found an increase in conversion rate with the increase in enzyme concentration during the bioconversion of nicotinamide to nicotinic acid using the acyltransferase activity of a bacterial strain, and the maximum conversion was observed at 0.7 mg dcw/mL resting. Similarly, Pandey et al. (2011) used 300 mM of acetamide and 800 mM of hydroxylamine to produce the acetohydroxamic acid using resting cells of *Bacillus* sp. Likewise, a study by Devi et al. (2022), reported optimized conditions for the bioconversion process of acetohydroxamic acid using the acyltransferase activity of *Rhodococcus pyridinivorans* using 300 mM of acetamide and 500 mM of hydroxylamine-HCl which led to product conversion a rate of 89% at 45° C in a 30 min reaction (Devi et al., 2022).

Effect of the time course of enzyme reaction using resting cells at different temperatures

The conversion of butyramide to butyrohydroxamic acid was faster at higher temperatures and time. At 50°C, the conversion was slow, but at 55°C, 100 mM butyramide was completely converted within 5 h for resting cells (Figure 3). Devi et al. (2022), reported 60°C as the optimum temperature for the activity of acyltransferase using resting cells The highest acyltransferase activity of strain APB-6 was observed at 45°C.
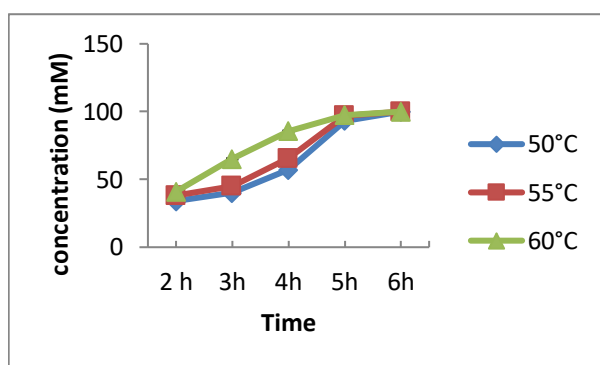
Figure 3. Time course of butyrohydroxamic acid production at different temperatures using resting cells.

Similar results were obtained during the bioconversion process of nicotinamide to nicotinic acid by using the acyltransferase of strain IITR6b2, where the highest conversion was achieved at 55°C (Agarwal et al., 2013).

Effect of the time course of butyramide conversion with a corresponding increase in substrate concentration

We have observed an increase in product formation about increasing substrate concentration along with time. Butyramide with 50 mM and 100 mM concentrations was completely converted within 5 h with resting cells (Figure 4).
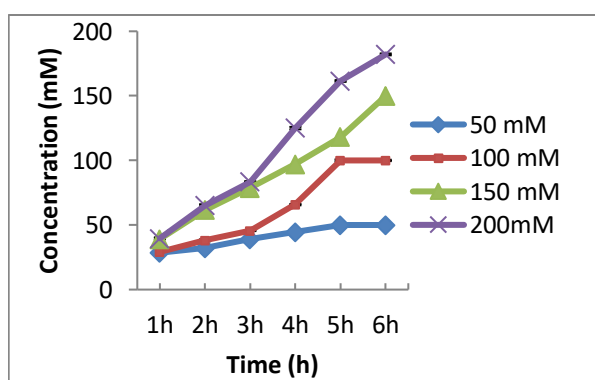
Figure 4. Time course of butyrohydroxamic acid production at various substrate concentrations using resting cells.

Singh et al. (2020), reported the time course for bioconversion of N'-phenyloctanediamide (10 mmol l^{-1}) to N-hydroxy-N'- phenyloctanediamide and reported maximum conversion after 12 hr at 40°C. Whereas,

maximum conversion of acetamide (300 mM), and hydroxylamine-HCl (800 mM) was observed after 30 min at 45°C by using the acyltransferase activity of *Rhodococcus pyridinivorans* (Devi et al., 2022).

Time course of butyramide conversion with a corresponding increase in substrate and resting cell concentration

The product formation increased with an increase in the concentration of butyramide and resting cells. The highest conversion was achieved with 1.578 mg dcw/mL and 100 mM butyramide. Devi et al. (2022), reported optimum conversion using resting cells with 576 U/mg-dcw residual activity using 300 mM of acetamide.

Batch and fed-batch reactions to produce butyrohydroxamic acid using resting cells

Batch and fed-batch reactions on a 50 mL scale were done in a 250 mL Erlenmeyer flask to increase the molar yield. HPLC analysis of commercial hydroxylamine HCl, butyrohydroxamic acid, and butyramide was done. The zero-hour sample (before the reaction started) showed the peaks of both substrates (butyramide and hydroxylamine HCl) in HPLC (Figure 5a).

Sr. No.	Name	RT	Area	Height
1.	Hydroxylamine HCl	1.696	1437875	193232
2.	Butyrohydroxamic Acid	2.285	2013205	238412
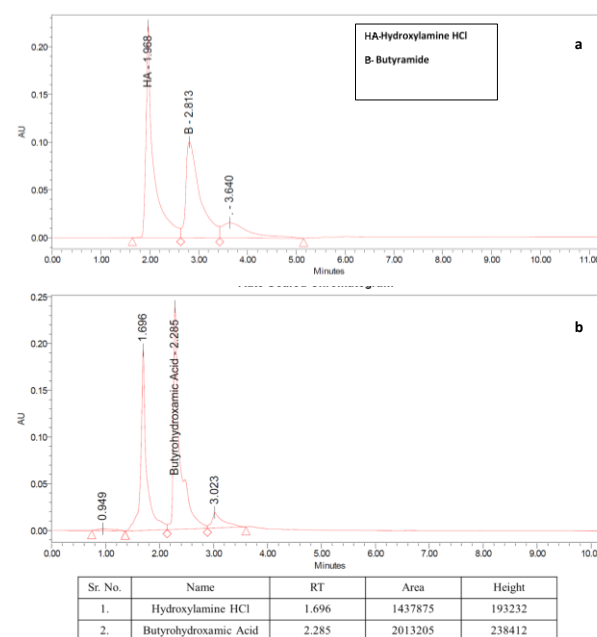
Figure 5. HPLC chromatogram of zero h sample (a), and HPLC chromatogram of butyrohydroxamic acid in batch reaction (b).

The batch reaction using resting cells produced 100% butyrohydroxamic acid and the total product concentration was 100 mM at 50 mL scale. The HPLC chromatogram showed the peaks of butyramide (product) and hydroxylamine, which were used in excess (1:12) compared to butyramide and remained unreacted (Figure 5b).

The product concentration before and after each feeding in the fed-batch reaction was measured by HPLC. The fed-batch reaction was not successful, as the conversion rate decreased after the feeding, even though the total product amount increased. Before the

feeding of substrates (after 5 hrs), 100 mM butyramide was completely converted to butyrohydroxamic acid (Figure 6). Bhatia et al. (2013), performed a 50 mL scale fed-batch reaction and applied five feedings of benzamide (50 mM) and hydroxylamine (250 mM) at time intervals of 20 min for benzohydroxamic acid production at 50°C.
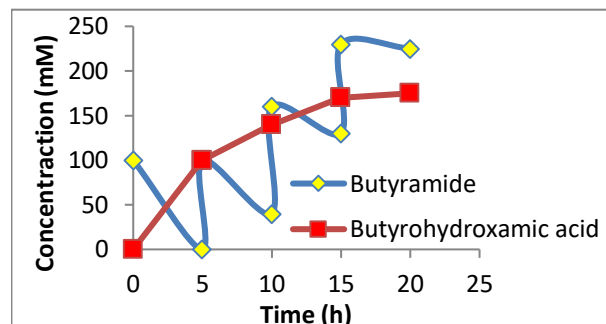
Figure 6. Synthesis of butyrohydroxamic acid using resting cell in 50 mL scale fed-batch reaction.

Also, a thermostable amidase from *Xinfangfangia* sp. DLY26 with optimal activity at 60°C and broad substrate specificity was reported by Xi et al. (2021). The maximum product formation was observed at the fourth feeding. After the feeding of substrates (after 10 hrs), the conversion was only 40%. Whereas, the result obtained in batch reaction with a tremendous conversion rate highlights the importance of the current study. This is the highest conversion rate report for butyrohydroxamic acid production. Therefore, the results further motivate us to upscale to bench scale (1L) for the synthesis of butyrohydroxamic acid.

Bench scale (1L) bioconversion of butytamide and hydroxylamine to butyrohydroxamic acid

A bench scale (1 L) process was performed in a fermenter vessel with a temperature of 55°C and an impeller speed of 200 rpm (Figure 7).

Figure 7. New Brunswick Scientific BioFlow C-32 fermenter (1.5 L) showing the reaction containing resting cells of APB-6 for the biotransformation of butyramide to butyrohydroxamic acid.

The reaction lasted for 5 hrs and produced 100 mM butyrohydroxamic acid (100% molar conversion yield). The conversion of 100 mM butyramide to butyrohydroxamic acid was almost complete within four and a half hours, which was faster as compared to 50 mL reaction. The reason behind this may be the kinetic change in the reaction and increased interaction surface area of the enzyme and substrate at the 1 L scale. After removing the resting cells and residual buffer a creamish white powder was obtained. Further, the purified product was analyzed by HPLC and showed a peak of pure butyrohydroxamic acid (RT: 2.273 min, Figure 8).
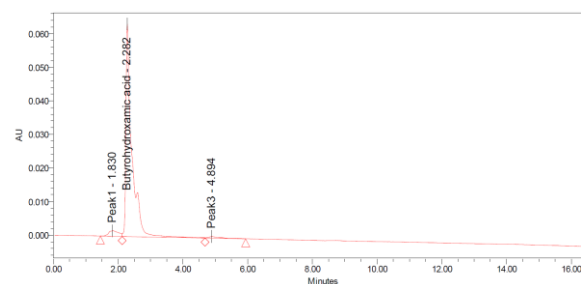
Figure 8. HPLC chromatogram of recovered butyrohydroxamic acid.

The HPLC analysis confirmed the yield of butyrohydroxamic acid as 100 mM (100%). In the 1 L batch mode reaction using resting cells, 10.23 g of butyrohydroxamic acid with 95% purity, 1.44 g/g/h catalytic productivity, and 2.273 g/L/h volumetric productivity were produced. Recombinant *Rhodococcus* sp. R312 amidase as an insoluble biocatalyst (10 g) produced 1 L of acetohydroxamic acid in 1 hr and 30 min with a bioconversion rate of 55 to 60% (mol/mol) (Fournand et al., 1997). Sharma et al. (2022), reported a 64% recovery rate for bench scale production of butyrohydroxamic acid with 96% purity. Singh et al. (2020), reported 83% recovery for the product vorinostat from the substrate N'-phenyloctanediamide. A bioconversion rate of 95% (mol/mol) has been reported for acetohydroxamic acid production by use of *Geobacillus pallidus* resting cells in 20 min at 50°C (Sharma et al., 2012). A 93% molar conversion yield at 1 L scale was obtained to produce acetohydroxamic (280 mM) acid by using the amidase of *Bacillus* sp. APB-6, while 0.26 M of acetohydroxamic acid was obtained in 80 min by using amidase of *G. pallidus* BTP-5X (Bhatia et al., 2013). Bhatia et al. (2015), obtained nicotinyl hydroxamic acid (190 mM) with 95% yield in 30 min at 1L scale, which was slightly higher than at a 50 mL scale. The catalytic productivity and volumetric productivity of the recovered nicotinyl hydroxamic acid were 13 g/h/dcm and 32 g/L/h, respectively (Boodhoo et al., 2022). Our data from bench scale 1L reaction reported higher molar conversion for the hydroxamic acid as compared to previous reports for acetohydroxamic acid and benzohydroxamic acid production. The bench scale reaction recovered 70% of the resting cells with 40%

residual amidotransferase activity. These cells were reused in a 50 mL reaction mixture and converted 34% of 100 mM butyramide to butyrohydroxamic acid. The standardized conditions with a high conversion rate at the bench scale can be further upscaled to industrial-level fermenters for the commercial production of butyrohydroxamic acid intended for various applications.

NMR spectrum of butyrohydroxamic acid

The OH proton is indicated by a singlet at 5.7009 (Figure 9).

Figure 9. Proton NMR spectrum of butyrohydroxamic acid.

There is no coupling between the methylene protons and the hydroxyl protons. The methylene protons resonate at a lower field due to the adjacent oxygen atom and appear as a quartet at 0.875 ∂ for 2H. The methylene protons show a multiplet at 5.481 ∂. The methyl protons appear as a triplet at 1.9752 ∂ for 3H. This data indicated the presence of butyrohydroxamic acid.

Conclusion

The present study showed the production of 100 mM butyrohydroxamic acid (100% molar conversion yield) on a 1 L bench scale. Also, bench scale reaction recovered 70% of the resting cells with 40% residual enzyme activity, which can be further reused in subsequent reactions.

This is the first report on the amidotransferase activity of the amidase from *Bacillus* sp. APB-6 with high butyramide tolerance. The optimized process against different parameters for the effective production of butyrohydroxamic acid by biotransformation can be upscaled and may find applications for various industrial bioprocess products, including anticancer compounds, antimicrobial compounds, and anti-inflammatory agents.

Conflict of Interest

The authors have declared that no conflict of interest exists.

Author Contributions

PK: experimentation, data collection; MP: data collection, and visualization, formal analysis and interpretation of the data original draft, review, and editing; AK: review and editing; DC: review and editing, supervising the work.

References

Adebayo, G. P., Oduselu, G. O., Aderohunmu, D. V., Klika, K. D., Olasehinde, G. I., Ajani, O. O., & Adebiyi, E. (2024). Structure-based design, and development of amidinyl, amidoximyl and hydroxamic acid based organic molecules as novel antimalarial drug candidates. *Arabian Journal of Chemistry*, *17*(2), 105573. https://doi.org/10.1016/j.arabjc.2023.105573

Agarwal, S., Gupta, M., & Choudhury, B. (2013). Bioprocess development for nicotinic acid hydroxamate synthesis by acyltransferase activity of *Bacillus smithii* strain IITR6b2. *Journal of Industrial Microbiology and Biotechnology*, *40*(9), 937-946. https://doi.org/10.1007/s10295-013-1299-x

Bhatia, R. K., Bhatia, S. K., Kumar, V., & Bhalla, T. C. (2015). Bi-substrate kinetic analysis of acyl transfer activity of purified amidase from *Pseudomonas putida* BR-1. *Catalysis Letters*, *145*, 1033-1040. https://doi.org/10.1007/s10562-014-1467-2

Bhatia, R. K., Bhatia, S. K., Mehta, P. K., & Bhalla, T. C. (2013). Bench scale production of benzohydroxamic acid using acyl transfer activity of amidase from *Alcaligenes* sp. MTCC 10674. *Journal of Industrial Microbiology and Biotechnology*, *40*(1), 21-27. https://doi.org/10.1007/s10295-012-1206-x

Boodhoo, K. V. K., Flickinger, M. C., Woodley, J. M., & Emanuelsson, E. A. C. (2022). Bioprocess intensification: A route to efficient and sustainable biocatalytic transformations for the future.

Chemical Engineering and Processing-Process Intensification, *172*, 108793. https://doi.org/10.1016/j.cep.2022.108793

Brammar, W. J., & Clarke, P. H. (1964). Induction and repression of *Pseudomonas aeruginosa* amidase. *Microbiology*, *37*(3), 307-319. https://doi.org/10.1099/00221287-37-3-307

Devi, N., Patel, S. K., Kumar, P., Singh, A., Thakur, N., Lata, J., Pandey, D., Thakur, V., & Chand, D. (2022). Bioprocess scale-up for acetohydroxamic acid production by hyperactive acyltransferase of immobilized *Rhodococcus pyridinivorans*. *Catalysis Letters*, *152*(4), 944-953. https://doi.org/10.1007/s10562-021-03696-4

Fournand, D., Bigey, F., Ratomahenina, R., Arnaud, A., & Galzy, P. (1997). Biocatalyst improvement for the production of short-chain hydroxamic acids. *Enzyme and Microbial Technology*, *20*(6), 424-431. https://doi.org/10.1016/S0141-0229(96)00170-6

Kanwar, K., Sharma, D., Singh, H., Pal, M., Bandhu, R., & Azmi, W. (2024). In vitro effects of alginate lyase SG4+ produced by *Paenibacillus lautus* alone and combined with antibiotics on biofilm formation by mucoid *Pseudomonas aeruginosa*. *Brazilian Journal of Microbiology*, 1-15. https://doi.org/10.1007/s42770-024-01334-w

Končić, M. Z., Barbarić, M., Perković, I., & Zorc, B. (2011). Antiradical, chelating and antioxidant activities of hydroxamic acids and hydroxyureas. *Molecules*, *16*(8),6232-6242. https://doi.org/10.3390/molecules16086232

Kumari, P., Chand, D. (2017) Immobilization of whole resting cell of Bacillus sp. APB-6 exhibiting amidotransferase activity on sodium alginate beads and its comparative study with whole resting cells. *Journal of Innovations in Pharmaceutical and Biological Sciences*, *4*, 121-127. https://jipbs.com/index.php/journal/article/view/247

Kumari. P., Devi, N., & Chand, D. (2017) Enhanced production of amidotransferase from *Bacillus* sp. ABP-6 by optimization of nutritional parameters using statistical experimental design. *International Journal of Engineering Science Invention*, 12-22. https://www.ijesi.org/papers/Vol(6)9/Version4/B0609041222.pdf

Lin, H., Xu, P., & Huang, M. (2022). Structure-based molecular insights into matrix metalloproteinase inhibitors in cancer treatments. *Future Medicinal Chemistry*, *14*(1), 35-51. https://doi.org/10.4155/fmc-2021-0246

Mountanea, O. G., Mantzourani, C., Kokotou, M. G., Kokotos, C. G., & Kokotos, G. (2023). Sunlight-or UVA-Light-Mediated Synthesis of Hydroxamic Acids from Carboxylic Acids. *European Journal of Organic Chemistry*, *26*(13), e202300046. https://doi.org/10.1002/ejoc.202300046

Pandey, D., Singh, R., & Chand, D. (2011). An improved bioprocess for synthesis of acetohydroxamic acid using DTT (dithiothreitol) treated resting cells of *Bacillus* sp. APB-6. *Bioresource Technology*, *102*(11), 6579-6586. https://doi.org/10.1016/j.biortech.2011.03.071

Sharma, H., Singh, R. V., Ganjoo, A., Kumar, A., Singh, R., & Babu, V. (2022). Development of effective biotransformation process for benzohydroxamic acid production using *Bacillus smithii* IIIMB2907. *3 Biotech*, *12*(2), 44. https://doi.org/10.1007/s13205-022-03109-2

Sharma, M., Sharma, N. N., & Bhalla, T. C. (2012). Biotransformation of acetamide to acetohydroxamic acid at bench scale using acyl transferase activity of amidase of *Geobacillus pallidus* BTP-5x MTCC 9225. *Indian Journal of Microbiology*, *52*, 76-82. https://doi.org/10.1007/s12088-011-0211-5

Singh, R. V., Sharma, H., Ganjoo, A., Kumar, A., & Babu, V. (2020). Novel amidase catalysed process for the synthesis of vorinostat drug. *Journal of Applied Microbiology*, *129*(6), 1589-1597. https://doi.org/10.1111/jam.14753

Syed, Z., Sonu, K., Dongre, A., Sharma, G., & Sogani, M. (2020). A review on hydroxamic acids: Widespectrum chemotherapeutic agents. *International Journal of Biology and Biomedical Engineering*, *14*, 75-88. https://doi.org/10.46300/91011.2020.14.12

Victorino da Silva Amatto, I., Gonsales da Rosa-Garzon, N., Antonio de Oliveira Simoes, F., Santiago, F., Pereira da Silva Leite, N., Raspante Martins, J., & Cabral, H. (2022). Enzyme engineering and its industrial applications. *Biotechnology and Applied Biochemistry*, *69*(2), 389-409. https://doi.org/10.1002/bab.2117

Wang, M., Tang, T., Huang, Z., Li, R., Ling, D., Zhu, J., Jiang, L., Li, J., & Li X. (2022). Design and synthesis of novel hydroxamic acid derivatives based on quisinostat as promising antimalarial agents with improved safety. *Acta Materia Medica*, *1*(2), 212-223. https://doi.org/10.15212/AMM-2022-0007

Wu, Z., Liu, C., Zhang, Z., Zheng, R., & Zheng, Y. (2020). Amidase as a versatile tool in amide-bond cleavage: From molecular features to biotechnological applications. *Biotechnology Advances*, *43*, 107574. https://doi.org/10.1016/j.biotechadv.2020.107574

Xi, L., Tan, W., Li, J., Qu, J., & Liu, J. (2021). Cloning and characterization of a novel thermostable amidase, Xam, from *Xinfangfangia* sp. DLY26. *Biotechnology Letters*, *43*, 1395-1402. https://doi.org/10.1007/s10529-021-03124-y

BIOTECH STUDIES

RESEARCH PAPER

Cloning of glucoamylase gene from *Aspergillus niger* and its expression in *Pichia pastoris*

Meryem Damla Ozdemır Alkıs[1] iD, Dilek Gokturk[1]* iD, Osman Gulnaz[2] iD, Mehmet Inan[3,4] iD

[1]Adana Alparslan Türkeş Science and Technology University, Faculty of Engineering, Department of Bioengineering, Adana, Türkiye.
[2]Cukurova University, Faculty of Education, Department of Mathematics and Sciences Education, Adana, Türkiye.
[3]Akdeniz University, Department of Food Engineering, Antalya, Türkiye
[4]İzmir Biomedicine and Genome Center, İzmir, Türkiye.

Abstract

Glucoamylase (1,4-α-glucosidase) is a crucial commercial enzyme responsible for the conversion of starch, glycogen, and oligosaccharides into D-glucose through the hydrolysis of their non-reducing terminal glycosidic bonds. While many microorganisms, including bacteria, yeasts, and fungi, can produce glucoamylase, fungal glucoamylase is the preferred choice for industrial applications. The goal of this study was to produce the glucoamylase enzyme recombinantly in *Pichia pastoris*. To achieve this, the *glaA* gene from *Aspergillus niger*, responsible for encoding the glucoamylase enzyme, was cloned into a plasmid (pGAPZα-A) under the control of the GAP promoter and subsequently transferred into *P. pastoris*. The gene was verified through sequence analysis, while the effectiveness of transfection was validated using colony PCR and enzyme activity assays. The results demonstrated that the recombinant *P. pastoris* strain successfully secreted a substantial amount of glucoamylase (307.05 mg/L). The activity of the recombinant enzyme was measured at 79 U/mL.min. The enzyme exhibited robust activity over a broad range of temperatures (50-80°C) and various pH levels (pH 5-10), retaining 92-60% of its maximum activity. In conclusion, this study highlights the potential for laboratory-scale production of the glucoamylase enzyme, crucial for various industries, from a cost-effective and easily cultivable recombinant yeast strain, *P. pastoris.*

Introduction

Glucoamylase (GA), also known as 1,4-α-D-glucanglucohydrolase (EC 3.2.1.3), is an exoenzyme with a pivotal role in catalyzing the hydrolysis of glycosidic bonds within various substrates such as glycogen, starch, and oligosaccharides. Specifically, it targets the non-reducing ends of substances such as glycogen, starch, and oligosaccharides, cleaving these bonds and releasing D-glucose as a product. All sorts of α -glycosidic linkages between two glucosyl components, including α-(1→4) and α-(1→6) glycosidic linkages, can be broken

down by GA, with the exception of the α-α-trehalose bond (Aehle, 2007; Sauer et al., 2000). This enzymatic activity has significant industrial relevance and comes in second place globally in terms of sales and distribution (Li et al., 2017). The importance of GA to industry stems from its function in starch hydrolysis. Starch has a significant role in industry, particularly in the food, textile, pharmaceutical, and paper industries. The food industry primarily utilizes starch to manufacture bioethanol, glucose, high-fructose syrups, and other

biochemicals. Since the 1960s, GA has been utilized in the industry for the purpose of processing starch, and this is one of the major breakthroughs. Because starch hydrolysis was previously accomplished using inorganic acids before GA. However, enzymatic hydrolysis offered several benefits over acidic hydrolysis, including higher efficiency, lower energy consumption, and lower cost (Christakopoulos & Topakas, 2012; Hua et al., 2014; Satyanarayana et al., 2004).

Most bacteria, yeasts, and fungi have the ability to produce GA in a variety of forms, but fungal GA is particularly significant for industry (Bagheri et al., 2014; Li et al., 2017). The filamentous fungi are excellent providers of GA due to their high production capacity, thermostability, and stability over a broad pH range. A filamentous fungus called *Aspergillus niger* has been identified as the source of the first GA. Due to its great activity at neutral pH levels (3.5 to 5) and thermostability (optimally active at 50-60°C), the GA obtained from *A. niger* is primarily preferred in industry, notably in starch processing (Bagheri et al., 2014; Karim et al., 2016; Li et al., 2017; Norouzian et al., 2006; Sauer et al., 2000).

This study aimed to clone the GA encoding gene (*glaA*) from *A. niger* to *P. pastoris*. Recombinant technology was applied since recombinant enzymes could more economically and efficiently meet the demands in this field (Longoni et al., 2015). GA can be produced from fungi by different methods, but fungi grow slowly and are challenging to manage in the fermenter due to their complicated morphology (Adrio & Demain, 2010; Norouzian et al., 2006; Wucherpfennig et al., 2011). Additionally, there are significant drawbacks to using a fungus-like *A. niger* to produce homologous overexpressed proteins, such as the restricted types of plasmid vectors that may be employed and their inability to be sustained over an extended period. In other words, *A. niger* can generate a significant amount of GA, which is suitable for the industry, but producing GA from *A. niger* as a heterologous in a particular host will be more effective for industrial processes (Fleißner & Dersch, 2010; Storms et al., 2005). Herein, *P. pastoris* is a commonly used and very prospering host (Karakaş et al., 2010).

Materials and Methods

Strains, plasmids, and culture media

In this study, the *glaA* gene sourced from *A. niger* (NRRL3, ATCC 9029, CBS 120.49) was chosen as the target for cloning. For this purpose, mycelia from *A. niger* were cultured in Luria-Bertani (LB broth) medium (Merck, cat no:110285) containing 4 g/L starch at 37°C for propagation. The expression of the glucoamylase enzyme was achieved using *P. pastoris* X33, and the expression vector pGAPZα-A. *Escherichia coli* (DH5α), chemically competent, was used for plasmid proliferation and cultured in LB Lennox medium containing 25 μg/mL of the antibiotic Zeocin (Invivogen,

cat no: ant-zn-05) at 37°C. *P. pastoris* was cultured in YPD medium (Sigma-Aldrich, cat no: Y1375) at 30°C with orbital shaking (250 rpm). For the GA activity assay, cells were cultured in starch added M9 minimal medium (M9 salts (64 g/L $Na_2HPO4.7H_2O$, 15 g/L KH_2PO_4, 2,5 g/L NaCl, 5 g/L NH_4Cl), 1M $MgSO_4$, 1M $CaCl_2$).

Cloning of *glaA* and sequencing

The total RNA of *A. niger* was obtained using the Total RNA Purification Kit (Sigma, GenElute). cDNA was synthesized using the High-Capacity cDNA Reverse Transcription Kit (Applied Biosystems™). Polymerase chain reaction (PCR) was conducted using the High Fidelity PCR Kit (Roche) in which the cDNA was employed as the template (primers: 5'GGCTGAAGCTGAATTCATGTCGTTCCGATCTCTACTCGC 3' (sense), 5'GAGTTTTTGTTCTAGACTACCGCCAGGTGTCAGTCACC3' (antisense)). The PCR product containing the *glaA* gene was recovered from an agarose gel (0.8%) using a proper kit (Thermo Scientific™, GeneJET). EcoRI and NotI restriction enzymes were used to digest PCR products and the PGAPZαA carrier plasmid. Subsequently, a ligation reaction utilizing the Rapid DNA Ligation Kit (Thermo Scientific™) and plasmid isolation utilizing the Maxiprep Kit (Thermo Scientific™, GeneJET) were performed. The DNA amount was determined using a Qubit Fluorometer (Invitrogen). Sequence analyses of isolated plasmids were performed (by Sentegen Biotech) to confirm the absence of any potential mutations that might have occurred during PCR.

Transformation and expression of the *glaA* in *Pichia pastoris*

The plasmid was linearized with the restriction enzyme XmaJI within the GAP promoter and purified using a PCR purification kit (Qiagen, MinElute) before transformation. Transformation into *P. pastoris* (X33) was conducted via electroporation (Bio-Rad, Gene Pulser II) following the manufacturer's protocols. Yeast cells were then cultured on agar (YPD with Zeocin (100 μg/mL)). After 48 h of growth, the clones were collected, and colony PCR was performed as described in the manual of the PCR kit (Sigma, CORET). PCR conditions are initial denaturation at 95°C for 30 s, denaturation at 95°C for 30 s (35 cycles), annealing at 60°C for 30 s (35 cycles), extension at 68°C for 2.5 min (35 cycles), and final extension at 68°C for 5 min.

Starch agar plate test

To determine if the transfected gene (*glaA*) had starch hydrolyzing activity, the starch agar test was carried out. First, minimal medium agar plates with starch were made. To compare the transfected and normal cells, the transfected cells were cultured on one side of the plate and the normal yeast cells were cultured on the other side. After three days of cell incubation, iodine vapor was used to stain the plates.

Protein quantitation

Protein quantitation was performed using the supernatants of 72-h cultured recombinant yeast and normal yeast, as well as *A. niger* (NRRL3) cell cultures. The assay was conducted using the BCA Protein Assay Kit (Thermo Scientific™, Pierce).

Enzyme purification

The GA enzyme purification from the supernatant was carried out through ammonium sulfate precipitation, following the protocol of "Bulk Precipitation of Proteins by Ammonium Sulfate" (Simpson, 2006). The precipitated enzyme was dissolved in phosphate-buffered saline (PBS) (Merck, pH 7.4). The enzyme was separated from ammonium sulfate using a centrifugal filter system (Merk-Amicon) and collected in 500 µL of PBS.

Glucoamylase enzyme activity assay

Enzyme activity was estimated using a dinitrosalicylic acid (DNS) assay (Bernfeld, 1955) measuring the change in optical density at 540 nM (Shimadzu UV–VIS, UV mini-1240). A calibration curve was plotted using the optical densities of standard glucose solutions (20, 40, 60, 80, and 100 µg/mL). The enzyme was diluted 1/100 with PBS, and this diluted enzyme was used in all enzyme activity assays, with all assays conducted in triplicate. Enzyme activity (U/mL.min) was calculated using the calibration curve. In the specified test conditions, a single unit of GA enzyme activity was defined as the amount of enzyme capable of releasing 1 µmol of glucose per minute. The relationship between enzyme activity, temperature, and time was investigated at 25°C, 34°C, and 55°C for 15, 30, and 60 minutes. 500 µL of 10 g/L starch solution was treated with 500 µL of 1/100 diluted enzyme. The thermostability of the enzyme was determined by incubating 500 µL of 1/100 diluted enzyme with 500 µL of 10 g/L starch solution for 60 min at various temperatures (40°C, 50°C, 60°C, 70°C, and 80°C). The effect of pH on enzyme activity was measured using a citrate buffer (0,1 M). A 500 µL solution of 10 g/L starch was treated with 500 µL of 1/100 diluted enzyme. The enzymatic reactions were conducted at various pH levels (5, 6, 7, 8, 9, and 10) for 60 min.

Statistical analyses

All assays were performed in triplicate. The enzyme activity was calculated from three replicates, and the results were consistent. The standard deviation was extracted using Excel with previously obtained averages. The data were subjected to analysis of variance, and the means were compared between groups at the $p \leq 0.05$ level with ANOVA, One-Way and post-hoc Tukey test.

Results

Verification of cloning by colony PCR

In the initial stage, colony PCR was performed to confirm the effectiveness of cloning. Colony PCR was carried out using *E. coli* cells containing the recombinant plasmid. The results indicated that the empty plasmid had a size of approximately 500 bp, whereas the plasmid containing *glaA* was 2410 bp in size (Figure 1a). Additionally, to determine whether yeast cells successfully received the recombinant plasmid DNA, a colony PCR analysis was conducted. The gel image displayed a PCR product size of 2410 bp, providing clear evidence of successful transformation (Figure 1b).

Starch agar plate test

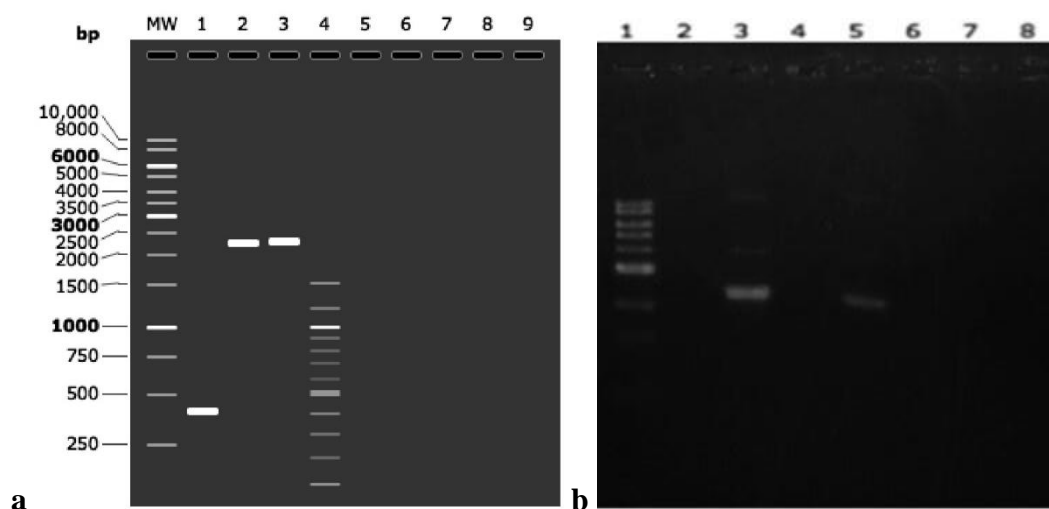Glucoamylase is a type of exoamylase that breaks the α-(1→4) and α-(1→6) glycosidic linkages found in

Figure 1. a. Colony PCR was made with *E.coli* cells containing recombinant plasmid. In the first well, PGAPZαA (the empty plasmid) is found; In the 2. and 3. well recombinant PGAPZαA (plasmid + glucoamylase) is found. b. The gel image of colony PCR after transfection. In the first well, 1kb DNA ladder (GeneRulerTM Thermo Scientific, Cat. No. SM0311) is found; In the third well the PCR product in which recombinant PGAPZαA plasmid was used as the template is found; In the fifth well the PCR product in which recombinant yeast cell lysate was used as the template is found (The PCR product size is between 2000 and 2500 bp).

starch (Li et al., 2017). The starch polymers are bound by the iodine, resulting in a blue-black color (Pfister et al., 2016; Xiao et al., 2006). When GA hydrolyzes the starch on the plate, which is secreted by recombinant *P. pastoris* cells, iodine vapor treatment causes the starch-containing portions to become discolored. In Figure 2. a, part B of the iodine vapor-treated plate displayed a significant blue-black color staining, whereas part A remained clear (unstained). This result clearly demonstrated that, while host cells cannot digest starch by secreting GA, recombinant cells can.

Protein quantitation assay

The protein concentrations in the liquid phase of transformed and untransformed yeast and *A. niger* cultures were determined using a standard curve. The quantity of protein released by untransformed P. pastoris, recombinant P. pastoris, and A. niger cells was found to be zero, 307.05325 g/mL and 361.033 g/mL respectively (Figure 2.b).
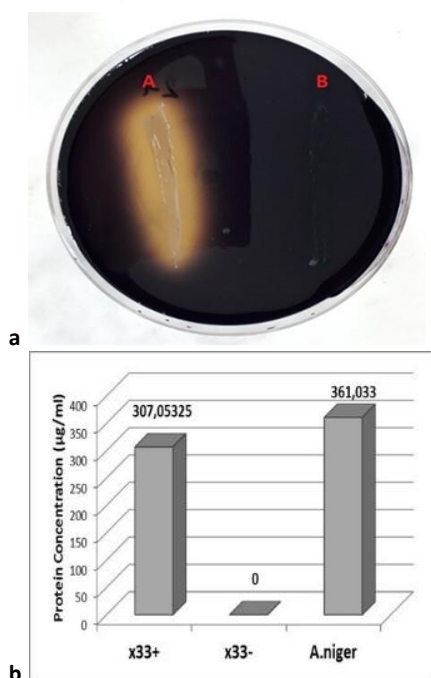
Figure 2. a. Starch agar plates stained with iodine vapor. A. Recombinant yeast cells, B. Normal yeast cells (the color didn't change as a result of the breakdown of starch by GA produced by recombinant yeast cells). b. The amount of protein found in the supernatants of recombinant (X33⁺), untransformed *P. pastoris* (X33⁻), and *A. niger* which were the source organism cultures.

Determination of enzyme activity

Enzyme activity was assessed through a DNS (3,5-dinitrosalicylic acid) assay and evaluated under different circumstances. The DNS assay results showed that 71.2 mg/L of glucose was released per minute. Since a single unit of GA enzyme activity is defined as the amount of enzyme that can release 1 μmol of glucose per minute, the enzyme activity was calculated as 79 U/mL.

The enzyme activities at room temperature (25°C), culture temperature (34°C), and industrial temperature

(55°C) were remarkably similar when the enzyme was treated with a starch solution (10 g/L) for 60, 30, and 15 min (Figure 3). Enzyme activities at room and industrial temperatures were similar and not much lower than at culture temperatures. The optimal enzyme activity of the recombinant GA obtained in this study was recorded at 40°C, whereas the enzyme activity at 55°C and 60°C was 92% and 88% of its optimal activity (Figure 4). The enzyme activity of recombinant GA was also investigated at different pH levels (Figure 5). The highest enzyme activity was recorded at pH 7, and the enzyme activity at pH 5 and 6 had 90% and 97% of the highest activity, respectively. It was 68% of its maximum activity at pH 10.

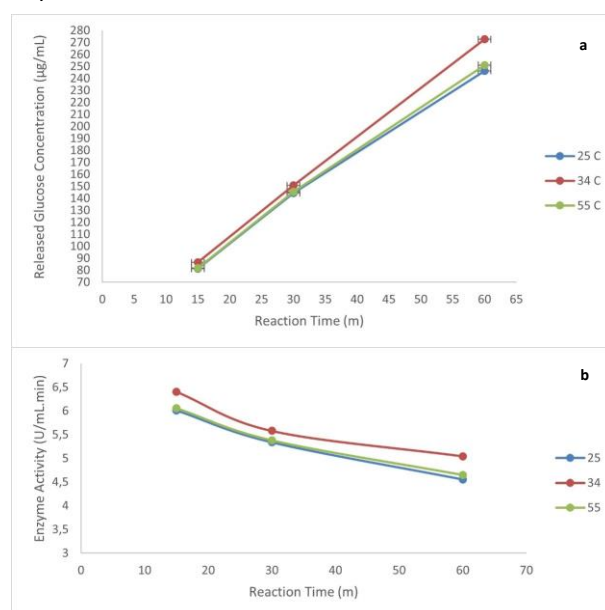**Figure 3.** The relation of (a) released glucose and (b) enzyme activity with temperature and time. (Blue: 25°C, Red: 34°C, Green: 55°C) ($p<0.05$).
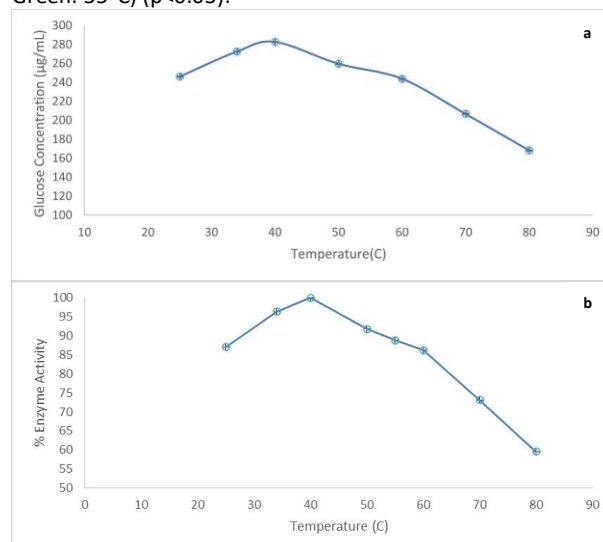

Figure 4. The relation between enzyme activity percent and temperature. The enzyme was incubated with 10 g/L soluble starch at different temperatures for 1 hour. Released glucose concentration (a) and enzyme activity (b) were calculated ($p<0.05$).
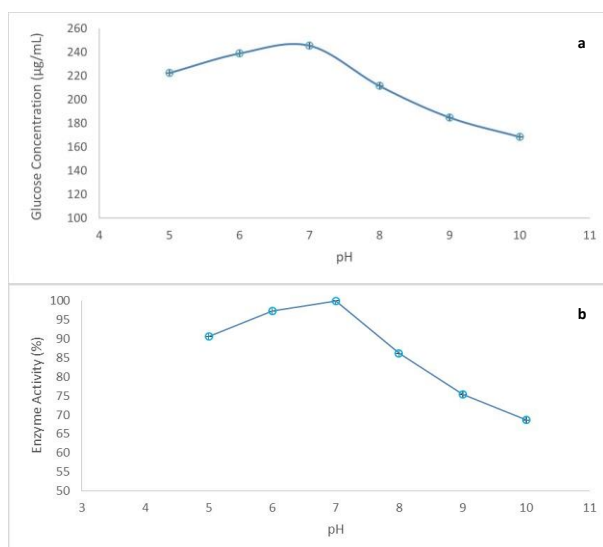
Figure 5. The relation between (a) released glucose and (b) enzyme activity (%) with pH (p<0.05).

Discussion

Pichia pastoris has gained considerable attention as an effective system for expressing recombinant proteins (Pan et al., 2022). Studies in the literature have demonstrated that *P. pastoris* cells exhibit a tendency to secrete relatively modest amounts of endogenous proteins, which is one of the characteristics rendering them suitable hosts for recombinant protein production (Burgard et al., 2020; Macauley-Patrick et al., 2005). This indicates that yeast cells do not normally synthesize extracellular proteins under these conditions. It can be assumed that the quantity of protein released from recombinant yeast cells is equivalent to the quantity of GA enzyme secreted. *A. niger* can produce a variety of extracellular proteins depending on the source of carbon present in the medium, with varying amounts (Lu et al., 2010). When *A. niger* is grown in a medium that contains just starch as a carbon source, GA represents more than 50% of its extracellular proteome. (Kwon et al., 2012). The levels of extracellular protein released by *A. niger* (361.033 g/mL), and recombinant yeast (307.05325 g/mL) were quite similar. The difference is likely due to the different exoproteins of *A. niger,* and the GA enzyme level of the transformed *P. pastoris* in this study is thought to be nearly as high as or possibly higher than that of the donor organism.
No studies have been found in the literature regarding the cloning of the GA gene region from *A. niger* into *P.*

pastoris. However, there is a study reporting the cloning of the GA gene region from *Aspergillus awamori*, which has been shown to be identical to that of *A. niger.* The results indicate that recombinant glucoamylase produced in *P. pastoris* exhibits enzymatic, chemical, and physicochemical properties that are very similar to those of the source organism (Fierobe et al., 1997). Additionally, several studies have been published on GA derived recombinantly from *P. pastoris* using different source organisms. (Table 1). It was reported that GA enzyme activity obtained from recombinant *P. pastoris* cells transfected with the GA encoding gene from *Bispora sp.* (MEY-1) reached 34.1 U/mL (Hua et al., 2014). Recombinant *P. pastoris* cells cloned with the *Chaetomium thermophilum* GA gene produced a GA activity of 16.73 U/mL (Chen et al., 2007). The cDNA that encodes glucoamylase GA from the thermophilic fungus *Thermomyces lanuginosus* was cloned into *P. pastoris* yielding an activity of approximately 7.4 U/ml (Thorsen et al., 2006). In a study aiming to increase the secretion of GA in *P. pastoris*, GA from *Rhizopus oryzae* was cloned into *P. pastoris* by combining it with a modified signal peptide and a gene encoding a protein associated with secretory vesicles. As a result, the GA activity obtained from systems containing different combinations and various copy numbers of the gene was minimum 0.126 U/mL and maximum 12.619 U/mL (Liu et al., 2005). The activities of GA secreted by recombinant *P. pastoris*, which was cloned with the GA gene from *Rasamsonia emersonii* and *Talaromyces leycettanus*, were 38.6 U/mL and 9.2 U/mL, respectively (Tong et al., 2022). These examples from the literature suggest that the GA enzyme activity obtained in this study (79 U/mL) was notably higher.

GA is a highly demanded and main enzyme for industrial processes involving starch (Li et al., 2017). It is involved in fermentation processes such as alcohol and vinegar, in the production processes of vitamins, antibiotics, and organic acids whose substrate is glucose, together with cellulose in the recycling of straw and other agricultural wastes, and in the de-inking process in paper recycling (Kumar & Satyanarayana, 2009; Pasin et al., 2024; Zong et al., 2022). Recently, GA used in industry primarily sourced from filamentous fungi such as *Aspergillus niger*, *Aspergillus awamori,* and *Rhizopus niveus* (Bagheri et al., 2014; Tong et al., 2021). In the literature, it is reported that the ideal temperature for GA obtained from *A. niger* and various other filamentous fungi is between 40-60°C, although

Table 1. Enzyme activities of recombinant glucoamylases expressed in *Pichia pastoris*

Source	Host	Enzyme Activity	Reference
Thermomyces lanuginosus	*P. pastoris*	7,4 U/mL	(Thorsen et al., 2006)
Chaetomium thermophilum	*P. pastoris*	16.73 U/mL	(Chen et al., 2007)
Bispora sp. MEY-1	*P. pastoris*	34.1 U/mL	(Hua et al., 2014)
Aspergillus flavus (NSH9)	*P. pastoris*	8.24 U/mL	(Karim et al., 2016)
Penicillium oxalicum	*P. pastoris*	81.2 U/mg	(Xu et al., 2016)
Rasamsonia emersonii	*P. pastoris*	38.6 U/mL	(Tong et al., 2022)
Talaromyces leycettanus		9.2 U/mL	

the majority are below 55°C ([Kumar & Satyanarayana, 2009](#); [Pandey, 1995](#); [Paszczvdski & Miedziak, 1982](#)). However, GA enzyme is used at temperatures above 55°C in processes that hydrolyze starch, such as bioethanol and glucose syrup production, and at temperatures between 40-50°C in paper recycling processes ([James & Lee, 1997](#); [Pasin et al., 2024](#)). Hence, if the obtained GA is thermostable, it will be more suitable for industry as it will not lose its activity at high temperatures. The recombinant GA enzyme obtained in this study preserved 92% of its optimum activity at 55°C and even showed more than half of its optimum activity at 80°C. This will be highly favorable regarding use in industrial applications. The commercially available GA derived from *A. niger* is normally active at acidic pH levels ([Norouzian et al., 2006](#)). The liquefaction stage of starch conversion processes occurs at pH 5.5-6 ([Hua et al., 2014](#)). After liquefaction, the liquefied starch is processed with GA to produce glucose syrup, high conversion syrups, or substrates for alcohol fermentation. During these processes pH will vary from 4.5 to 5.5 ([James & Lee, 1997](#)). In addition, in the paper recycling process, which is another usage area of GA, the enzyme should be stable between pH 4-6 ([Pasin et al., 2024](#)). The enzyme activity of the recombinant GA produced in this work was significantly high at acidic pH levels and was active across a wide pH range (5-10). Thus, it is considered that the recombinant GA obtained in this study is suitable for industrial use.

Within the scope of this study, we successfully conducted the molecular cloning and expression of the glucoamylase gene (*glaA*) derived from *A. niger* in *P. pastoris*. The transformation of *P. pastoris* with the recombinant plasmid was not only efficient but also resulted in recombinant yeast cells that demonstrated a remarkable capability to secrete GA, comparable to the original *A. niger* organism.

One of the key findings of our study was the high activity level of the recombinant GA, reaching 79 U/mL.min. This level of activity suggests that the recombinant enzyme holds great promise for industrial applications. Moreover, we assessed the enzyme's performance across a range of temperatures and pH levels, revealing its versatility and suitability for various industrial processes.

Furthermore, the recombinant *P. pastoris* used in this study showed the potential to produce a substantial quantity of industrially relevant GA. This finding implies that large-scale production of this industrially significant enzyme can be achieved more cost-effectively and with higher yields using recombinant *P. pastoris*.

Conclusion

In conclusion, this research underscores the potential of recombinant glucoamylase-expressing *P. pastoris* as a valuable tool for industrial enzyme production. This approach offers a more economical and efficient means of obtaining glucoamylase on a large scale, with broad industrial applications.

Author Contributions

MDOA: Formal analysis, Investigation, Writing - Original Draft, Visualization; DG: Conceptualization, Methodology, Resources, Writing - Review & Editing, Supervision; OG: Methodology, Resources, Writing - Review & Editing MI: Validation, Resources, Writing - Review & Editing

Conflict of Interest

The author(s) declare that they have no known competing financial or non-financial, professional, or personal conflicts that could have appeared to influence the work reported in this paper.

Acknowledgements

References

Adrio, J. L., & Demain, A. L. (2010). Recombinant organisms for production of industrial products. *Bioengineered Bugs*, *1*(2), 116–131. https://doi.org/10.4161/bbug.1.2.10484

Aehle, W. (2007). *Enzymes in Industry: Production and Applications, 3rd Edition* (W. Aehle, Ed.; third). WILEY-VCH Verlag GmbH & Co. KGaA, Weinheim.

Bagheri, A., Khodarahmi, R., & Mostafaie, A. (2014). Purification and biochemical characterisation of glucoamylase from a newly isolated *Aspergillus niger*: relation to starch processing. *Food Chemistry*, *161*, 270–278. https://doi.org/10.1016/j.foodchem.2014.03.095

Bernfeld, P. (1955). Amylases, α and β. In *Methods in Enzymology*, *1*, 149–158. https://doi.org/10.1016/0076-6879(55)01021-5

Burgard, J., Grünwald-Gruber, C., Altmann, F., Zanghellini, J., Valli, M., Mattanovich, D., & Gasser, B. (2020). The secretome of *Pichia pastoris* in fed-batch cultivations is largely independent of the carbon source but changes quantitatively over cultivation time. *Microbial Biotechnology*, *13*(2), 479–494.

https://doi.org/10.1111/1751-7915.13499

Chen, J., Zhang, Y.Q., Zhao, C.Q., Li, A.N., Zhou, Q.X., & Li, D.C. (2007). Cloning of a gene encoding thermostable glucoamylase from Chaetomium thermophilum and its expression in *Pichia pastoris*. *Journal of Applied Microbiology*, *103*(6), 2277–2284. https://doi.org/10.1111/j.1365-672.2007.03475.x

Christakopoulos, P., & Topakas, E. (2012). Editorial Note: Advances in Enzymology and Enzyme Engineering. *Computational and Structural Biotechnology Journal*, *2*(3), 1. https://doi.org/10.5936/csbj.201209001

Fierobe, H. P., Mirgorodskaya, E., Frandsen, T. P., Roepstorff, P., & Svensson, B. (1997). Overexpression and characterization of *Aspergillus awamori* wild-type and mutant glucoamylase secreted by the methylotrophic yeast *Pichia pastoris*: comparison with wild-type recombinant glucoamylase produced using *Saccharomyces cerevisiae* and *Asperg*. *Protein Expression and Purification*, *9*(2), 159–170. https://doi.org/10.1006/prep.1996.0689

Fleißner, A., & Dersch, P. (2010). Expression and export: recombinant protein production systems for *Aspergillus*. *Applied Microbiology and Biotechnology*, *87*(4), 1255–1270. https://doi.org/10.1007/s00253-010-2672-6

Hua, H., Luo, H., Bai, Y., Wang, K., Niu, C., Huang, H., Shi, P., Wang, C., Yang, P., & Yao, B. (2014). A thermostable glucoamylase from *Bispora* sp. *MEY-1* with stability over a broad pH range and significant starch hydrolysis capacity. *PLoS ONE*, *9*(11), e113581. https://doi.org/10.1371/journal.pone.0113581

James, J. A., & Lee, B. H. (1997). Glucoamylases: microbial sources, industrial applications and molecular biology — A Review. *Journal of Food Biochemistry*, *21*(6), 1–52. https://doi.org/10.1111/j.1745-4514.1997.tb00223.x

Karakaş, B., Inan, M., & Certel, M. (2010). Expression and characterization of *Bacillus subtilis* PY22 α-amylase in *Pichia pastoris*. *Journal of Molecular Catalysis B: Enzymatic*, *64*(3–4), 129–134. https://doi.org/10.1016/j.molcatb.2009.07.006

Karim, K. M. R., Husaini, A., Hossain, M. A., Sing, N. N., Mohd Sinang, F., Hussain, M. H. M., & Roslan, H. A. (2016). Heterologous, expression, and characterization of thermostable glucoamylase derived from *Aspergillus flavus* NSH9 in *Pichia pastoris*. *BioMed Research International*, *2016*(1), 5962028. https://doi.org/10.1155/2016/5962028

Kumar, P., & Satyanarayana, T. (2009). Microbial glucoamylases: characteristics and applications. *Critical Reviews in Biotechnology*, *29*(3), 225–255. https://doi.org/10.1080/07388550903136076

Kwon, M. J., Jørgensen, T. R., Nitsche, B. M., Arentshorst, M., Park, J., Ram, A. F. J., & Meyer, V. (2012). The transcriptomic fingerprint of glucoamylase over-expression in *Aspergillus niger*. *BMC Genomics*, *13*(1), 1-18. https://doi.org/10.1186/1471-2164-13-701

Li, Z., Ji, K., Dong, W., Ye, X., Wu, J., Zhou, J., Wang, F., Chen, Q., Fu, L., Li, S., Huang, Y., & Cui, Z. (2017). Cloning, heterologous expression, and enzymatic characterization of a novel glucoamylase GlucaM from *Corallococcus* sp. strain *EGB*. *Protein Expression and Purification*, *129*(June), 122–127. https://doi.org/10.1016/j.pep.2015.06.009

Liu, S. H., Chou, W. I., Sheu, C. C., & Chang, M. D. T. (2005). Improved secretory production of glucoamylase in *Pichia pastoris* by combination of genetic manipulations. *Biochemical and Biophysical Research Communications*, *326*(4), 817–824. https://doi.org/10.1016/J.BBRC.2004.11.112

Longoni, P., Leelavathi, S., Doria, E., Reddy, V. S., & Cella, R. (2015). Production by tobacco transplastomic plants of recombinant fungal and bacterial cell-wall degrading enzymes to be used for cellulosic biomass saccharification. *BioMed Research International*, *2015*(1), 289759. https://doi.org/10.1155/2015/289759

Lu, X., Sun, J., Nimtz, M., Wissing, J., Zeng, A.-P., & Rinas, U. (2010). The intra- and extracellular proteome of *Aspergillus niger* growing on defined medium with xylose or maltose as carbon substrate. *Microbial Cell Factories*, *9*, 1-13. https://doi.org/10.1186/1475-2859-9-23

Macauley-Patrick, S., Fazenda, M. L., McNeil, B., & Harvey, L. M. (2005). Heterologous protein production using the *Pichia pastoris* expression system. *Yeast*, *22*(4), 249–270. https://doi.org/10.1002/yea.1208

Norouzian, D., Akbarzadeh, A., Scharer, J. M., & Moo Young, M. (2006). Fungal glucoamylases. *Biotechnology Advances*, *24*(1), 80–85. https://doi.org/10.1016/j.biotechadv.2005.06.003

Pan, Y., Yang, J., Wu, J., Yang, L., & Fang, H. (2022). Current advances of *Pichia pastoris* as cell factories for production of recombinant proteins. *Frontiers in Microbiology*, *13*, 1059777. https://doi.org/10.3389/fmicb.2022.1059777

Pandey, A. (1995). Glucoamylase Research: An Overview. *Starch - Stärke*, *47*(11), 439–445. https://doi.org/10.1002/star.19950471108

Pasin, T. M., Betini, J. H. A., de Lucas, R. C., & Polizeli, M. de L. T. de M. (2024). Biochemical characterization of an acid-thermostable glucoamylase from *Aspergillus japonicus* with potential application in the paper bio-deinking. *Biotechnology Progress*, *40*(1), e3384. https://doi.org/10.1002/btpr.3384

Paszczvdski, A., & Miedziak, I. (1982). A simple method of affinity chromatography for the purification of

glucoamylase obtained from *Aspergilus niger C. FEBS letters*, *149*(1), 63-66.

Pfister, B., Sánchez-Ferrer, A., Diaz, A., Lu, K., Otto, C., Holler, M., Shaik, F. R., Meier, F., Mezzenga, R., & Zeeman, S. C. (2016). Recreating the synthesis of starch granules in yeast. *ELife*, *5*(NOVEMBER2016), 1–29. https://doi.org/10.7554/eLife.15552

Satyanarayana, T., Noorwez, S. M., Kumar, S., Rao, J. L. U. M., Ezhilvannan, M., & Kaur, P. (2004). Development of an ideal starch saccharification process using amylolytic enzymes from thermophiles. *Biochemical Society Transactions*, *32*(Pt 2), 276–278.

Sauer, J., Sigurskjold, B. W., Christensen, U., Frandsen, T. P., Mirgorodskaya, E., Harrison, M., Roepstor, P., & Svensson, B. (2000). Glucoamylase: structure/function relationships, and protein engineering. *Biochimica et Biophysica Acta (BBA)-Protein Structure and Molecular Enzymology, 1543*(2), 275-293.

Simpson, R. J. (2006). Bulk precipitation of proteins by ammonium sulfate. *Cold Spring Harbor Protocols*, *2006*(1), pdb. prot 4308. https://doi.org/10.1101/pdb.prot4308

Storms, R., Zheng, Y., Li, H., Sillaots, S., Martinez-Perez, A., & Tsang, A. (2005). Plasmid vectors for protein production, gene expression and molecular manipulations in *Aspergillus niger*. *Plasmid*, *53*(3), 191–204. https://doi.org/10.1016/j.plasmid.2004.10.001

Thorsen, T. S., Johnsen, A. H., Josefsen, K., & Jensen, B. (2006). Identification and characterization of glucoamylase from the fungus Thermomyces lanuginosus. *Biochimica et Biophysica Acta (BBA) - Proteins and Proteomics*, *1764*(4), 671–676.

https://doi.org/10.1016/J.BBAPAP.2006.01.009

Tong, L., Huang, H., Zheng, J., Wang, X., Bai, Y., Wang, X., Wang, Y., Tu, T., Yao, B., Qin, X., & Luo, H. (2022). Engineering a carbohydrate-binding module to increase the expression level of glucoamylase in *Pichia pastoris*. *Microbial Cell Factories*, *21*(1), 95. https://doi.org/10.1186/s12934-022-01833-1

Tong, L., Zheng, J., Wang, X., Wang, X., Huang, H., Yang, H., Tu, T., Wang, Y., Bai, Y., Yao, B., Luo, H., & Qin, X. (2021). Improvement of thermostability and catalytic efficiency of glucoamylase from *Talaromyces leycettanus* JCM12802 via site-directed mutagenesis to enhance industrial saccharification applications. *Biotechnology for Biofuels*, *14*(1), 202. https://doi.org/10.1186/s13068-021-02052-3

Wucherpfennig, T., Hestler, T., & Krull, R. (2011). Morphology engineering - osmolality and its effect on *Aspergillus niger* morphology and productivity. *Microbial Cell Factories*, *10*, 1–15. https://doi.org/10.1186/1475-2859-10-58

Xiao, Z., Storms, R., & Tsang, A. (2006). A quantitative starch – iodine method for measuring alpha-amylase and glucoamylase activities. *Analytical Biochemistry*, *362*(MAY 2006), 146–148. https://doi.org/10.1016/j.ab.2006.01.036

Xu, Q.-S., Yan, Y.-S., & Feng, J.-X. (2016). Efficient hydrolysis of raw starch and ethanol fermentation: a novel raw starch-digesting glucoamylase from *Penicillium oxalicum*. *Biotechnology for Biofuels*, *9*, 216. https://doi.org/10.1186/s13068-016-0636-5

Zong, X., Wen, L., Wang, Y., & Li, L. (2022). Research progress of glucoamylase with industrial potential. *Journal of Food Biochemistry*, *46*(7), e14099. https://doi.org/10.1111/jfbc.14099

CONTENTS